UNIVERSITY OF CAPE TOWN

RHEOLOGICAL EFFECTS ON GAS DISPERSION IN A PILOT SCALE MECHANICAL FLOTATION CELL

A thesis submitted to the faculty of
ENGINEERING AND THE BUILT ENVIRONMENT
of the
UNIVERSITY OF CAPE TOWN
in Fulfillment of the Requirements of the Degree of
MASTER OF SCIENCE IN ENGINEERING
MSc (Eng)

By
Ntokozo Zinhle Precious Shabalala
BSc. (Chem Eng), University of Cape Town

Centre for Minerals Research
University of Cape Town
Rondebosch 7700
South Africa
August 2013

Declaration

I know the meaning of plagiarism and declare that all the work in the document, save for that which is properly acknowledged, is my own.

Signed by candidate

Ntokozo Shabalala

Acknowledgements

First, I would like to convey my sincere thanks and appreciation to Prof. Dave Deglon for his perceptive guidance and advice. I would like to thank him for persistently ensuring that I am on the right track.

I would also like thank my co-supervisor, Mr. Martin Harris for his enthusiasm and invaluable advice.

I would also like to acknowledge the following people:

Mintek and Dr. Mike Bryson for their consistent support.

The CMR staff at UCT especially Kenneth Masuku and Monde Bhekaphi for assisting with the preparation of samples.

Veruscha Verster from CPUT for assisting with the rheology testing and allowing me to use their facilities.

My friends, for believing in me.

My family, most especially my mother for her unfailing support, love and encouragement.

Abstract

Froth flotation is a separation method used for the beneficiation of a considerable portion of the world's mineral ores. The majority of flotation occurs in mechanical flotation cells, where effective gas dispersion is a primary requirement for particle-bubble contacting. Due to the mineralogical complexity of ores, it is required that particles be ground even finer to liberate valuable minerals. Mining operations tend to run flotation circuits at fairly high solids concentrations in order to maximise residence time, accommodate higher tonnages and limit water consumption. Mineral slurries processed at fine particle sizes and high solids concentrations have been shown to exhibit non-Newtonian rheological behaviour.

The effect of slurry rheology on gas dispersion in a 100 litre mechanical flotation cell was investigated by varying the solids concentration. The study was conducted using kaolin, Bindura nickel and Platreef slurries. All three ores displayed typical non-Newtonian rheological behaviour where the slurry yield stress and viscosity increased exponentially with solids concentration.

Bubble size varied from 0.55 to 1.10 mm for all the ores tested. At low solids concentration bubble size was found to decrease with impeller speed, a characteristic trend that was expected. At moderate solids concentrations bubble size was found to either increase/remain relatively constant with impeller speed; this trend was also expected. Unexpectedly, at the highest solids concentration, a dramatic decrease in bubble size was observed. This unexpected drop in bubble size was attributed to slurry rheology. It was also observed that there was a slight increase in bubble size at the highest solids concentration with increasing impeller speed. This increase was attributed to a trade-off relationship between the rheology of the slurries and the existing hydrodynamics (as a result of the rotating impeller).

Gas hold-up varied from 2 to 15% across all the ores tested. At low solids concentrations gas hold-up increased with impeller speed as expected. At moderate solids concentration, gas hold-up was viewed to either increase/remain relatively constant with impeller speed. A significant drop in gas hold-up was observed at the highest solids concentration. The gas hold-up however still increased with impeller

speed albeit at a lower rate at the highest solids concentrations. This drop in gas hold-up at the highest solids concentration (along with the decrease in bubble size) was attributed to the effect of slurry rheology.

At high solids concentrations, all three slurries (kaolin, Bindura nickel and Platreef) exhibit non-Newtonian behaviour illustrated by means of high viscosities and yield stresses. High viscosities result in turbulence damping in the cell which inhibits bubble break-up, resulting in larger bubbles and correspondingly lower gas hold-up. It was concluded in this study that the yield stress is the dominant rheological property due to the significant changes observed with increasing solids concentration.

High yield stresses resulted in the formation of a 'cavern' of slurry around the impeller region. Within this 'cavern', high power intensities exist around the impeller where small bubbles are formed. However due to the formation of the 'cavern', the slurry in the bulk cell remains relatively stagnant. As a result small bubbles formed around the impeller remain localised in the 'cavern' and cannot be dispersed throughout the cell. This localization and poor dispersion of bubbles resulted in low gas hold-ups.

It was thus concluded that slurry rheology in fact has a significant effect on gas dispersion particularly at the highest solids concentrations where significant yield stresses are observed.

TABLE OF CONTENTS

List of Figures

List of Tables

Nomenclature

A	dimensionless constant
A_{bubble}	bubble surface area (mm^2)
A_{cell}	cell cross sectional area (m^2)
d_b	mean bubble size (mm)
d_{max}	maximum stable diameter (m)
d_{32}	Sauter mean diameter (m)
D	impeller diameter (m)
J_g	superficial gas velocity (cm/s)
K	consistency index
M	torque of the impeller (Nm)
n	flow behaviour index
N	impeller speed (rpm)
N_p	power number
N_{Re}	Reynolds number
P	power draw (kW)
P_d	probability of detachment
Q_g	measured volumetric aeration rate (m^3/min)
r	particle size
r_{max}	maximum particle size
S_b	bubble surface area flux (s^{-1})
V	cell volume (m^3)
V_L	liquid volume (L)
We	Weber number

Greek letters

ε	energy dissipation rate per unit mass (m^2/s^3)
ε_G	gas hold-up (volume %)
ε_H	hold-up (-)
ρ	liquid density (kg/m^3)
ρ_{SL}	slurry density (kg/m^3)

μ_A	apparent viscosity of fluid (Pa.s)
μ_G	gas viscosity (Pa.s)
μ_L	suspending liquid viscosity (Pa.s)
μ_W	viscosity of water (Pa.s)
σ	surface tension (N/m)
τ	shear stress (Pa)
τ_B	Bingham yield stress (Pa)
γ	shear rate (s^{-1})
η	fluid viscosity (Pa.s)
η_C	Casson apparent viscosity (Pa.s)
η_B	Bingham apparent viscosity (Pa.s)

CHAPTER 1 Introduction

Mining operations are increasingly required to grind ores to finer and finer particle sizes in order to liberate valuable minerals from finely disseminated ore bodies. In ultra-fine grinding, stirred mills such as Isamills (Pease *et al*., 2006) have been employed to achieve these ultra-fine particle sizes (P_{80} of less than 10 μm) under wet conditions. In order to achieve satisfactory grades and recoveries during flotation, it is essential that the desired valuable minerals be liberated from gangue minerals at the grinding stage.

There is a growing awareness that, in future, plants will be required to run at higher solid densities to cut back on water usage, as water shortage is increasingly becoming a problem. Running at high solids densities also promotes higher tonnages and maximises residence time in flotation circuits. It is believed that slurry rheology will increasingly become important with increasing solids concentration particularly at fine particle sizes. Fine particle sizes and concentrated slurries enhance inter-particle interaction which often results in difficult slurry behaviour characterised by high yield stresses and apparent viscosities as a consequence of particle aggregation. These ultra-fine particles have been found to be problematic in downstream processes such as flotation where they have been reported to reduce product recovery and grade (King, 1982; Yoon, 2000; George *et al*., 2004; Waters *et al*., 2008).

In flotation it has also been observed that slurries (at varying solids concentrations and particle sizes) exhibit varying rheological behaviour; the significance of the ore mineralogy was also found to influence slurry rheology, particularly for ores containing phyllosilicates (Ndlovu *et al*., 2010). Many valuable minerals are associated with naturally floating gangue minerals such as talc and graphite (Du, 2008) which report to the froth surface with the valuable minerals, thus reducing the concentrate grade. These minerals also affect the rheology of the slurry in the cell; they are usually known as the ‘problematic’ minerals that lead to difficulties when handling ores bearing these gangue minerals.

The effect of slurry rheology in wet grinding has been well studied (Klimpel, 1988; Yue and Klein, 2004; He and Forssberg, 2007); He *et al*., 2006) and has been found to affect the grindability and the resulting particle size distribution. Elevated grinding times result in increased product fineness characterised by a very fine product size. At high slurry concentrations the surface properties tend to predominate in the system (Gao and Forssberg, 1993; Wang and Forssberg, 1995). However, few studies on the effect of slurry rheology in flotation have been carried out, particularly in mechanical flotation where effective gas dispersion is a primary requirement for particle-bubble contact. Independent research on gas dispersion and rheology in stirred tanks has been done in the general chemical engineering field, thus most of the literature will be drawn from this field.

It is believed that slurry rheology will increasingly become important in flotation whether as a consequence of increasing solids concentration or reduced particle size. In mechanical flotation cells it is believed that slurry rheology will affect how gas is dispersed throughout the cell, ultimately affecting the recovery of minerals.

In this study, slurry rheology tests were conducted at different solids concentrations using kaolin, Bindura nickel and Platreef ores. The rheology tests were conducted to determine the rheological behaviour of slurries as a function of solids concentration. Gas dispersion measurements of bubble size and gas hold up were then conducted in a pilot mechanical flotation cell for each of the ores tested at different solids concentrations. The rheology tests were conducted prior to the gas dispersion tests at different solids concentrations so that the rheological behaviour at specific slurry concentrations could be established. The prior knowledge of the rheological properties was believed necessary to assist in the interpretation of the gas dispersion results. The rheological properties of yield stress and viscosity were related to the gas dispersion measurements at the different solids concentrations that were tested for each of the ores tested.

The aim of this thesis is thus to investigate the effect of slurry rheology on gas dispersion in mechanical flotation cells. Chapter 2 reviews the relevant literature on flotation, slurry rheology and gas dispersion. The available literature on the effect of varying rheological behaviour on gas dispersion is also reported. Most of this

information is drawn from the chemical engineering literature with respect to stirred tanks. The experimental section then follows in Chapter 3. This chapter explains in detail the equipment, materials as well as the procedure followed to carry out experiments. The results with relevant observations are presented in Chapter 4 followed by the discussion. Conclusions and recommendations are then summarised in Chapter 5.

CHAPTER 2 Literature Review

This study focuses on the effect of rheology on gas dispersion in mechanical flotation cells. This chapter begins with an overview of the flotation process and the flotation cells usually applied in industry. The outcome of the flotation process occurs as a result of hydrodynamics existing in the flotation cell. In turn, the rheology of slurries influences the hydrodynamics in the cell. The hydrodynamics in the cell ultimately affect how gas is dispersed throughout the cell.

Froth flotation is reviewed by looking at the different processes involved to achieve flotation together with the typical flotation cells that are used. Rheology is then reviewed followed by the review of the hydrodynamics in mechanical flotation cells. Gas dispersion is reviewed under the headings of bubble size, superficial gas velocity and gas hold-up. Lastly the results of previous studies on the effect of rheology on hydrodynamics in mechanical flotation cells is presented and reviewed. The chapter then ends with the scope and objectives of this study.

2.1 Froth Flotation

2.1.1 Overview of Froth Flotation

Froth flotation is a separation process that is widely used in the mining industry to extract valuable minerals from ore. Originally patented in 1906, flotation has permitted the mining of low-grade and mineralogically complex ore bodies which would have been otherwise been regarded as uneconomic (Wills, 1997). In 1860, Haynes patented the use of selective clinging of particles at an oil-water interface (Pryor, 1965). In 1886, Carrie Everson patented some reagents after observing the response of galena during the laundering of textiles which had been in contact with the ore.

Due to the complex nature of mineral ores, valuable minerals are usually liberated from gangue minerals by grinding the ore to ultra-fine particle sizes. The flotation process uses the differences in physico-chemical surface properties of particles of

various minerals. The slurry is treated with reagents to modify the surface properties of the solid particles, rendering the mineral particles hydrophobic or hydrophilic. The hydrophobic particles are transported to the froth layer at the surface of the cell by means of air bubbles formed by introducing air into the pulp; the froth layer is removed and usually comprises the concentrate. The hydrophilic particles remain submerged in the pulp. The hydrophilic particles at the bottom of the cell are known as tailings, these are recycled or passed on to other cells for further treatment until a desired target mineral grade is achieved. This is called direct flotation; in reverse flotation the gangue is recovered at the top of the cell while the valuable minerals sink or remain in the cell. Figure 2.1 below (adopted from Van der Westhuizen, 2004) demonstrates the fundamentals of the flotation process.

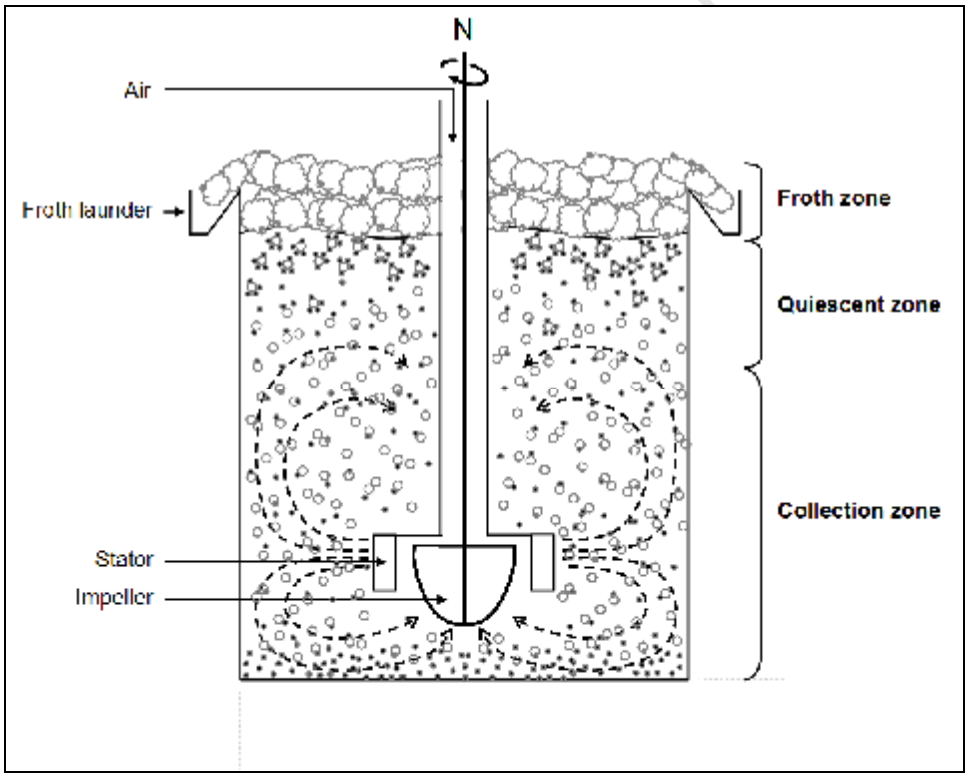

Figure 2.1 Schematic of a mechanical flotation cell showing different zones in cell (from Van der Westhuizen, 2004).

Reagents such as collectors, activators, frothers and depressants are used to treat the slurry and to activate the surface properties of the particles. The role of these reagents is further discussed in Section 2.1.2.1.

The efficiency of the flotation process depends significantly on the prevailing chemical and hydrodynamic conditions in the cell. Authors such as Gorain *et al.* (1995a, 1995b, 1997), Grau and Heiskanen (2003, 2005) and Quinn *et al.* (2007) have investigated both the effect of different frothers and varying operating conditions on the flotation process by evaluating gas dispersion properties (bubble size, gas hold-up and superficial gas velocity) in flotation cells. These studies demonstrate that there are various factors to be considered to achieve a desired recovery and grade in flotation; hence flotation is found to be a rather complex process.

In particular, there are problems associated with the flotation of very fine particles (e.g entrainment, high froth stability). Studies have shown that the recovery of very fine particles by flotation can be much lower than for the same material in larger sizes. King (1982) reviewed the literature on the flotation of fine particles by reviewing studies of various authors (Woodburn *et al.*, 1971; King *et al.*, 1974; Trahar and Warren, 1976). It is believed however that the effect of particle size is dominated by the physical processes of collision, adhesion and detachment; these processes are described in Sections 2.1.2.2.

2.1.2 The Flotation Process

2.1.2.1 Conditioning

In order for particles to float they initially have to be suspended into an agitated slurry through the action of an impeller. Reagents such as collectors, activators, depressants and frothers are added to the cell. The various reagents perform different roles in the flotation process. Collectors are used to render the surface of valuable minerals hydrophobic in the slurry. Activators selectively activate certain valuable minerals within the slurry and allow for the collector to render them hydrophobic. Depressants are used to increase the selectivity of flotation by suppressing certain minerals in the slurry, thus rendering the minerals hydrophilic. Frothers are added to reduce the gas-liquid surface tension, reduce bubble coalescence during gas dispersion and to stabilise the froth layer at the surface of the cell.

2.1.2.2 Collection

Once the conditioning stage has been completed, particle collection follows; the extent to which it occurs depends on the hydrophobicity of the particles as well as the chemical conditions that render the bubbles sufficiently stable. Air is introduced into the flotation cell and is sheared into small bubbles by the impeller. The efficiency of particle collection has to be investigated in a flotation cell. This is done by expressing the probability of collection as a function of three micro processes occurring in the cell, viz. collision, attachment and detachment; these processes are discussed in this order. The probability of particle collection ($P_{collect}$) can be expressed as the product of the probabilities of particle-bubble collision, (P_c), attachment, (P_a) and detachment, (P_d) as shown in equation 2.1.

$$P_{collect} = P_c P_a (1 - P_d) \quad 2.1$$

Collision

Before a particle can be recovered by flotation it must collide with a bubble and adhere. The mechanism of collision in the highly turbulent conditions usually encountered in mechanical flotation cells becomes rather complex. The particle must have sufficient momentum to resist the tendency to follow the streamlines of the water that flows around the bubble. This is typical of very fine particles which tend to skirt around the bubble without making any direct contact. The probability of collision can be expressed as:

$$P_c \propto \frac{d_p^{\,m}}{d_b^{\,n}} \quad 2.2$$

where m and n vary between 1-2 and 2-3, respectively

Attachment

After the collision of the particle with the bubble, successful attachment is achieved only if the particle penetrates the skin of the bubble within a certain time. The bubble surface deforms and the water film between the particle and the bubble thins until it finally ruptures. The particle will attach to the bubble only if the induction time is less

than the time taken by the particle to slip over the surface and into the water. The probability of attachment is defined as the fraction of particles that remain attached to bubbles after collision has occurred, and is commonly modelled in terms of contact and induction times. The contact time is the time that a particle and a bubble are in contact for after colliding, while the induction time is the time taken for the disjoining film to drain, rupture and form a stable contact angle.

Detachment

The particle-bubble aggregate that is formed during attachment has to be sufficiently buoyant to rise through the pulp and must be sufficiently stable to endure any disturbances in the pulp. The turbulent and gravitational forces acting on the particle-bubble aggregate however have been known to cause detachment of the particle from the bubble. A portion of the particles that successfully formed aggregates with bubbles detach while the bubble rises to the surface. This is an unwanted micro-process, controlled by both the stability of particle-bubble aggregates and external shear stresses in the flotation cell. Woodburn *et al.* (1971) developed a relationship estimating the probability of detachment as a function of particle size (r). The authors observed the tension developed in the skin of the bubble as it accelerates in a turbulent field. As the bubble accelerates, the particle lags behind due to its inertia thus causing a strain of the bubble skin. The authors went on to deduce that the maximum strain in the bubble skin is proportional to the particle size to the power of 1.5.

The successful completion of the collection stage produces stable and buoyant particle-bubble aggregates containing the floatable particles, in conditions allowing these aggregates to rise towards the froth phase, and other particles to remain in the slurry phase in the flotation cell.

2.1.2.3 Separation

After the particle collection stage particle-bubble aggregates rise upwards through the froth layer and are subsequently removed from the top of the flotation cell as

concentrate. At the slurry-froth interface, the particle-bubble aggregates need to separate from the hydrophilic gangue minerals, which should remain in the slurry. However, due to bubble crowding at the slurry-froth interface considerable *entrainment* of slurry into the froth occurs. Froth *stability* is very important as liquid film drainage and rupture of bubbles with age causes some of the particles to return to the pulp from the froth (dropback). The rate of froth *flow* is dependent on a number of factors, most notably aeration rate, pulp chemistry and cell geometry. The slurry stream containing the gangue minerals is normally removed lower down in the cell. An unwanted sub process related to slurry discharge is called *short-circuiting* and occurs when particles from the feed stream bypass the collection stage and discharge directly into the tailings stream. The successful completion of the separation phase produces a froth loaded with the floatable particles and very few unattached particles, as well as a slurry discharge stream containing only particles that were unsuccessfully contacted with air bubbles (Van der Westhuizen, 2004).

2.2 Flotation Cells

Flotation cells can be classified into three different categories viz. flotation columns, novel cells and mechanical flotation cells. These cells are discussed in succession in the following sub-sections.

2.2.1 Column Flotation Cells

The flotation column is the most widely used of the pneumatic flotation cells and derives its name from the geometric shape of the vessel. Its concept has been around for nearly 40 years but it attracted attention with the copper mining problems of the early 1980s (Fuerstenau and Han, 2003). The ore is fed into the column near the top of the cell usually at a height that is about one-third from the top. Air bubbles are generated at the bottom of the column by a sparger; the floatable particles flow to the top and the non-floatable material is removed at the bottom. Industrial flotation columns vary in height ranging from 9 to 14 m and can have a diameter of up to 3.5 m. The cross-section of the tank can either be round, square or rectangular depending

on the specific application. The column cell has a smaller surface area than a conventional cell of equivalent volumetric capacity. The small area is favourable for promoting froth stability and allowing very deep froth beds to be formed.

The most important feature of the column cell is the froth washing system. This system provides an additional means for removing unwanted impurities from the flotation froth. Wash water is added at the top of the column and filters through the froth zone displacing process water and entrained particles trapped between bubbles. In addition, the froth wash water serves to stabilize the froth by separating bubbles into a 'packed bed' of spherical and therefore very strong bubbles.

2.2.2 Novel Flotation Cells

A number of novel flotation cells have been developed in an attempt to improve the various sub processes of flotation (Deglon, 2004). The driving forces for the development of these cells are the improvement of gas dispersion through micro-bubble generation and the improvement of particle-bubble contacting through both high levels of turbulence and decoupling the processes of solid suspension and gas dispersion. These improvements contribute to a better understanding of flotation fundamentals which has led to an appreciation of the micro-environment necessary for optimising flotation performance. The Jameson cell is an example of a novel flotation cell; it was invented in 1986 and since then 225 Jameson cells have been installed in a variety of applications. Wills (2006) described the operation of the cell as follows. Contact between the feed and the air stream is made in a mixing device at the top of the vertical downcomer. The air-liquid mixture flows downwards to discharge into a shallow pool of pulp in the bottom of a short cylindrical column. The bubbles disengage and rise to the top of the column to overflow into a concentrate launder; the tails are discharged from the bottom of the cell. This type of cell is very effective for rapid collection of particles in the downcomer where primary contact of pulp and air bubbles takes place; this cell is also known for its typical shorter residence times (Çinar *et al*., 2007).

2.2.3 Mechanical Flotation Cells

This is the most widely used class of flotation cells and is characterised by a mechanically driven impeller, which is responsible for the processes of solids suspension, gas dispersion and particle-bubble contact. The design of impeller and dispersion baffles varies significantly from one machine to the other. The characteristic feature of mechanical flotation cells is the high degree of turbulence required in the pulp. The high level of agitation required for efficient particle suspension and gas dispersion in these cells makes them better suited for flotation of fine and intermediate sized particles (Deglon, 2004). For coarser particles vigorous agitation causes strong detachment which is an unwanted effect as it lowers the efficiency of flotation. A highly turbulent region is required to provide particle-bubble contact, but also a quiescent zone adjacent to the froth layer in which the bubbles carrying minerals can rise without turbulent disruption of particles adhering to the bubble surface (Gorain ***et al***., 2007).

Mechanical flotation cells can be classified by the method of air supply to the flotation cell. In self-aerated cells the rotation of the impeller causes a pressure drop which is the driving force for air to flow into the cell from ambient pressure. Typical self-aerated cells are the Denver and the Wemco cells; Figure 2.2 shows a typical Wemco cell.

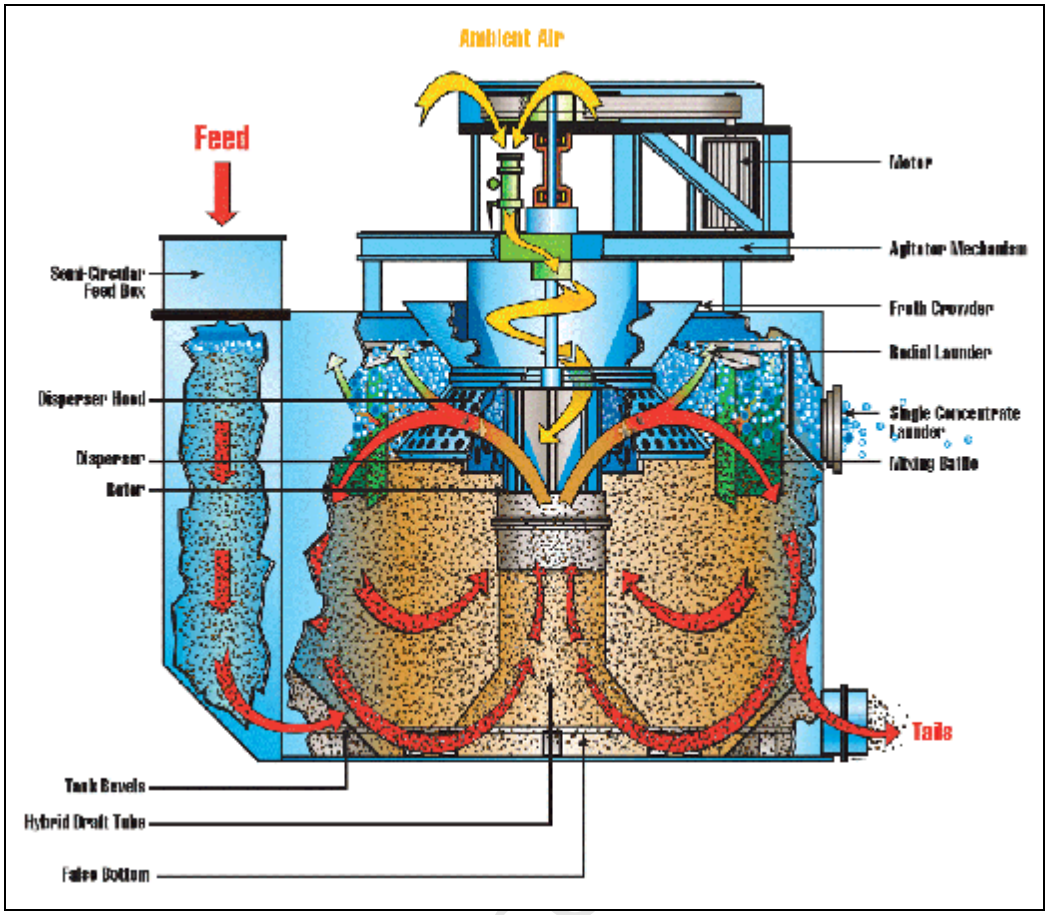

Figure 2.2 Wemco SmartCell (from Van Der Westhuizen, 2004).

In forced-aerated cells, additional pressure is supplied to the air fed into the cell by compressors or air blowers. The impeller is located close to the cell bottom with a deeper impeller submergence. This is typical of the Outotec cell shown in Figure 2.3.

Figure 2.3 Outotec Cell (from Van der Westhuizen, 2004).

2.3 Hydrodynamics in Mechanical Flotation Cells

Hydrodynamics involves the study of fluid motion. In mechanical flotation cells this motion is caused by the rotation of the impeller which establishes a flow pattern. Hydrodynamics is responsible for the sub-processes of solids suspension, gas dispersion and particle collection in the cell. The hydrodynamics in the cell is influenced by vessel and slurry characteristics such as energy dissipation, impeller type and speed, aeration conditions, frother dosage, solids concentration and slurry rheology. These properties are responsible (directly or indirectly) for the generation of turbulence in the cell. Knowledge of hydrodynamics in mechanical flotation cells is important for understanding gas dispersion behaviour and solid suspension characteristics. It is also useful for the prediction of design parameters concerned with mixing, velocity profiles, turbulence and mass transfer coefficients (Egya-Mensah, 1998). The outcome of the flotation process depends on the hydrodynamics existing in the cell.

In mechanical flotation cells different flow patterns are generated by different types of impellers. These are divided into radial and axial impellers, depending on the type of flow patterns they generate. Radial impellers produce a radial flow pattern with high mean velocities existing around the impeller. The typical flow pattern of radial flow impellers is shown in Figure 2.4. Fluctuations in mean velocities exist at distances away from the impeller but decrease as the cell wall is approached (Mujumdar *et al.*, 1970 from Egya-Mensah, 1998).

Radial flow impellers are most commonly used in mechanical flotation cells as they are believed to be suitable for effective solid suspension and gas dispersion throughout the cell. Radial impellers however are known to consume a high degree of power as compared to other impellers. The Rushton turbine is typical of radial impellers. Axial flow impellers generate axial flow with the radial flow only proportional to the projected blade area. These types of impellers are known to generate more flow than the radial flow impellers at the same power input.

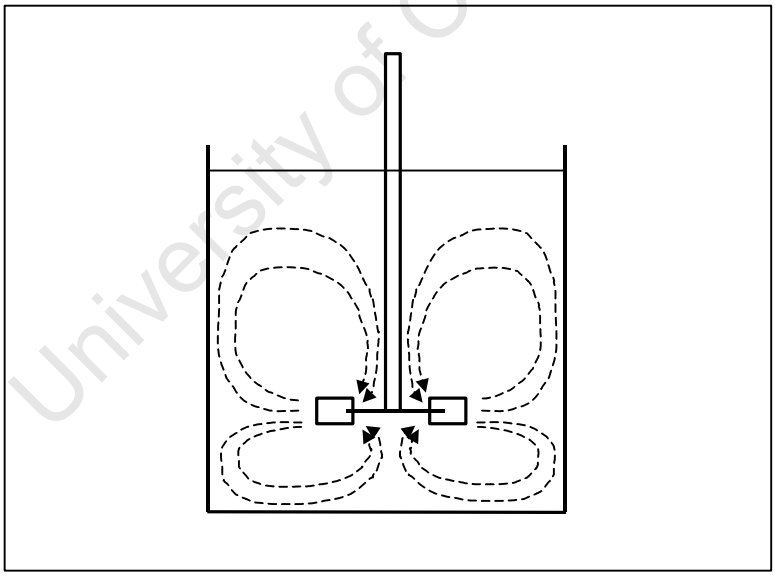

Figure 2.4 Schematic of the flow patterns generated by radial impellers in mechanical flotation cells (from Lewis, 2003).

The properties affecting the hydrodynamics are reviewed under the sub headings of power input, gas dispersion, and the effect of rheology on the hydrodynamics in mechanical flotation cells.

2.4 Rheology

Rheology is defined as the science of deformation and flow of matter. The rheological properties of fluids are commonly represented in the form of flow curves where the shear stress is plotted against the shear rate; these flow curves (also known as rheograms) are shown in Figure 2.5. The flow behaviour of fluids can be characterised as either Newtonian or non-Newtonian. Typical fluids exhibiting Newtonian behaviour are water, oil, glycerol and sugar solutions where the viscosity (depicted by the slope of the line) is constant with varying shear rate. Paints, emulsions, paper pulp, polymeric and mineral slurries are some examples of non-Newtonian fluids. The majority of mineral suspensions are known to exhibit pseudo-plastic behaviour, with or without a yield stress, followed by Bingham plastic behaviour (Tangsathitkulchai and Austin, 1989). Two properties, the viscosity and the yield stress, are commonly used to describe the rheological behaviour of fluids.

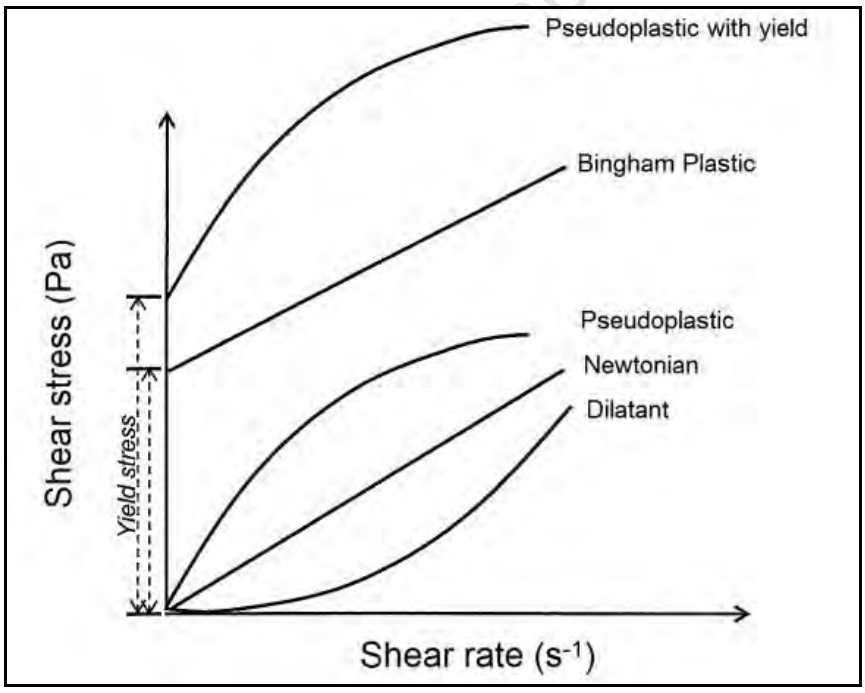

Figure 2.5 Flow curves for Newtonian and non-Newtonian slurries (Vieira and Peres, 2012).

The viscosity of a fluid is defined as the resistance to flow by the fluid and is represented by the ratio of shear stress to shear rate ($\mu = \tau/\gamma$). Newtonian fluids have a

constant viscosity whereas, in non-Newtonian fluids, the viscosity varies as a function of the shear rate and is thus termed the 'apparent' viscosity.

The yield stress of a fluid is the minimum force required for the fluid to flow and is a characteristic property of Bingham plastic fluids and some pseudo-plastic fluids. The yield stress is used as a measure of flocculation in a suspension where the overall attractive forces between the suspended particles are a maximum (Barnes, 1999). Nguyen and Boger (1985) developed the vane method in order to accurately measure the yield stress at shear rates less than 1 s^{-1}. This method however is applicable only to concentrated slurry solutions at ultra fine particle sizes.

In recent years rheometers have been developed and widely used to measure the shear stress at a given shear rate range. Shear stress and shear rate data can then be fitted with a mathematical model and the yield stress and the apparent viscosity can be approximated. The most encountered rheological models used for mineral slurries are the Bingham, Casson, power law and Herschel-Bulkley models. The Bingham model is a simple two parameter equation whose coefficient (apparent viscosity) has physical significance (equation 2.3). This model has been widely used by authors such as Muster and Prestidge (1995) and Gao and Forssberg (1993).

$$t = t_B + \left(h_B \cdot g\right) \qquad 2.3$$

The rheological behaviour of mineral slurries is indicative of the level of inter-particle interaction in the slurry (He *et al.*, 2006; Muster and Prestidge, 1995). A number of factors influence the rheological behaviour of slurries: these include solid content, solid type, particle shape, and particle size, the surface chemistry of the particles and the mineralogy of the ore (solid type). These properties affect the viscosity of the slurry but it is also known that viscosity is not the only rheological property affecting mineral process performance. The rheological nature of the slurry (Newtonian, dilatant, pseudo plastic and the presence and value of a yield stress) also has a significant influence on the process (Shi and Napier-Munn, 1996). The factors that significantly affect slurry rheology are reviewed in detail in Section 2.7.1.

2.5 Gas Dispersion

Gas dispersion is defined as how well the air entering a flotation cell is dispersed throughout the volume of the cell, and is heavily dependent on the air flowrate and impeller speed (Schwarz and Alexander, 2006). It defines the efficiency of the process once the chemistry has been established (Gomez and Finch, 2002). Rennie and Valentin (1968) and Tatterson (1991) described the phenomenon of gas dispersion. Gas is sparged into the low pressure regions behind the impeller; the gas accumulates to form gas cavities where the gas flows and is then dispersed into small bubbles. The bubbles are then spread throughout the cell by means of the flow pattern generated by the impeller. A schematic of this gas dispersion action is shown in Figure 2.6.

Different types of cavities form depending on the impeller geometry, aeration rate, impeller speed and the gas recirculation rate. Rennie and Valentin (1968) were amongst the first to publish photographs illustrating the presence of trailing vortices forming behind the impeller blades.

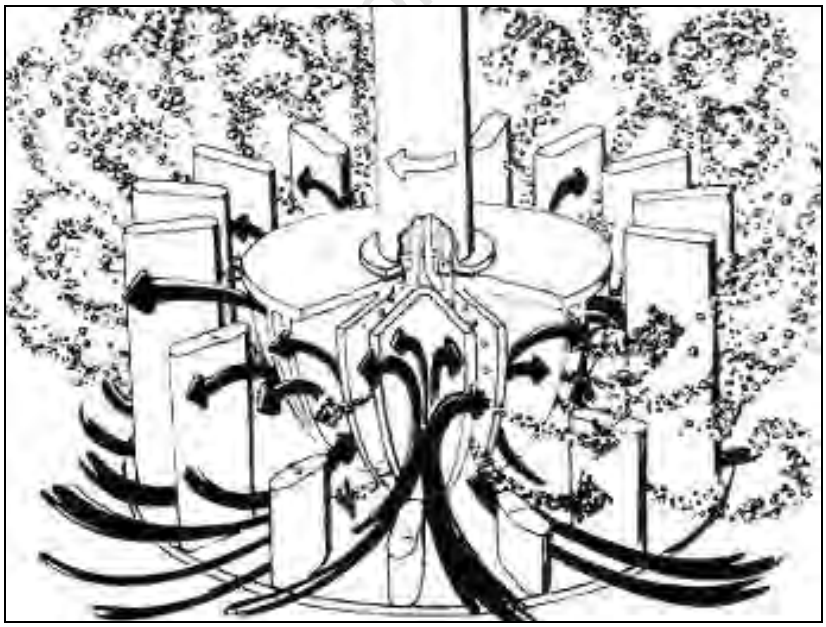

Figure 2.6 Schematic of the gas dispersion action in a mechanical flotation cell (Kelly and Spottiswood, 1982).

The distribution of air bubbles is affected by the rotation speed of the impeller and the behaviour of the solids in the cell. More specifically, the viscosity and the yield stress

of the slurry determine how air bubbles are distributed in the cell. Nienow and Ulbrecht (1985) presented a general review of the studies of gas dispersion in highly viscous and non-Newtonian liquids. They observed that gas dispersion in such liquids occurs at lower impeller Reynold's numbers because of high viscosities. A detailed review of these effects is discussed in Section 2.7.2.

Properties that describe gas dispersion in the cell include bubble size (d_b), gas hold-up (ε), superficial gas velocity (J_g) and a derived quantity, the bubble surface area flux (S_b). Gas dispersion has been regarded as the key hydrodynamic characteristic in flotation (Finch *et al.*, 2000). The bubble surface area flux has been considered a parameter of prime interest as it is linked to the flotation rate constant (Gorain *et al.*, 1997; Hernandez *et al.*, 2003). It has also been proved by Gorain *et al.* (1997) that it is possible to scale up from a 60 dm^3 cell to a 100 dm^3 cell on the basis of the bubble surface area flux. The following sub-sections review the literature of the properties of gas dispersion under the headings: bubble size, gas hold-up and superficial gas velocity.

2.5.1 Bubble Size

For flotation to occur, air has to be introduced into the collection zone of the cell in the form of bubbles, which form the carriers for hydrophobic particles. The dispersion of bubbles through-out the cell is important for particle-bubble interaction. Bubble size distribution occurs as a result of three processes, viz. bubble formation, bubble break-up and coalescence. The outcome of these processes determines the net bubble size.

The factors affecting bubble size in a flotation cell include air flowrate, power input, impeller speed, pulp density, viscosity and particle size. Chemical factors such as frother type and concentration, pH, ionic strength and temperature also affect bubble size significantly. The effects of air flowrate and impeller speed are reviewed in this section while the effect of solids content and viscosity are reviewed in Section 2.7.1 as these are the parameters that affect slurry rheology which is the main focus of this thesis.

Gorain *et al*. (1995a) performed experiments in a 2.8 m^3 flotation cell that was fitted in turn with four different impellers. They found that an increase in aeration rate results in an increase in bubble size. Grau and Heiskanen (2005) observed similar results; they observed that the influence of the air flow rate on bubble size is inherently related to the presence of air cavities behind the blades of the rotor. These air cavities enlarge with increasing air flow rate causing the power requirement to decrease; thus the shear forces responsible for shearing the cavities into small bubbles are reduced. The presence of air cavities and their size was found to affect the power input in the cell.

An increase in the impeller speed at constant aeration rate results in a decrease in the bubble size. Gorain *et al*. (1995a) demonstrated this effect. At low impeller speed, the shear forces generated by the impeller blades moving through the slurry are weak, resulting in the production of large bubble sizes. The shearing effect increases as the impeller speed is increased with the result that cavities are sheared into smaller bubbles. Grau and Heiskanen (2005) also observed this effect.

A review of industrial flotation data reported in literature showed that the typical range of mean bubble size observed in mechanical flotation cells is between 1 and 2 mm (Burgess, 1997; Vera *et al*., 1999; Yianatos *et al*., 1999; Power and Franzidis, 2000; Deglon *et al*., 2000; Chen *et al*., 2001; Yianatos *et al*., 2001; Schwarz and Alexander, 2006; Finch *et al*., 2006; Nesset *et al*., 2006).

2.5.1.1 Bubble Formation

Air is drawn into the low-pressure regions which form behind the impeller blades due to rotation, to form gas cavities. At a particular impeller speed, air from these gas cavities is entrained by the fluid vortices flowing around the impeller blades into the impeller discharge stream. A thin film, which ultimately breaks into bubbles, surrounds these trailing vortices; hence bubbles are formed and are then dispersed throughout the cell by the pumping action of the impeller (Tatterson, 1991 in Sawyerr *et al*., 1998). In the bulk region of the cell, bubble motion is controlled by the surrounding fluid circulation and by the bubbles' intrinsic buoyancy. Bubbles in this

region may collide and coalesce, then recirculate to the impeller region or rise out of the cell.

The level of turbulence dictates the size range of eddies in the inertial sub-range (Deglon *et al.*, 1993). These eddies determine the size of bubbles that form around the impeller region. The level of turbulence in the cell is highly dependent on the prevailing conditions as well as the rheological characteristics of the slurry. A combination of all these factors determines how effective gas dispersion will be in the cell. In a highly viscous slurry it has been found that the prevailing drag forces hinder the dispersion of bubbles throughout the cell. The resulting bubble sizes and distribution are dictated by all the events taking place in the cell, in particular the relative rates of bubble breakage and bubble coalescence in the cell (Sawyerr *et al.*, 1998).

2.5.1.2 Bubble Break-up

Flotation in a dynamic system is rather complex; it is difficult to independently characterise and model bubble break-up and coalescence in the cell. Thus, many authors consider either one of the processes by repressing one process so the other can be studied. In an instance where bubble break-up is studied, the fluid system must be non-coalescing, and therefore reagents such as frothers are added.

Machon *et al.* (1997) reviewed Calderbank's (1958) method to characterise the bubble break up process. Calderbank (1958) assumed that the bubble size in an aerated stirred vessel is controlled by breakage and applied the concept of a critical Weber number, *We*, to estimate the maximum stable bubble size. A balance between inertial forces and the surface tension forces controls bubble break-up. The ratio of the inertial forces to the surface tension is given by the Weber number (cf. equation 2.4), where α is a coefficient which can vary from 1 to 4 (Balerin *et al.*, 2006).

$$We = \frac{\eta \cdot \gamma \cdot d_{32}}{\alpha \cdot \sigma} \qquad 2.4$$

A critical Weber number exists where, if the ratio of inertial forces to surface tension exceeds a certain critical value, the bubble will break. The continuous phase viscosity (η) and the Weber number are directly proportional. The Weber number can also be used to determine the maximum bubble size that exists in a dispersion process. Weber numbers from 0.3 to 0.5 have been reported in literature for foaming applications (Kroezen & Groot Wassink, 1987; Djelveh & Gros, 1995; Djelveh *et al.*, 1999; De Lorgeril *et al.*, 2000; Thakur *et al.*, 2003). In order to use the Weber number to predict the maximum bubble size in this particular study, a fluid indicating a similar viscous nature as the slurry could be used.

For a given level of turbulence there is a maximum stable bubble size below which bubbles cannot be broken up by eddies. The maximum stable bubble size can be determined using an equation based on the Kolmogoroff concept of isotropic turbulence (equation 2.5) where the disruptive forces are expressed as a function of the local specific energy dissipation rate.

$$d_{max} = C\left(\frac{s^{\frac{3}{5}}}{e^{\frac{2}{5}} r^{\frac{3}{5}}}\right) \qquad 2.5$$

From the equation above it can be seen that an increase in energy dissipation results in a decrease in the maximum stable bubble diameter (d_{max}). An increase in solids content increases the viscosity of the slurry which further increases the damping effect on turbulence, thus the presence of solids causes energy dissipation to be damped (Nesse *et al.*, 1979), resulting in an increase in the maximum bubble diameter. In most studies where the effect of high solids content is significant the viscosity of the slurry is thought of as the key parameter used to characterise the rheological behaviour of the slurry. However, rheology studies have reported that viscosity is one of two properties that affect the behaviour of the slurry in the cell. The yield stress is an equally important property however no studies have been reported on the case where the yield stress governs the behaviour of the slurry in a flotation cell.

2.5.1.3 Bubble Coalescence

Bubble coalescence occurs as a consequence of three steps. Initially bubbles collide, trapping a small amount of liquid between them. The liquid drains until the film separating the bubbles thins and ruptures which results in coalescence; Figure 2.7 shows two mechanisms of coalescence. The rate at which bubbles come together depends on the fluid turbulence as well as the time they spend in close proximity. The probability of collision and coalescence has to be determined in order to determine whether coalescence will occur. Bubble coalescence can also occur when bubbles are drawn into the wakes of other bubbles (Preen, 1961). This type of coalescence however is difficult to model because it requires information concerning bubble sizes, wakes, frequency, and location of the surrounding bubbles (Tatterson, 1991).

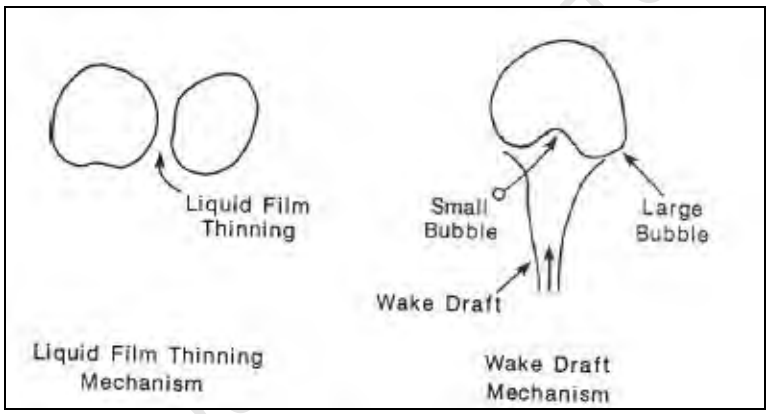

Figure 2.7 Bubble coalescence mechanisms (Preen, 1961 in Tatterson, 1991).

Bubbles formed by coalescence may not be stable enough to carry particles to the froth surface thus resulting in reduced recoveries and grades. It is desirable to keep the bubble size sufficiently small and stable enough to transport particles to the froth surface. This can be achieved by the addition of a frother at a concentration well above the critical coalescence concentration (CCC). The critical coalescence concentration (CCC) refers to the lowest frother concentration at which bubble coalescence does not occur. For a given frother, the bubble diameter decreases as frother concentration increases until a critical concentration is reached, above which the bubble diameter remains constant (Newell and Grano, 2007). The presence of small amounts of surface active reagents can lead to significant reductions in mean bubble size (Aston *et al.*, 1983; Tucker *et al.*, 1994; Sweet *et al.*, 1997; Aldrich and

Feng, 2000; Cho and Laskowski., 2002). The reduction occurs at concentrations at which there is very little change in static surface tension, and is attributed to the ability of the frother to prevent bubble coalescence (Cho and Laskowski, 2002).

Grau and Heiskanen (2005) investigated the effect of frothers on bubble size using three commercial frothers (DF-200, DF-1012 and DF-250). The authors found that DF-200 was the most effective frother with respect to bubble size reduction with the least effective frother being DF-1012. They also concluded that frothers do not only hinder coalescence but also affect bubble break-up under turbulent conditions. At concentrations exceeding CCC the bubble becomes stable enough to resist coalescence and to a certain extent oppose disruptive forces (Grau, 2006).

Cho and Laskowski (2002) investigated the effect of different frothers on bubble size by varying their concentrations. They found that with increasing frother concentration the degree of bubble coalescence decreases. They also found that at a particular concentration, the critical coalescence concentration (CCC), the coalescence of bubbles is completely prevented and the bubble size levels off. At low frother concentrations (C < CCC) they found that the bubble sizes were much larger indicating that coalescence was a main mechanism for determining bubble size. At frother concentrations above the CCC the system can be defined as non-coalescing; the bubble size will no longer depend on coalescence but on the hydrodynamic conditions existing in the cell. The value of the CCC is different for each type of frother.

Parthasarathy and Ahmed (1994) found that in non-coalescing systems the bubble size distribution generated in the impeller region is preserved in the various regions in the cell. They also found that in coalescing systems, there will be spatial variations of bubble size distribution due to an increase in coalescence in the quiescent regions of the cell.

2.5.2 Superficial Gas Velocity

Superficial gas velocity (J_g) is a measure of the aeration ability of a cell and has a direct influence on flotation kinetics (Ahmed and Jameson, 1989). This is an important parameter as it influences the performance of the flotation process. Its measurement gives an indication of how the incoming air is dispersed throughout the cell (Gorain *et al*., 1996). Various measurement techniques have been developed to measure the local superficial gas velocity. Gorain *et al*. (1996), Burgess (1997), and Deglon *et al*. (2000) used a Jg probe, which captures gas into a graduated probe. Falutsu (1994) developed a method that allows for direct measurement of the gas velocity by establishing a correlation that depends on factors such as the cell geometry and the characteristics of the slurry.

Gomez and Finch (2002) developed a pressure difference technique; in this method rising air bubbles are collected from the pulp into a probe that is sealed at the top during sampling. The continuous entrance of bubbles into the probe causes the gas to accumulate thus increasing the pressure and the liquid-froth interface is pushed down the probe. The superficial gas velocity can then be determined in relation to the rate of change in pressure inside the probe. The above mentioned techniques are applicable to measure the local superficial gas velocity. The global superficial gas velocity can be calculated as the overall volumetric air flow rate divided by the cell cross-sectional area.

Different values of J_g can be measured at different locations in the cell. Differences in Jg at different locations give an indication of the gas dispersion characteristics in the cell (Schubert *et al*., 1982). The uniformity of the J_g values at the different locations indicates a good distribution of air in the cell. A wide variation in J_g values thus indicates poor gas dispersion. Too high a J_g can result in increased entrainment into the froth and reduce the stability of the slurry-froth interface.

Gorain *et al*. (1996) investigated the effects of air flowrate and impeller speed on flotation performance. Gorain *et al*. (1996) measured superficial gas velocity values at six different locations in the cell. The superficial gas velocity increased with air

flowrate but was not affected by impeller speed at a constant air flowrate. Superficial gas velocity typically varies between 1 and 2 cm/s (Deglon *et al*., 1999) in industrial flotation cells but may be lower in large tank cells.

2.5.3 Gas Hold-Up

Gas hold-up (ε_G) refers to the volume fraction of air within the flotation cell. This parameter is easily measured, and gives further insight into the conditions existing in the cell (Newell and Grano, 2006). The gas hold-up is defined by bubble size, gas and liquid flow rate, mixing patterns and physical properties of the pulp such as density and viscosity (Finch and Dobby, 1990). These factors ultimately influence the flotation performance. It is also an important parameter for the precise control of gas-liquid mass transfer where reactions take place in a highly consistent media with complex rheology (Vlaev *et al*., 2002). In flotation, where the rheology of slurries becomes more complex with increasing solids content (characterised by a yield stress or apparent viscosity) the gas hold-up is important in describing how bubbles are dispersed throughout the cell.

Various techniques have been developed to measure the local and the global gas hold-up in a flotation cell. These techniques include estimating the gas hold-up via pressure difference measurements where initially pressure manometers were installed to measure pressure signals. Authors such as Gorain *et al.* (1995b), Deglon *et al.* (2000) and Yianatos *et al.* (2001) have conducted tests using a dual piston cylinder which is operated using a vacuum or manually. Grau and Heiskanen (2003) used a device which works on a phase separation basis. These aforementioned techniques are applied for estimating local gas hold-up at various locations within the flotation cell. These different values of gas dispersion are compared to investigate the different effects of gas dispersion at each of these locations. An average value is calculated from the gas hold-up values at varying locations. This value can be considered to represent the global gas hold-up.

Gomez *et al.* (2003) developed a gas hold-up sensor that is continuous and could be automated for industrial flotation cells. The sensor consists of two flow through cells

in which conductivity is measured in the presence and absence of air. The cells can be flush mounted to the internal wall of the cell for optimum performance. Maxwell's equation is then applied to compute the gas hold-up from the conductivities. As mentioned before, this technique has been applicable mainly to industrial flotation cells; it would require proper scaling down to fit a lab/pilot scale cell.

Gorain *et al*. (1995b) have investigated the effects of air flowrate and impeller speed on gas hold-up. They found that an increase in air flowrate resulted in an increase in gas hold-up in the cell. The high gas hold-up was attributed to the large number of small bubbles produced as a result of increased superficial gas velocity. Increasing the impeller speed at constant air flowrate increased the gas hold-up. This result was explained by the fact that at higher impeller speeds, the smaller bubbles produced have low rise velocities, resulting in longer residence time in the cell. Finch *et al*. (2000) and Grau and Heiskanen (2005) observed similar results.

In conventional flotation cells, typical gas hold-up values range from 3% to 20%. It has been found that increasing gas hold-up values to a certain point results in improved flotation kinetics due to a greater number of bubbles per unit volume (Ahmed and Johnson, 1989). However high gas hold-up values could lead to reduced flotation performance due to increased gas residence times, resulting in the detachment of particles from bubbles (Deglon *et al*., 1999). According to Deglon *et al*. (1999) the effect would have a more prominent effect in large flotation cells as the gas residence time is proportional to the cell height. The effects of impeller speed, air flow rate and solids concentration (w.r.t. viscosity and yield stress) on gas hold-up is reviewed in more detail in Section 2.7.3.3 as this is the main focus of this thesis.

2.6 Power Input

2.6.1 Power Draw

The power draw is the energy per time that is transferred from the impeller to the fluid. This is one of the most fundamental measurements used mainly for scale-up purposes; it is usually converted and translated into the specific power input (or power

intensity). The power draw is an integral parameter that influences metallurgical performance in the cell as it is dependent on aeration rate, impeller speed, impeller geometry and fluid properties and rheology. The power draw increases with an increase in the impeller speed and solids density. Introducing gas decreases the power draw; this is because of the streamlining of the impeller blade by the gas cavities which causes a reduction in the pressure drag of the blade. The pressure drop from the front of the blade to the back decreases.

One method of determining the actual power draw applied to the slurry in stirred tanks or flotation cells is to first measure the power draw/torque with the impeller running free; the power draw/torque in the presence of slurry and air is then measured. The difference between these power measurements and considering the frictional losses (e.g. applied by bearings) gives the 'load power', the actual power supplied to suspend solids in the cell (Brown *et al.*, 2004).

2.6.2 Power Intensity

The power input per cell volume (P/V) also known as the power intensity/specific power input is considered to be an important parameter as it influences the metallurgical performance in flotation cells. High power intensities are thought to improve the performance of flotation through improved aeration and particle-bubble contact (Schubert and Bischofberger, 1978).

As mentioned in Section 2.6.1, the power input is influenced by the impeller speed, impeller geometry and fluid properties. By rotating the impeller, energy (kinetic) is imparted to the fluid which dissipates through viscous dissipation (Kumar, 2010). Viscous dissipation refers to the energy dissipation due to viscous effects of a fluid. The energy dissipation thus can be characterised as a function of the viscosity of the fluid. The specific energy dissipation rate in a stirred tank is known to depend on the shear rate and shear stress (Sànchez Pérez *et al.*, 2006). In mechanical flotation cells the impeller rotates at high speeds and creates turbulent conditions in the cell. The rotation of the impeller is associated with a high shear stress around the impeller.

The shearing effect is reduced with an increase in distance away from the impeller. This affects the quality of gas dispersion in the cell. There are no relationships that have been developed to relate the power intensity to the parameters of rheology such as shear rate and shear stress for mechanical flotation cells. However, a few relationships have been developed for stirred tanks in the general chemical engineering literature. As the mixing effect in stirred tanks and mechanical flotation cells is fairly similar (depending on the type of impeller used and its clearance) these relationships may be applicable in attempting to relate power intensity to the rheological behaviour of the slurry. Such a relationship was developed by Sánchez Pérez ***et al***. (2006) as shown in equations 2.7 to 2.11.

The power intensity in an agitated vessel is related to the shear rate and shear stress as shown in Equation 2.7. It is known that in Newtonian fluids, the viscosity is the ratio of shear stress to shear rate (c.f. equation 2.8), for non-Newtonian fluids however the viscosity is a function of shear rate, equation 2.9 shows the power law model which relates the shear stress to shear rate for a non-Newtonian fluid. Equation 2.9 was incorporated into the Newtonian equation (equation 2.8) to determine the 'apparent' viscosity (equation 2.10), a property of a non-Newtonian fluid.

$$\left(\frac{P}{V}\right) = t \cdot g \qquad 2.7$$

$$m_a = \frac{t}{g} \qquad 2.8$$

$$t = Kg^{n} \qquad 2.9$$

$$m_a = \frac{t}{g} = Kg^{n-1} \qquad 2.10$$

Substituting equation 2.9 into 2.7 and re-arranging, the impeller shear rate can be determined by equation 2.11. K and *n* values obtained from rheology data can be used to determine the impeller shear rate. Once the shear rate is known, the power law

model can be used again to determine the corresponding impeller shear stress. The above equations help in calculating the power intensity present around the impeller as a function of slurry rheology. This further helps in understanding the hydrodynamics existing in the flotation cell.

$$g = \left(\frac{1}{K} \cdot \frac{P}{V} \right)^{\frac{1}{(n+1)}} \qquad 2.11$$

2.7 Effect of Rheology on Hydrodynamics in Mechanical Flotation Cells

Sections 2.3 to 2.6 have given a general overview of hydrodynamics in mechanical flotation cells, rheology, and gas dispersion in mechanical flotation cells. This section focuses on non-Newtonian rheology and how it affects the hydrodynamics and gas dispersion which form the central focus of this thesis. First the effects of different properties e.g. solids content, mineralogy are presented in Section 2.7.1, followed by the effect of rheology on the hydrodynamics in Section 2.7.2. Lastly the effect of rheology on gas dispersion is presented in Section 2.7.3.

2.7.1 Rheology

The literature on rheology pertaining to mineral slurries was introduced in Section 2.4. As mentioned, rheology is strongly influenced by solids concentration, particle size, the chemical nature of the slurry as well as the solid type (mineralogy). These effects are outlined in the following sub-sections.

2.7.1.1 Effect of Solid Content

He *et al*. (2004) investigated the effect of solids concentration on alumina A16 and zirconia Unitec suspensions and observed that the yield stress exponentially increases with increasing solids concentration (see Figure 2.8).

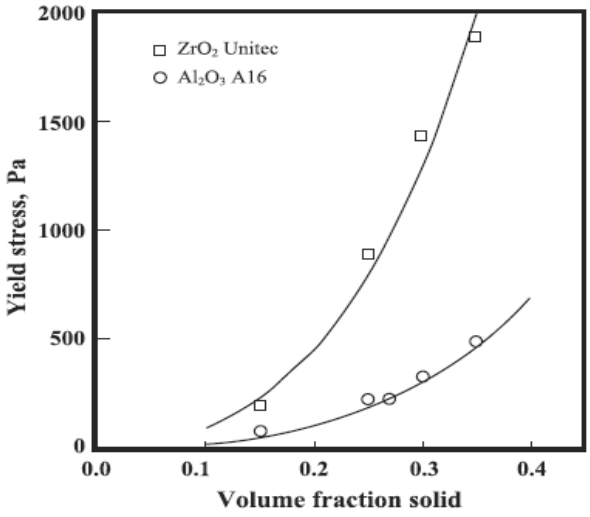

Figure 2.8 Exponential increase of the yield stress as a function of solids concentration (He *et al*., 2004)

He *et al*. (2006) studied the effect of varying solids content on limestone slurries and observed that the rheological behaviour transforms from a weakly dilatant characteristic (shear-thickening) to an evidently pseudo-plastic (shear-thinning) one with a yield stress when the solids concentration is increased from 35.71 vol% (60 wt%) to 57.49 vol% (78.5 wt%). They found that in a dilute slurry the inter-particle distance is so large that attractive van der Waals forces are non-existent allowing the particles to move freely as individuals. As the solids concentration increases the inter-particle distance between particles becomes smaller thus increasing the probability of collisions between particles resulting in more particles attracting each other.

In a study done for a mill slurry (Tangsathitkulchai, 2003) it was shown that for a typical ore three distinct regimes of rheological behaviour can be identified in relation to change in slurry concentration range. In a low concentration regime (20 vol% solids) the slurry exhibits almost no yield stress values and the rheological character resembles that of Newtonian fluids. Intermediate concentrations (30 – 45 vol% solids) possess some yield stresses and a rheological character of pseudo-plastic followed by Bingham plastic behaviour. A high concentration regime (54 – 65 vol% solids) is typified by substantial yield stresses and a true Bingham plastic behaviour.

Although deviation from Newtonian fluid behaviour occurred at high solids concentrations for the particular ore that they tested, this is indicative of the fact that different ores behave differently at the same solids concentration.

2.7.1.2 Effect of Particle Size

The inter-particle forces that arise from the solid-liquid solution interfacial chemistry increasingly dominate the interaction between neighbouring particles as the particle size of the slurry decreases. These forces in turn are responsible for the observed rheological properties of slurries (Huynh *et al.*, 2000).

He *et al.* (2006) investigated the effect of particle size and distribution on rheology using limestone materials. Three particle sizes (< 100 µm, < 74 µm and < 40 µm) were investigated. It was found that the slurries exhibit pseudo plastic flow with an evident yield stress in a lower shear rate range followed by a transition to an approximate Bingham plastic flow (with a higher extrapolated yield stress) in a higher shear rate range. The yield stress and apparent viscosity were found to increase with decreasing particle size and distribution. The extrapolated yield stress was found to increase exponentially with size distribution. Similar observations were made by Yang *et al.* (2001) for titanium oxide, Tangsathitkulchai and Austin (1989) for coal and for quartz slurries.

Yue and Klein (2004) investigated the influence of rheology on the performance of horizontal stirred mills using quartz material. They found that at 30% solids the influence of particle fineness on slurry rheology was negligible. As the solids content increased to 35% the yield stress variation became evident but the influence from particle fineness on yield stress was still relatively small. Increasing the solids content to 40% resulted in a more significant change in the slurry yield stress. As the particles became smaller, the change became larger. Gao and Forssberg (1993) observed similar results. These authors also found that the yield stress is the dominant rheological parameter that contributes most to the behaviour of the slurry and not the apparent viscosity. It was thus concluded by the authors that the significance of slurry rheology becomes greater with decreasing particle size, which is likely due to a

greater influence of surface properties that affect aggregation/dispersion and thereby the yield stress.

It has been shown that a single slurry can exhibit many rheological natures, depending only on the concentration and the size distribution of the solids (Shi and Napier-Munn, 1996). The rheological behaviour of mineral slurries has a significant influence on their processing performance and hence a slight change in any of these slurry properties could have a significant impact on the process. Many materials of commercial and technological importance in the minerals industry are handled in the form of highly concentrated suspensions and often with a fine particle size distribution.

2.7.1.3 Effect of Surface Chemistry

The chemical nature of the slurry has a significant impact on the rheological behaviour of the slurry. Inter-particle forces which arise from the solid-solution interfacial chemistry increasingly dominate the interaction between neighbouring particles as the particle size of the slurry decreases (Huynh *et al*., 2000). Altering the chemical nature of the particle surfaces alters the inter-particle interactions resulting in reduced or enhanced values of yield stress and apparent viscosity.

The addition of a suitable dispersant is useful especially in wet ultra-fine grinding in order to decrease the slurry viscosity and to reduce or eliminate the slurry yield stress (He *et al*., 2006). Extensive studies on the electrochemistry and surface chemistry of different ores have been carried out (Muster and Prestidge, 1995; Huynh *et al*., 2000; He *et al*., 2006; Burdukova *et al*., 2007) in relation to their effect on viscosity and yield stress.

2.7.1.4 Effect of Mineralogy

The mineralogy of ores has received significant attention particularly in mineral processing. Poor performance in flotation (low grade and recovery) in some cases occurs as a result of inefficient liberation of minerals during the grinding stage as well

as through the recovery of undesired minerals. The minerals may be in composites (e.g. binary or ternary) with other minerals or they may be ground to fine sizes resulting in entrainment rather than true flotation. Pease *et al*. (2006) performed such a study where they investigated the effect of ultra-fines in flotation. The gangue minerals are usually present in low-grade ores and have been found to be difficult to process. Gangue minerals of prime importance in this study are categorized as phyllosilicates, one of several groups that constitute silicates. Phyllosilicates are well known for their sheet-like structures that form as a result of the linkage of silicon tetrahedral rings through shared oxygen molecules. Typical phyllosilicates include the following: Antigorite, lizardite, chrysotile from the serpentine group (Dana, 1999), talc and mica. Phyllosilicates from the smectite group include montmorillonite, beidellite, nontronite and hectorite (Dana, 1999). The naturally floating behaviour exhibited by talc is due to its unique structure which consists of essentially neutral 't-o-t' (trioctahedral-octahedral-trioctahedral) layers held together by weak residual bonds. Antigorite (from the serpentine group) and kaolinite show prominent hydrophilic character because its structure is composed of 't-o' (trioctahedral-octahedral) layers held together by hydrogen bonding (Dana, 1999). Minerals from the smectite group naturally absorb water. Phyllosilicate minerals such as from the smectite group are known as 'swelling clays' (Ndlovu *et al*., 2011).

Serpentines

Serpentine minerals are magnesium rich silicates which may contain iron and nickel; they are generally described by the formula $(Mg,Fe)_3Si_2O_5(OH)_4$. Serpentines are alteration products of olivines and pyroxenes after hydrothermal metarmorphosis. They form convoluted and bent layered structures and different minerals of which fibrous chrysotile and lamellar antigorite may be the best known (Kirjavainen and Heiskanen, 2007). Serpentines are difficult to handle and have been associated with high viscosities particularly in low grade ores where the sulphides are finely disseminated and thus require fine grinding.

Kirjavainen and Heiskanen (2007) observed that shearing of ores containing serpentine lead to an increase in aggregation and viscosity of the slurry. During

flotation they found that at high shear rates around the impeller the slurry viscosity was low; at low rates the viscosity increased. Typical problems associated with serpentines in flotation are that air bubbles tend to coalesce, the flotation rate is lowered and mechanical recovery of the gangue is high.

Talc

Talc is a magnesium phyllosilicate with the general composition $Mg_3Si_4O_{10}(OH)_2$ and is considered to be a hydrated alteration product of the abundant anhydrous silicate orthopyroxene (Viti *et al*., 2005). It is a common component of ores containing platinum group minerals (PGMs) such as Platreef and Merensky ores from the Bushveld Igneous Complex. Talc is commonly found in low grade ores as a naturally hydrophobic gangue mineral which usually contributes 0.5 – 5% of the gangue (Parolis *et al*., 2007). Although its contribution to the gangue is quite small, talc has a significant influence on the efficiency of the flotation process. The natural hydrophobicity of talc renders the gangue mineral easily floatable and can thus lead to stabilised froths. Froth stability results in increased levels of entrainment and consequently lower grades of concentrate. Further processing of the concentrates involves a smelting stage; the presence of siliceous gangue in the concentrate makes it difficult to smelt and leads to elevated costs of smelting.

The presence of talc in minerals has a marked effect on the rheology of the slurry. High talc content in an ore leads to increased inter-particle interaction, thus increasing the slurry viscosity (Jahani and Ehsani, 2009).

The effect of talc on gas dispersion properties such as bubble size and gas hold-up has been found to be frother dependent. Kuan and Finch (2010) observed that the bubble size increases and gas hold-up decreases in the presence of F150. This effect was attributed to bubble coalescence. The authors also observed that the frothers DF250 and 1-heptanol did not have an effect on bubble size and gas hold-up. In the presence of 1-pentanol frother, a different observation was made where the bubble size remained the same and the gas hold-up initially decreased then increased.

To achieve optimum recovery, polysaccharides such as polyacrylamides, guar gums and carboxymethyl cellulose (CMC) have been used to effectively depress any naturally floatable silicate minerals (Jenkins and Ralston, 1997).

Kaolinites

Kaolinite is a major gangue mineral (aluminium-silicate) usually found in diasporic bauxite. Its structural formula is $Al_2(OH)_4Si_2O_5$. This mineral naturally occurs as a residual weathered product of granite and is important in many applications in the ceramics, cosmetics, pigments and paper industry. The kaolin particles are plate-like in shape. Their edges contain tetrahedral silica and octahedral alumina groups and bear a positive charge at low pH (Loginov *et al.*, 2008).

Loginov *et al*. (2008) found that the rheological response of concentrated kaolin suspensions depends on the degree of shear perturbations, the flow history and time of measurements. In a concentrated system, the particles are in close contact and aggregate to form continuous networks. High shearing rates may cause these networks to break and lead to the damage of inter-particle bonds. The authors have reported that at low shear rates the suspension exhibits shear-thinning behaviour with a transition to shear-thickening behaviour at high shear rates due to increased interaction between the differently charged edges and basal planes. Bingham yield stresses of 7 Pa and 15 Pa at 25 wt% (11 vol%) and 30 wt% (14 vol%) were reported by the authors. Bingham viscosities of 6 mPa.s and 8 mPa.s were observed at the mentioned solids concentrations. Due to the disseminated nature of kaolinite and its applications (cosmetics, ceramics, paper industry, etc.) it is usually ground to ultra-fine particle sizes.

2.7.2 Hydrodynamics

Some recent work involving the mixing of non-Newtonian fluids in a mechanical flotation cell has been done by Bakker *et al*. (2009, 2010). However, most research has been done in the chemical engineering field using stirred tanks. This work will be reviewed in this section. In the chemical engineering literature stirred tanks are widely

used to carry out chemical reactions; these tanks are mixed using impellers such as the six-bladed disk style impeller to achieve homogenous mixing. Since mechanically agitated flotation cells work on a similar principle, it is believed that the hydrodynamic conditions existing in tanks are applicable.

When a fluid demonstrating an apparent yield stress is stirred in a tank at low impeller speeds, a region of the fluid around the impeller is in motion; this mobile region is known as a 'cavern'. The fluid in the remainder of the vessel is apparently stationary and there is no motion on any reasonable time scale (Kushalkar and Pangarkar, 1995). Nagata *et al*. (1970) investigated the effect of impeller speeds on Bingham plastics; they found that at low impeller speeds the fluid was a solid-like structure and the impeller shear stresses were lower than the fluid yield stress. Increasing the power input led the solid-like internal structure being broken, consequently the apparent viscosity of the fluid decreased thus causing the power input in the tank to decrease at a constant impeller speed. The authors also observed the formation of a cavern around the impeller; this mixing phenomenon can be seen from Figure 2.9.

Nienow and Elson (1988) studied caverns in Rushton turbine agitated tanks and found that the cavern is usually cylindrical, centred on or around the agitator with a height/diameter ratio of 0.4. For a shear-thinning fluid this variation means that the apparent viscosity near the impeller is low, and high near the wall (Grenville and Nienow, 2004).

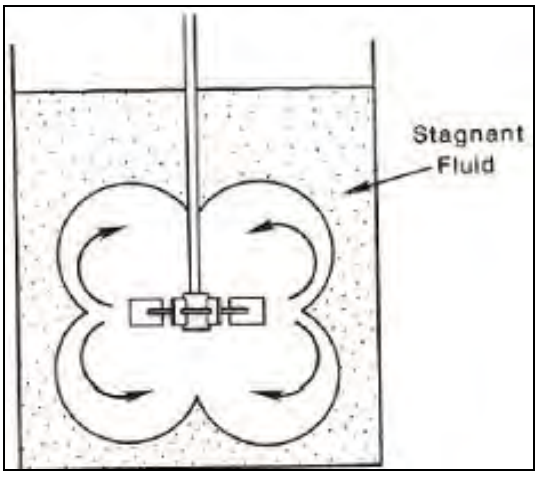

Figure 2.9 Cavern formed during mixing of a shear-thinning suspension (in Tatterson (1991), from Wichterle and Wein (1981)).

Wichterle and Wein (1975) also observed this phenomenon; they injected a dye tracer into the impeller region to visualise the 'cavern' of the fluid in motion. In 1981, these authors showed that in a stirred tank, a yield stress fluid is mobile around the impeller where shear stresses are high, whereas the same fluid is stagnant away from the impeller where shear stresses are low. Similar observations were made by other authors (Solomon *et al*., 1981; Elson *et al*., 1986; Moore *et al*., 1995; Fangary *et al*., 2000; Arratia *et al.*, 2006).

Bakker *et al*. (2009) conducted CFD simulations to investigate the effect of non-Newtonian slurries on the hydrodynamics in a mechanical flotation cell. The modelling was validated against published results showing experimental cavern measurements by modelling a pitch-blade turbine agitated tank. Bakker *et al*. (2009) went on to conduct experimental tests in a mechanical flotation cell using Bindura nickel slurries at 40 wt%, 50 wt% and 60 wt% solids concentrations. They found that a cavern in fact does form around the mobile region of the impeller due to the non-Newtonian (high yield stresses) nature of the slurries. The cavern boundaries in the flotation cell were identified using piezoelectric pressure sensors. The study conducted showed that the cavern forms around the stator and that the size of the cavern was inversely proportional to slurry yield stress and viscosity.

Bakker *et al*. (2010) went on to develop a semi-empirical model to determine the cavern height that forms in a mechanical flotation cell in non-Newtonian slurries. This model was based on the assumption that the cavern boundary was formed at the point where the shear stress imposed on the slurry equalled the slurry yield stress. Bakker *et al*. (2010) showed that according to the model, the cavern height was directly proportional to the product of the slurry density and the square of the impeller tip speed. They also found that the cavern height was inversely proportional to the slurry yield stress.

As mentioned in Section 2.6.2 it is assumed that the hydrodynamics in stirred tanks and mechanical flotation cells is similar. Therefore the behaviour of non-Newtonian fluids in stirred tanks can be used to describe the effect of non-Newtonian slurries in mechanically agitated flotation cells.

Oldshue (1983) concisely described the actions taking place in the tank during the mixing of pseudo plastic fluids. The author divided the viscosity in the cell into the impeller viscosity and the process viscosity. The impeller viscosity is the viscosity that the impeller 'sees' at a particular shear rate; this is the viscosity used in power calculations. The process viscosity is the viscosity that the process 'sees'; it is found at the process shear rate. The author went on to explain that for pseudo plastic fluids the impeller shear rate is always higher than the process shear rate meaning that the impeller viscosities are much lower than the process viscosities.

Metzner and Otto (1957) developed the most widely known definition to estimate the shear rate at the impeller in an agitated vessel. They performed studies on Newtonian and non-Newtonian shear-thinning fluids where they measured the power number using a variety of impellers in the laminar regime. They used the power law model to mathematically describe the behaviour of shear-thinning fluids. The authors postulated that the shear rate is related to the impeller speed by the following relationship (c.f. equation 2.12) where the shear rate is proportional to the impeller speed:

$$\dot{g} = \left(\frac{m_A}{K} \right)^{1/(n-1)} = k_s N \qquad 2.12$$

The disadvantage of this method, however is that it is applicable only in the laminar regime. The correlations by Sánchez Pérez *et al*. (2006) reviewed in Section 2.6.2 are applicable in the turbulent regime and have thus been applied in this thesis to relate rheological characteristics of the slurry to the cell hydrodynamics.

2.7.3 Gas Dispersion

In the following sections the hydrodynamic effects of gas dispersion are investigated with respect to varying solids content.

2.7.3.1 Bubble Size

Solids in a flotation cell have an effect on bubble size and on the overall dispersion of gas in the cell. The presence of solids in a flotation cell has been found to dampen energy dissipation (Nesse *et al*., 1979; Schubert, 1999). This damping effect increases with increasing solids content and is greater for fine particles. O'Connor *et al*. (1990) investigated the effects of pulp density, pulp viscosity and particle size on bubble size. They found that decreasing the pulp density (equivalent to a decrease in viscosity) decreases bubble size. It was suggested that this was due to the formation of a liquid film at the points of bubble formation, leading to the formation of smaller bubbles. They also found that decreasing the particle size resulted in the reduction in the size of bubbles formed in the cell.

Grau and Heiskanen (2005) also investigated the effect of solids concentration on bubble size using quartz material at a solids range between 0 and 30 wt%. They observed that the bubble size increased with more addition of quartz with a significant influence observed at 20 wt% solids. They also observed that the presence of solids dampens the turbulent intensity in the cell, which produces an increase in the amount of bubbles in the larger classes; Tucker *et al*. (1994) reported similar results.

2.7.3.2 Superficial Gas Velocity

To date there has not been any literature on the effect of solids concentration, viscosity or yield stress on the superficial gas velocity. However, the authors speculate that the solids will affect gas dispersion which will lead to wide variation in superficial gas velocity (local).

2.7.3.3 Gas Hold-Up

The effect of solids concentration, i.e. the rheological behaviour of slurries, on the gas hold-up has not been extensively investigated in minerals processing. The existing literature applies mostly in the general chemical engineering literature. Most of the literature reported involves two-phase systems where fluids such as high/low viscosity polymers are used to determine how effective gas dispersion is in an agitated vessel

(usually a continuously stirred tank). The majority of the information is drawn from this field and is applicable in this work as mechanical flotation cells are thought to have similar hydrodynamic properties.

Cooke *et al*. (2008) investigated the effect of increasing solids concentration of glass ballotini on the gas hold-up and mass transfer in a stirred tank. They found that the gas hold-up decreased with increasing solids concentration, which they attributed to the displacement of the small bubbles by solids in the slurry.

Vlaev *et al*. (2002) investigated the effect of rheology on gas hold-up with more emphasis placed on the pseudo-plasticity of the fluid. Tests were carried out using non-Newtonian aqueous solutions of xanthan gum with concentrations from 0.5 to 5 kg/m^3 and Newtonian glycerol solutions of 450 and 800 kg/m^3 containing 5% electrolyte. The authors performed these tests around three regions within the cell i.e. the impeller region, the wall region and the bulk region. The gas hold-up of the Newtonian solutions was found to increase with increasing polymer concentration both in the wall and the impeller region; this was due to the fact that the apparent viscosity was constant throughout the vessel. The average gas hold-up was found to be the same at varying speeds. This was not the case however with the non-Newtonian fluid where two distinct regions were formed; a mobile region where the circulation loop shrunk with increased agitation and a stagnant region at the wall. The gas hold-up was found to increase in the impeller region and to decrease or remain the same at the vessel wall. The authors concluded that the majority of bubbles were produced around the impeller region thus increasing gas hold-up; the stagnant region at the vessel wall receives fewer bubbles thus gas hold-up decreases. This effect resulted in poor liquid and gas circulation outside the impeller area.

Machon *et al*. (1980) investigated the effects of the shear-thinning nature of a liquid on the gas holdup using CMC solutions where the gas hold-up varied between 1% and 8%. When the shear-thinning nature of the fluid was increased, the gas hold-up decreased. This was attributed to an increase in the proportion of large bubbles produced, which have a shorter residence time in the tank. They concluded that the large bubbles were present due to the inability of the impeller to disperse the gas and not because of coalescence.

2.8 Scope of Thesis

Mining operations are increasingly processing mineralogically complex ores that are liberated by grinding the ores to very fine particles. Ultra fine grinding technologies such as Isamills are usually applied to achieve these very fine particle sizes. Froth flotation continues to be the separation method that is used for the beneficiation of a large portion of the world's mineral ores. The majority of flotation occurs in mechanical flotation cells where effective gas dispersion is a primary requirement for particle-bubble contacting.

Mining operations are also faced with running flotation circuits at fairly high solids concentrations in order to accommodate high tonnages and limit water consumption. Mineral slurries containing fine particles at high solids concentrations exhibit non-Newtonian rheological behaviour. The rheology of these slurries in turn significantly impacts on the hydrodynamics existing in the cell. Very little research on the effect of rheology on cell hydrodynamics in flotation cells has been conducted until recently by Bakker *et al*. (2009, 2010). Bakker *et al* (2009, 2010) found that slurries characterised by rheologies with a high yield stress may result in the formation of a yielded 'cavern' of slurry around the impeller, with slurry in the bulk cell remaining unyielded, and therefore stagnant.

Cell hydrodynamics significantly affect gas dispersion in the cell. Gas dispersion is characterised by the measurements of bubble size, gas hold-up, superficial gas velocity and bubble surface area flux. Extensive studies of gas dispersion in mechanical flotation cells have been conducted (Gorain *et al*., 1995a, b; Deglon *et al*., 2000; Finch *et al*., 2000, Grau and Heiskanen, 2003, 2005; Nesset *et al*., 2006; Schwarz and Alexander, 2006). However little or no work has been published on the effect of slurry rheology on gas dispersion in flotation cells. Independent research on gas dispersion and rheology in stirred tanks has been conducted in the general chemical engineering field.

Some work conducted in the area of flotation by Nesse *et al*. (1979) and Schubert (1999) showed that slurries containing fine particles led to turbulence damping, presumably through an increase in slurry viscosity. Tucker *et al*. (1994) and Grau and

Heiskanen (2005) investigated the effect of solids concentration on gas dispersion. They found that bubble size increases at higher solids concentration.

Due to the limited studies relating slurry rheology to gas dispersion particularly in mechanical flotation cells, it is believed that this study will make an important contribution in mineral processing.

The main objective of this study is thus to investigate the effect of rheological behaviour of slurries on gas dispersion in mechanical flotation cells. The effect of increasing solids concentration is investigated by performing rheology tests on three ores, viz. kaolin, Bindura nickel and Platreef (PGM) ore. The thesis then explores the effect of rheology (increasing solids concentration) and impeller speed on gas dispersion in a pilot scale mechanical flotation cell. Gas dispersion properties, i.e. bubble size and gas hold-up are investigated.

CHAPTER 3 Experimental

Experimental testwork was conducted in the Chemical Engineering experiential lab at the University of Cape Town using three ore types, viz., Bindura nickel, Platreef and kaolin ores. Rheology tests were conducted to determine the rheological behaviour of the slurries at different solids concentrations for each ore type. Gas dispersion parameters viz. bubble size and gas hold-up were measured at different solids concentrations and impeller speeds.

The chapter begins with a brief description of the mineral ores used for test work as well as the method of sample preparation used. The description of the experimental rig as well as the measurements carried out follows. The experimental design which explains the method used to determine the range of impeller speeds used is described. The experimental programme detailing the order in which experiments were carried out then follows. Finally, repeatability is accounted for by the error analysis section.

3.1 Mineral Ores

Three ores were used for experimental test work: Bindura nickel, Platreef and kaolin. Kaolin ore was used as a benchmark ore as it is a well studied ore in the rheology field (Street and Buchanan, 1956; Goodwin and Ottewill, 1969; Williams and Williams, 1977; Johnson *et al.*, 1998; Sjöberg *et al.*, 1999; Loginov *et al.*, 2008). Bindura nickel and Platreef ores were chosen because they are believed to exhibit very difficult rheological behaviour, particularly at high solids concentrations and fine particle sizes. Mineralogical information on each of the ores is detailed in the following sections. X-ray diffraction (XRD) was used to identify the minerals existing in each ore type (as well as identify the ‘problematic’ gangue minerals) and to qualitatively determine mineral contents in powdered materials. These ores are discussed in succession in the following sub-sections.

3.1.1 Kaolin Ore

Kaolin was obtained from Serina mine in Noordhoek, Cape Town. Kaolin is a clay mineral that is usually made up of three main minerals: kaolinite, mica and quartz. The kaolin used in this study consists mainly of kaolinite as the basic mineral with small traces of mica and quartz. Its structural formula is $Al_2(OH)_4Si_2O_5$. This is the standard kaolin chemical formula.

3.1.2 Bindura Nickel Ore

Bindura nickel ore was obtained from the Trojan nickel deposit, located in Harare, which occurs in serpentinized Archaean ultramafic lavas of the Mazoe greenstone belt (Tyndale-Biscoe, 1972). The type of nickel sulphide ore used is disseminated and forms part of the hanging wall ore body. This type of ore constitutes the major part of the mine. The sulphides often occur as discrete blebs up to 1 cm wide in serpentinite (Chimimba and Ncube, 1986). The major sulphide minerals are, in order of abundance: pyrrhotite, pentlandite and chalcopyrite.

Bindura nickel ore was chosen because it contains minerals such as smectite, talc ad antigorite that cause slurries to exhibit highly viscous non-Newtonian rheological properties. This high viscosity has been found to adversely affect materials handling particularly through the slurry section of pressure leaching process plants (Avotins ***et al***., 1979; Kyle and Furfaro, 1997; Motteram ***et a***l., 1997; Chalkey and Toirac, 1997; Whittington and Muir, 2000).

3.1.3 Platreef Ore

The Platreef is located in the northern limb of the Bushveld Complex situated 30 km northwest of Mokopane. It has an estimated platinum and palladium reserve of 16.3 million ounces (Cawthorn, 1999). The Platreef is composed of a complex sequence of medium to coarse grained pyroxenites, melanorites, and norites, in places pegmatoidal

and serpentinzed, containing metasedimentary xenoliths of the floor rocks. It contains sporadic enrichments of nickel (Ni), copper (Cu), and platinum-group element mineralization which locally make it of economic significance (Gain and Mostert, 1982).

The major sulphide minerals existing in Platreef in order of abundance are pyrrhotite (sometimes pyrite), pentlandite and chalcopyrite. Minor cubanite, sphalerite, bornite, millerite, cuprite, galena, and alabandite also occur (Gain and Mostert, 1982). Talc is found on the rims of chalcopyrite. Talc is usually associated with high viscosities and yield stress. This ore was chosen because it is also well known as a difficult ore when handled in industry, particularly at fine particle sizes.

3.2 Sample Preparation

100 kg of kaolin was sorced from Serina mine as a product that was packaged in 25 kg batches, therefore four batches were received. 150 kg of Bindura nickel ore was received through Mintek (as part of their studies) as a mill product. 250 kg of Platreef ore was received as a milled product from Anglo Platinum. Each of these ores was individually physically blended using shovels to homogenise each sample as much as possible. The riffle splitter was then used to split the sample until 10 kg batches were obtained. One 10 kg batch per ore type was then further split using a rotary splitter to obtain 1 kg batches.

The 1 kg batch from each ore was further split into 100 g batches where the 100 g batch was used for particle size analysis and density measurements. The particle size distributions (PSD) of the ores were determined using a Malvern Particle Size Analyzer. The PSD's for each of the ores are shown in Figure 3.1. Kaolin particles have a d_{50} of 5 µm with 80% passing 10µm. Bindura nickel solids have a d_{50} of approximately 20 µm and 80% passing 75µm. Platreef ore particles have a d_{50} of 9 µm with 80% passing 25 µm.

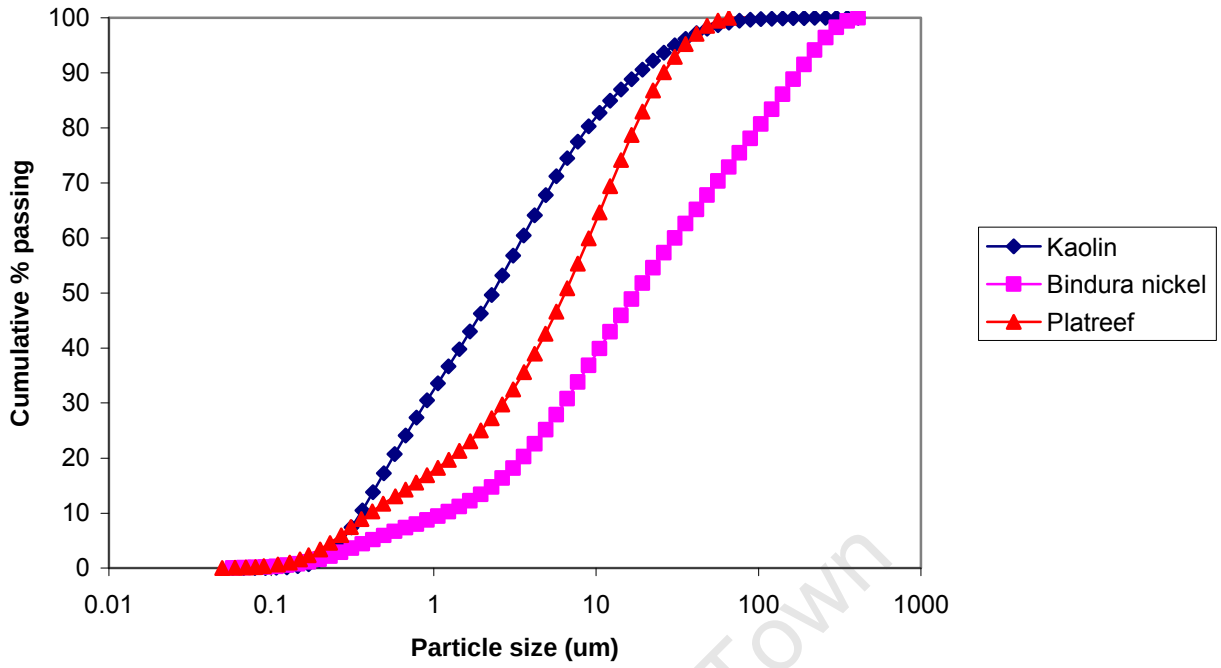

Figure 3.1 Particle size distribution for kaolin, Bindura nickel and Platreef ores.

The density of the kaolin, Bindura nickel and Platreef ores were found to be 2600 kg/m^3, 2999.4 kg/m^3 and 3016.8 kg/m^3 respectively. The slurry densities at different solids concentrations were then determined based on equations adopted from Van der Westhuizen (2004). These equations were used to determine the mass of solids and water required at each solids concentration. Each of the ore samples was then packaged into bags according to their required dry masses.

Mineralogical samples were prepared by first splitting the samples using a small riffle-rotary splitter. The samples were then micronised to ensure they were ultra-fine for XRD tests. A total sample of 3 g each was packed and sent for tests at the University of Pretoria; Table 3.1 shows the mineralogy of each of the ores used.

Table 3. 1 Ore mineralogy for kaolin, Bindura nickel and Platreef ores.

Ore type	Major minerals	Minor minerals
Kaolin	Kaolinite	Mica Quartz
Bindura nickel	Serpentine Olivine	Talc Chlorite Brucite Olivine Pentlandite Pyrrhotite Actinolite (amphibole)
Platreef	Pyroxenes Base Metal Sulphides	Talc

Synthetic plant water was prepared and used to carry out all the tests (rheology and gas dispersion) mainly because it is typical of industrial water (Wiese *et al.*, 2010). Synthetic plant water was also used because it reduces the effect of the electrical double layer of the particles which makes rheology difficult as would be encountered in industrial mineral processes. The specifications for the 100 litre batches that were used in each test are shown in Table 3.2.

Table 3. 2 Specifications for plant water.

Salt	Formula	Amount (g)
Magnesium sulphate	$MgSO_4 \cdot 7H_2O$	61.50
Sodium chloride	NaCl	35.60
Magnesium nitrate	$Mg(NO_3)_2 \cdot 6H_2O$	10.70
Calcium nitrate	$Ca(NO_3)_2 \cdot 4H_2O$	23.60
Calcium chloride	$CaCl_2$	11.10
Sodium carbonate	Na_2CO_3	3.00

3.3 Experimental Rig

The flotation rig used was adopted from the work of Van der Westhuizen (2004), Van der Westhuizen and Deglon (2007, 2008) and Bakker *et al*. (2009, 2010) where the effect of solids suspension in the cell was investigated. The experimental setup is shown schematically in Figure 3.2. Experiments were carried out in a cylindrical 0.54 m diameter (T) mechanically stirred tank fitted with a flat bottom. The capacity of the tank with the static liquid level (Z) kept at 80% to the tank diameter (Z = 0.8T = 0.44 m) is 100 litres. The cell was fitted with a cover to minimise overflow of froth out of the cell. A six bladed Bateman impeller with a maximum diameter (D_{max}) of 0.150 m and a stator mechanism were used. The impeller clearance from the tank bottom was kept at 15% of the tank diameter (83 mm). The air flowrate was adjusted by a hand valve and measured by an air rotameter (metric 47G). The impeller speed was measured using a variable speed drive.

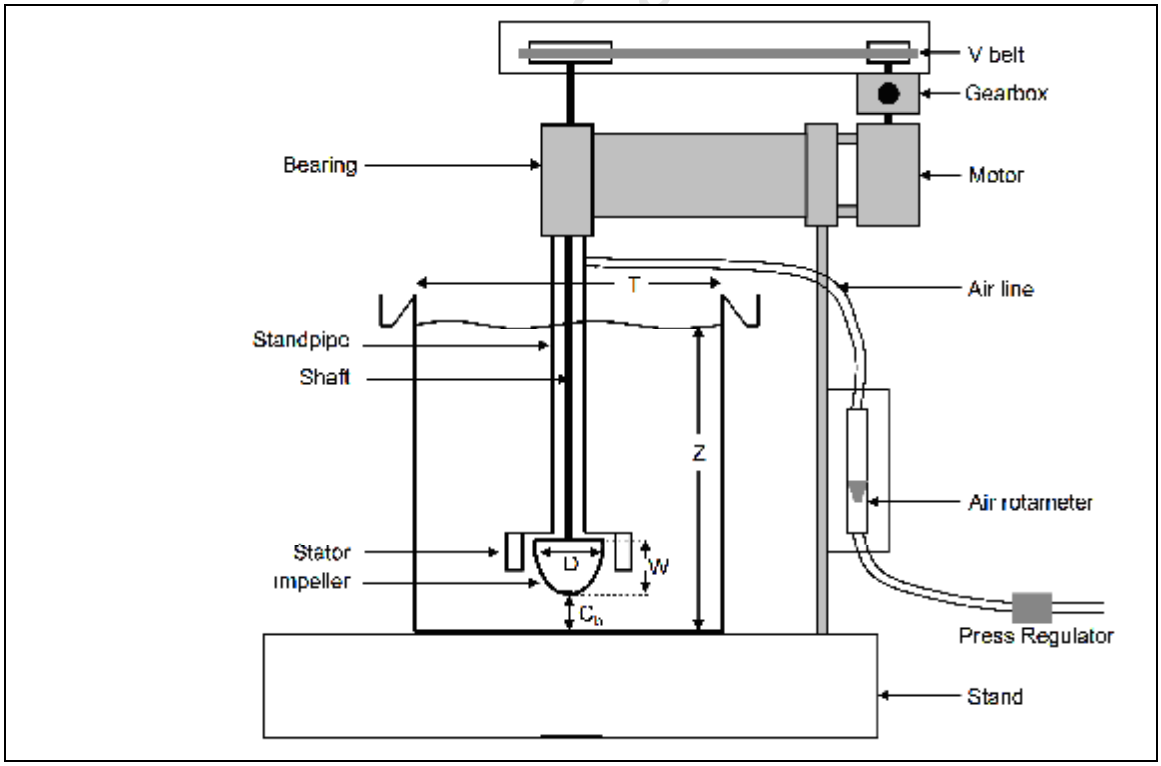

Figure 3.2 Experimental rig (van der Westhuizen, 2004).

3.4 Experimental Measurements

3.4.1 Rheology

Rheological measurements were carried out at the Cape Peninsula University of Technology (CPUT) using a MCR 300 rheometer (cf. Figure 3.3) with a cup and bob geometry. The instrument generates torque and the rotation speed of the bob which can be adjusted. The torque and speed measurements were converted to shear stress (τ) and shear rate (γ). The range of shear rate values used was between 0.1 and 1000 s^{-1}. This range was chosen in order to obtain complete flow curves and to allow for complete suspension and shearing of the suspension. The working range used for tests in the flotation cell was between 100 and 800 s^{-1}, which was determined by means of an experimental design using equations developed by Sànchez Pérez *et al*. (2006); Equations 2.7 to 2.11 are shown in Section 2.6.2. The experimental design is outlined in Section 3.5.

The temperature was maintained constant at 23°C; however, temperature sweeps were also carried out to investigate the rheological behaviour of the slurry over a specific temperature range. Smooth-walled rheometers are known to cause slip, particularly at high solids concentration (Cheng and Richmond, 1978 in Chhabra & Richardson, 1999); to minimise this effect a sandblasted bob was used.

Settling tests were carried out in order to determine the settling velocity of the suspension and the measurement period of the tests. For each test, a 100 ml sample of slurry was prepared using plant water. The rheological behaviour of the slurry was manipulated by varying the solids concentration for each ore type. The rheograms were plotted in order to observe the behaviour of the slurries. Rheological properties such as yield stress and the apparent viscosity were determined by fitting the shear stress and shear rate data with the Bingham model.

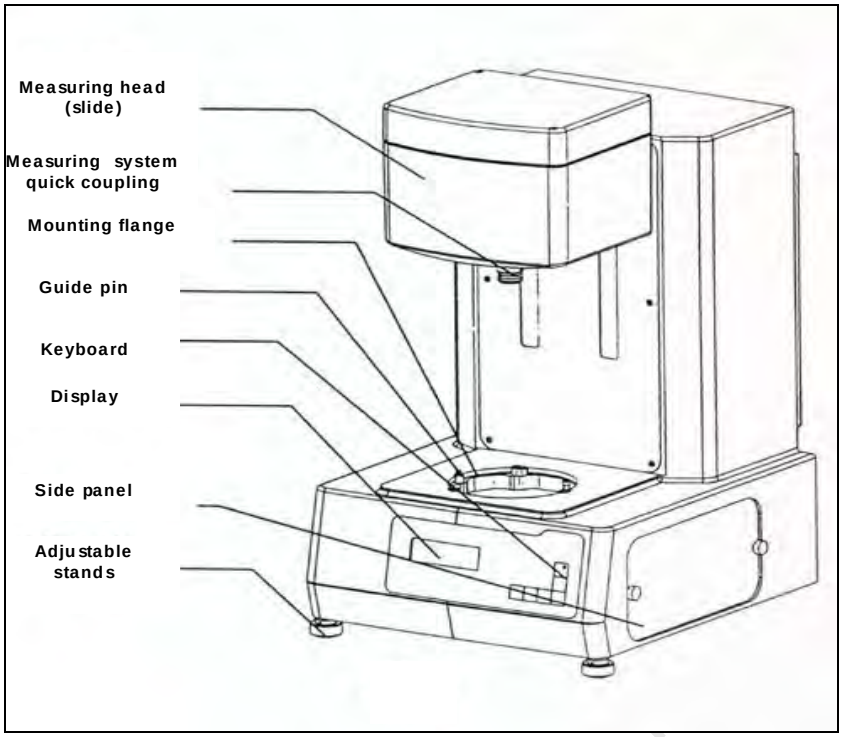

Figure 3.3 Schematic diagram of MCR 300 rheometer.

3.4.2 Bubble Size

To determine the bubble size in the stirred tank at various impeller speeds and slurry solids concentrations, the Anglo Platinum Bubble Size Analyser (Naik and van Drunick, 2007) was used. A schematic of the APBS is shown in Figure 3.4. The APBS consists of a sampler tube, a viewing chamber and an image acquisition system. The sampler tube was partially immersed in the pulp phase, below the froth-slurry interface, at an equidistant position between the impeller and the cell wall.

The APBS works on the principle of maintaining an unbroken column of water from deep within the flotation cell where bubbles are collected, to the viewing pane where images of the bubbles are captured using a digital camera. The viewing pane is situated above the flotation cell. The bubble sizer has a portable power supply that provides back lighting when capturing images. This power supply was charged for 14 to 16 hours to prevent images from being underexposed. The images were processed using bubble sizer software which displays 2-dimensional bubble areas of images were obtained from the viewing pane. Mean bubble areas were obtained and the mean

bubble diameters of the bubbles were calculated by assuming that the bubbles were spherical.

Figure 3.4 Anglo Platinum Bubble Size Analyser.

3.4.3 Gas Hold-Up

Due to the size of the cell, it was not possible to measure the local gas hold-up in the cell. Therefore, the global gas hold-up in the cell was determined by measuring the difference in height of the froth slurry interface in the presence and the absence of air. The difference between the two heights represents the volume of gas present in the cell during flotation. In this study, the global gas hold-up is thus considered to be the most reliable measurement.

3.4.4 Impeller Speed

The impeller speed is the only machine variable that was varied in the testwork. The impeller speed was measured by an electromagnetic pickup and displayed. A tachometer was used to confirm the impeller speed readings.

3.4.5 Power Draw

The power input was measured using a three-phase wattmeter. The load power draw was determined by subtracting the no load power obtained by measuring the power with the impeller running free.

3.5 Experimental Design

The experimental design outlined in this section illustrates the method used to determine the range of impeller speeds which would correspond to the impeller shear rates used to study gas dispersion in the presence of solids in the cell. The highest impeller speed was chosen according to motor limitations. The impeller speeds were also chosen to straddle and exceed the power intensities that are typical in industry (Deglon 2005). The equations by Sànchez Pérez *et al.* (2006) were used to determine the shear rate as outlined in Section 2.6.2 in Chapter 2.

Rheology tests were conducted on Platreef ore at different solids concentrations using the MCR 300 rheometer at shear rate range from 0.1 to 1000 s^{-1}. A yield stress value of 14 Pa was obtained from modelling of the shear rate and shear stress data, this value is comparable to yield stresses found in rheology measurements. The impeller speeds were selected based on 5 equidistant values of mean shear stress (c.f. Figure 3.5). The power intensity (P/V) was calculated after measuring the power of the pilot scale mechanical flotation cell at varying impeller speeds. The volume of slurry occupying cell was known and thus the power intensity could be calculated.

The power intensities at different slurry concentrations were then determined using the density ratio (density of slurry to water at different solids concentrations). An assumption was made where the impeller shear stress equals the slurry yield stress as a result of a boundary in the fluid where the fluid becomes stagnant. This assumption was made based on the literature that is presented in Section 2.7.2, such that the impeller shear stress could be substituted by the slurry shear stress (yield stress in this case). Consequently, Equation 2.7 was then used to calculate the impeller shear rate

which was found to correspond to the slurry shear rate range tested. The experimental design was therefore based on the mean shear stress (in this case a single value of yield stress) in fluids as it is known that the fluid yield stress impacts slurry rheology significantly. These values were used throughout all tests carried out in the cell for all ore types.

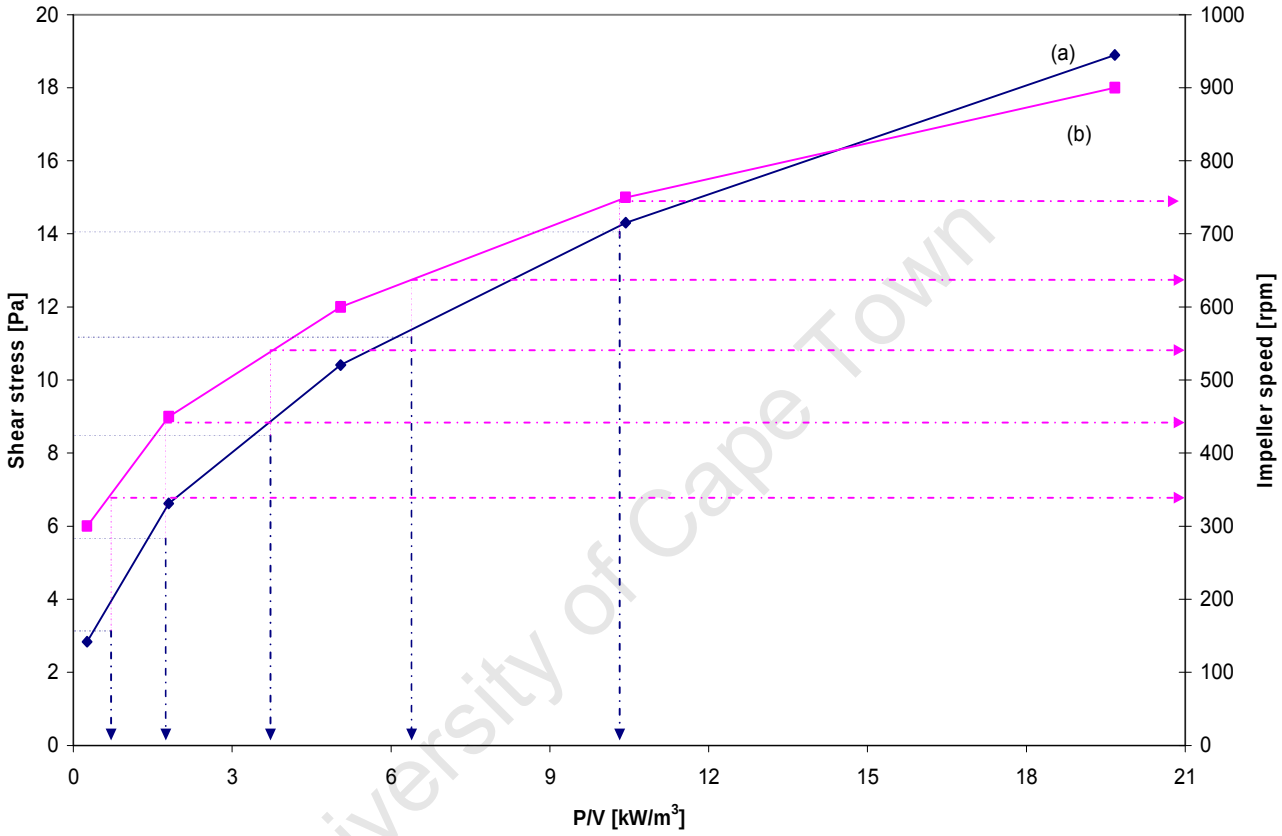

Figure 3.5 (a) Plot of shear stress vs. power intensity to determine working range of impeller speeds (b) Plot of impeller speed vs. power intensity to determine the impeller speed range used in the flotation cell.

3.6 Experimental Programme

Table 3.3 shows the variables considered in this study for kaolin, Bindura nickel, and Platreef ores. The solids concentration was varied so as to obtain different rheological behaviours. The aeration rate was kept constant as well as the frother concentration (cf. Table 3.4); the frother concentration was chosen because it is a concentration above the CCC to ensure a non-coalescing system (Newell and Grano, 2007). The only machine variable varied in the cell was the impeller speed to study gas dispersion while varying the rheology of the slurry.

Table 3. 3 Experimental variables used in this study.

Ore type	Density [kg/m^3]	Variable	Unit	Range
Kaolin	2600	Solids concentration	wt%	15, 25, 30, 40
			vol%	6, 11, 14, 20
Bindura nickel	2999		wt%	20, 25, 30, 35, 40, 50, 60
			vol%	8, 10, 13, 15, 18, 25, 33
Platreef	3017		wt%	20, 25, 30,35, 40, 50, 60
			vol%	8, 10, 12,15, 18, 25, 33
All ores		Impeller speed	rpm	300, 440, 550, 650, 730

Table 3. 4 Experimental conditions used in the flotation cell.

	Symbol	Unit	Value
Aeration rate	JG	cm/s	1.5
Frother dosage	MIBC	ppm	20

Rheology tests were carried out first followed by gas dispersion tests. In measuring gas dispersion properties in the cell, the gas hold-up was measured first followed by bubble size measurements. This order was followed because there is a slight increase in the slurry volume during bubble size measurements. Water (3 L) from the APBS reservoir ends up in the cell via the sampling tube.

5 runs were carried out per test for a single solids concentration by varying the impeller speed. A total of 95 runs were carried out for the whole range of solids concentrations.

3.7 Error Analysis

For each of the experiments carried out repeats were performed to account for the error and reproducibility of the results. Mean values of bubble size and gas hold-up were determined and the standard deviations were calculated. The standard error was also calculated in order to fully analyze experimental results. Table 3.5 shows a summary of standard deviation and errors calculated for bubble size and gas hold-up for kaolin, Bindura nickel and Platreef ores. Detailed tables are in the Appendix.

Table 3. 5 Standard deviation and errors on bubble sizes and gas hold-up for all ores.

Ore type	**Standard deviation**		**Standard error**	
	Bubble size (mm)	**Gas hold-up (vol%)**	**Bubble size (mm)**	**Gas hold-up (vol%)**
Kaolin	0 - 0.1	0 - 2.9	0 - 0.07	0 - 2.1
Bindura nickel	0 - 0.05	0.3 - 2.5	0 - 2.8	0.1 - 1.4
Platreef	0.001 - 0.2	0 - 0.5	0.001 - 0.2	0 - 0.3

CHAPTER 4 Results and Discussion

This chapter presents results obtained from the rheology and gas dispersion tests. The rheology results are first presented and discussed, followed by the gas dispersion results. The effect of solids concentration on rheology is investigated for three ores (kaolin, Bindura nickel and Platreef). Once the rheological behaviour of the ores is established, gas dispersion results are presented where the effect of impeller speed and solids concentration on the measured bubble size and gas hold-up is discussed. The effect of slurry rheology on each of these gas dispersion properties is discussed. The chapter concludes with an attempt to explain the gas dispersion results obtained in terms of a generic rheological parameter, the slurry yield stress.

4.1 Rheology Results

The shear stress against shear rate curves for kaolin, Bindura nickel and Platreef are shown in Figures 4.1 to 4.3 respectively. The shear rate range that was considered for analysis is between 100 and 1000 s^{-1} as this corresponds to the conditions used in the flotation cell for gas dispersion measurements. The ores exhibit Bingham plastic behaviour in the range between 100 and 1000 s^{-1}. This is typical of mineral slurries and has been observed in literature by Tangsathitkulchai (2003) and He *et al*. (2006), as noted in Section 2.7.1.1.

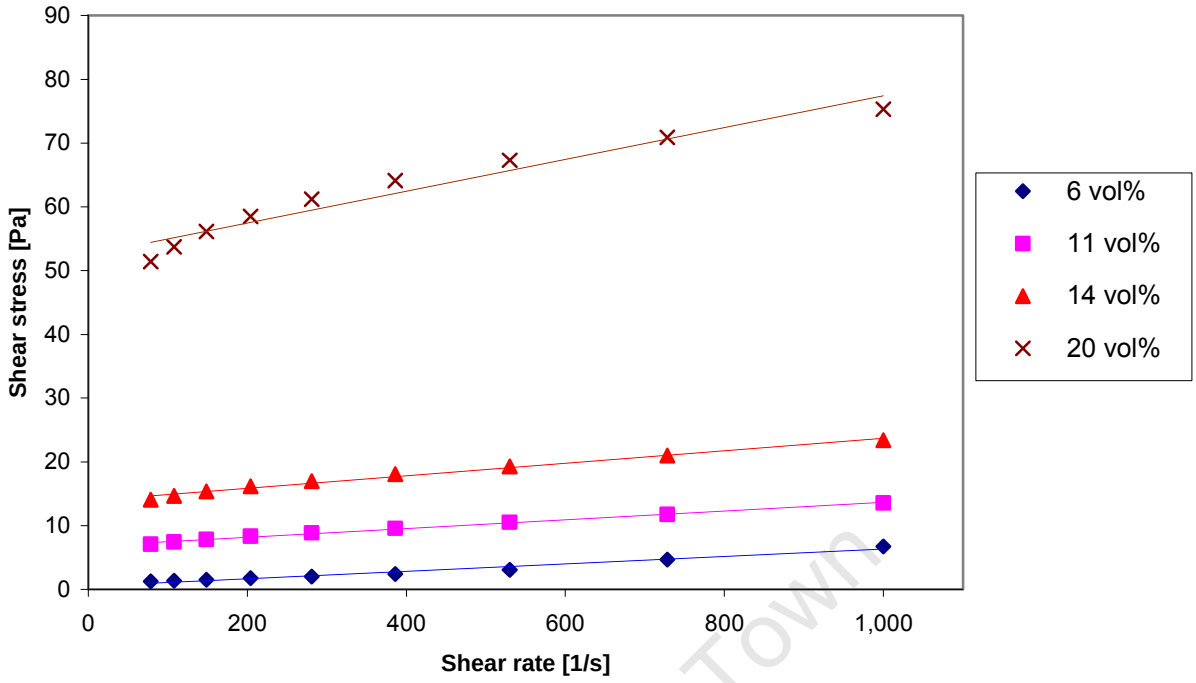

Figure 4.1 Rheograms for kaolin ore at different solids concentration.

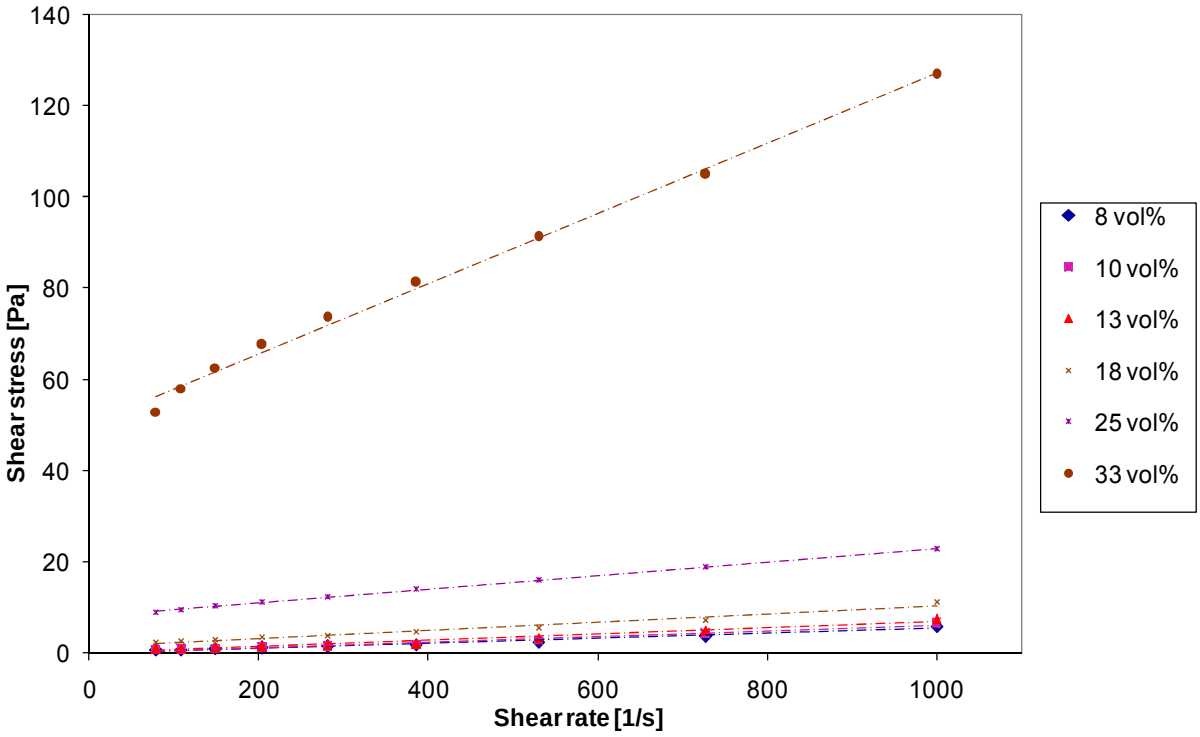

Figure 4.2 Rheograms for Bindura nickel ore at different solids concentration.

It can be seen that the Bingham yield stress (depicted by the y-intercept of each line) increases with solids concentration for each ore type, with a more significant jump at

20 vol% for kaolin ore and 33 vol% for Bindura nickel and Platreef ores. The slope of the curves does not change significantly with increasing solids concentration, particularly at the lower solids concentrations. This suggests that the Bingham yield stress is the dominant rheological characteristic for each ore type. It thus follows that an increase in the solids concentration affects the slurry rheology, with the yield stress exhibiting the most notable effect.

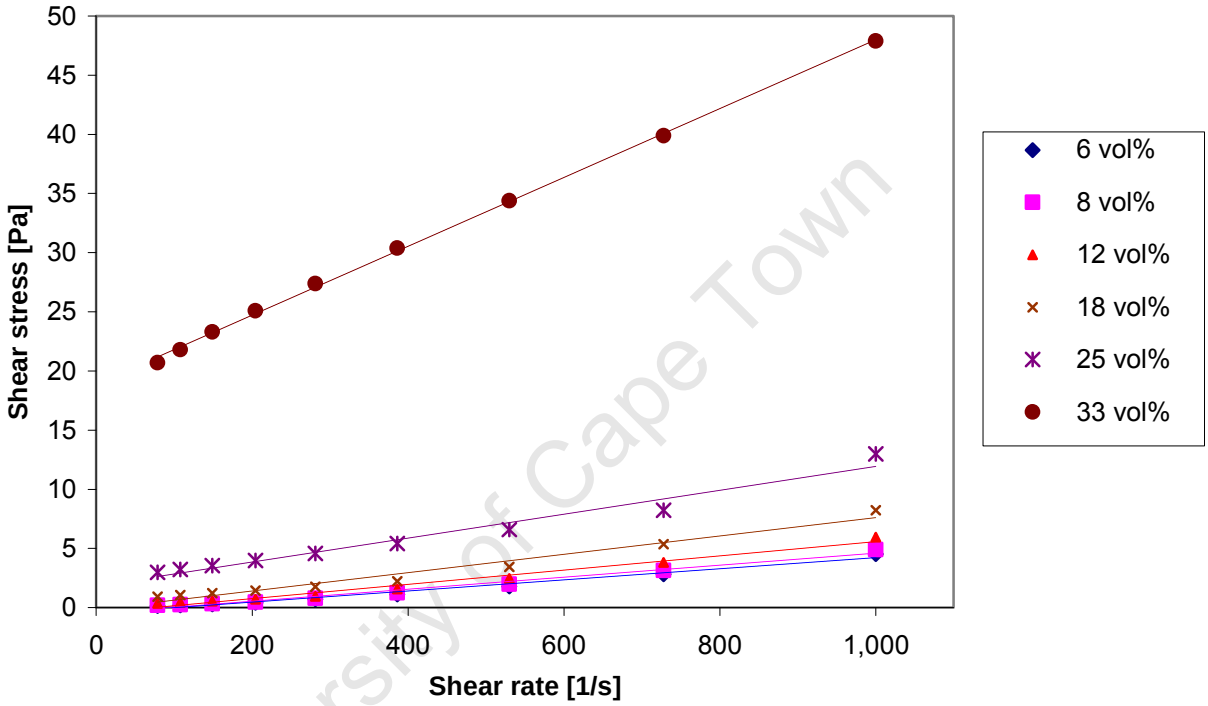

Figure 4.3 Rheograms for Platreef ore at varying solids concentrations.

A comparison of the three figures shows that kaolin has a higher yield stress compared to the other ores, even though its maximum solids concentration is only 20 vol%. This is because kaolin ore has a much finer particle size (c.f. Figure 3.1) compared to Bindura nickel and Platreef ores.

Figure 4.4 shows a plot of yield stress against solids concentration for each ore type. The yield stress varies from 0.52 to 52.4 Pa for kaolin, from 0.03 to 50.3 Pa for Bindura nickel and from 0.50 to 18.9 Pa for Platreef ore. It can be seen that the yield stress increases exponentially with solids concentration, with major increases from 14 vol% for kaolin and 25 vol% for Bindura nickel and Platreef ores. This exponential relationship between yield stress and solids concentration has been observed in

various studies in literature for various ore types, including sulphide slurries (Muster and Prestidge, 1995), alumina and zirconia suspensions (He *et al.*, 2004) and quartz particles (Yue and Klein, 2004).

At low solids concentrations the slurry is dilute and the distance between particles is large such that attractive van der Waals forces are very weak, or non-existent. This allows particles to move freely and not to coagulate, which results in a low yield stress. At high solids concentrations, however, the opposite effect is observed. Here, the inter-particle distance is small and strong attractive van der Waals forces exist, which results in particle coagulation and thus a high yield stress.

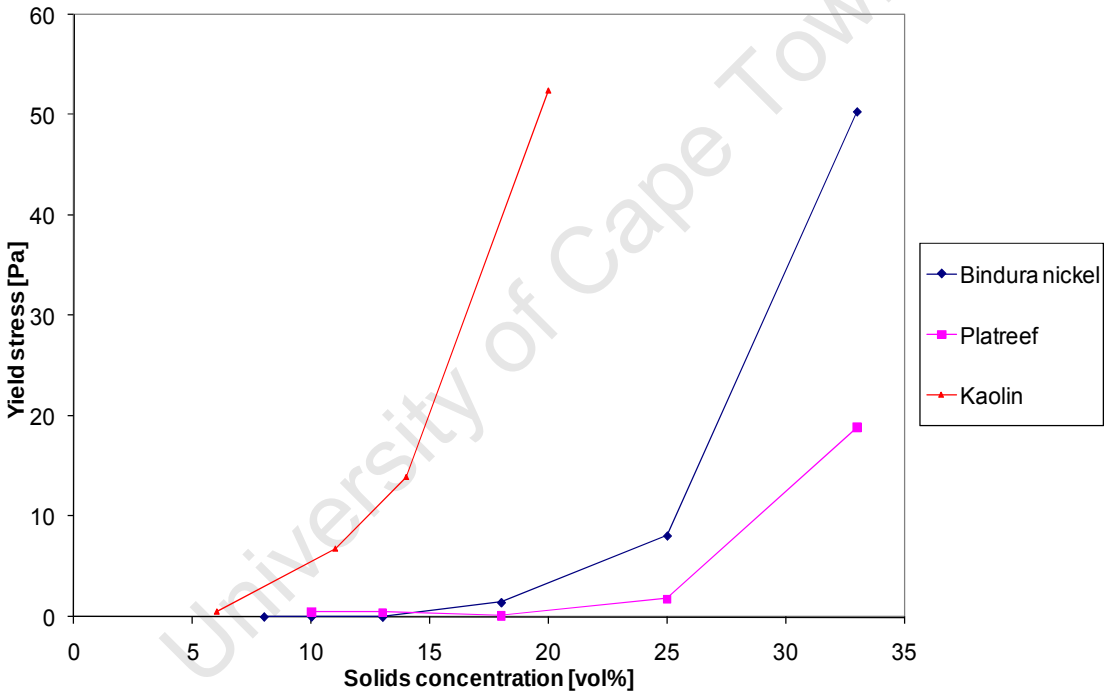

Figure 4.4 Graph of yield stress against solids concentration for three different ores.

Figure 4.5 shows a plot of viscosity against solids concentration for each ore type. The viscosity varies from 0.006 to 0.025 Pa.s for kaolin, from 0.006 to 0.077 Pa.s for Bindura nickel and from 0.005 to 0.029 Pa.s for Platreef ore. Loginov *et al.* (2008) observed similar values of viscosity for kaolin ore at similar solids concentrations. It can be seen that an exponential relationship also exists between the viscosity and solids concentration. However, the overall increases in viscosity are considerably smaller than those in the yield stress, where changes of up to two orders of magnitude

were observed. This exponential relationship has been observed in the literature by Gao and Forssberg (1993), Muster and Prestidge (1995) and Yue and Klein (2004).

The mineralogical nature of the ores also plays an important role. Section 3.2 Table 3.1 shows the XRD results for the kaolin, Bindura nickel and Platreef ores. Kaolinite is a major mineral in kaolin; this may explain the significant increase in yield stress at high solids concentration as a result of the complex structure of kaolinite. Bindura nickel has major minerals of serpentine and olivine, serpentine has been associated with high viscosities as mentioned in Section 2.7.1.4. It can be seen from Figure 4.5 that Bindura nickel in fact does have the highest values of viscosity at the solids concentrations that were tested. Platreef ore contains talc as a minor mineral, which could explain why both the yield stress and viscosity of Platreef of is lower than the other two ores tested.

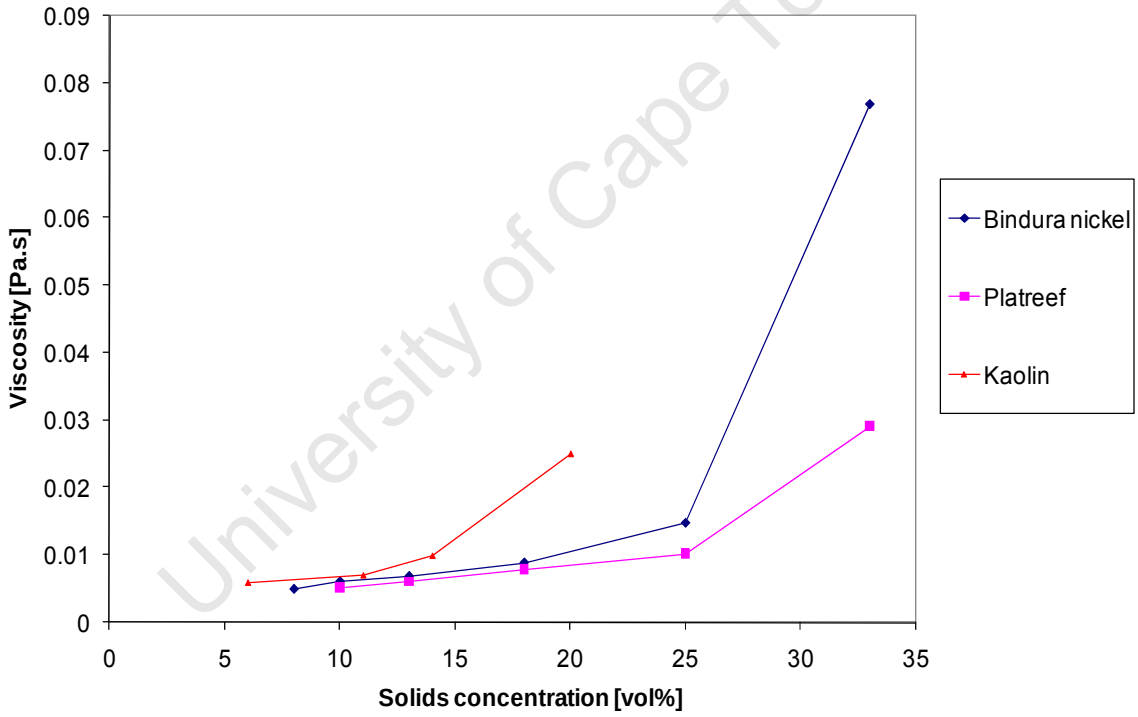

Figure 4.5 Graph of apparent viscosity against solids concentration for three different ores.

4.2 Gas Dispersion Results

Gas dispersion results are shown for the three ores at different impeller speeds and solids concentrations. Firstly, the effect of impeller speed and solids concentration on

bubble size is discussed and then the effect of impeller speed and solids concentration on gas hold-up. Each of these sections concludes with a discussion on the effect of slurry rheology on the gas dispersion results obtained. It should be noted that data corresponding to solids concentrations at three distinct solids concentrations to represent low, intermediate and high solids concentrations is presented in this study (for all ores tested) for clarity and for better interpretation of the results.

4.2.1 Bubble Size

4.2.1.1 Effect of Impeller Speed

Figures 4.6, 4.7 and 4.8 show the effect of impeller speed on bubble size for kaolin, Bindura nickel and Platreef ores respectively. Here, bubble sizes range from 0.55 to 1.10 mm. This bubble size range is slightly lower than the range of between 1 and 2 mm observed in industrial flotation cells (see Section 2.5.1). However, this range is typical of smaller flotation cells operating at high power intensities, particularly in this study where power intensities were as high as 10 kW/m^3 (Deglon, 2005).

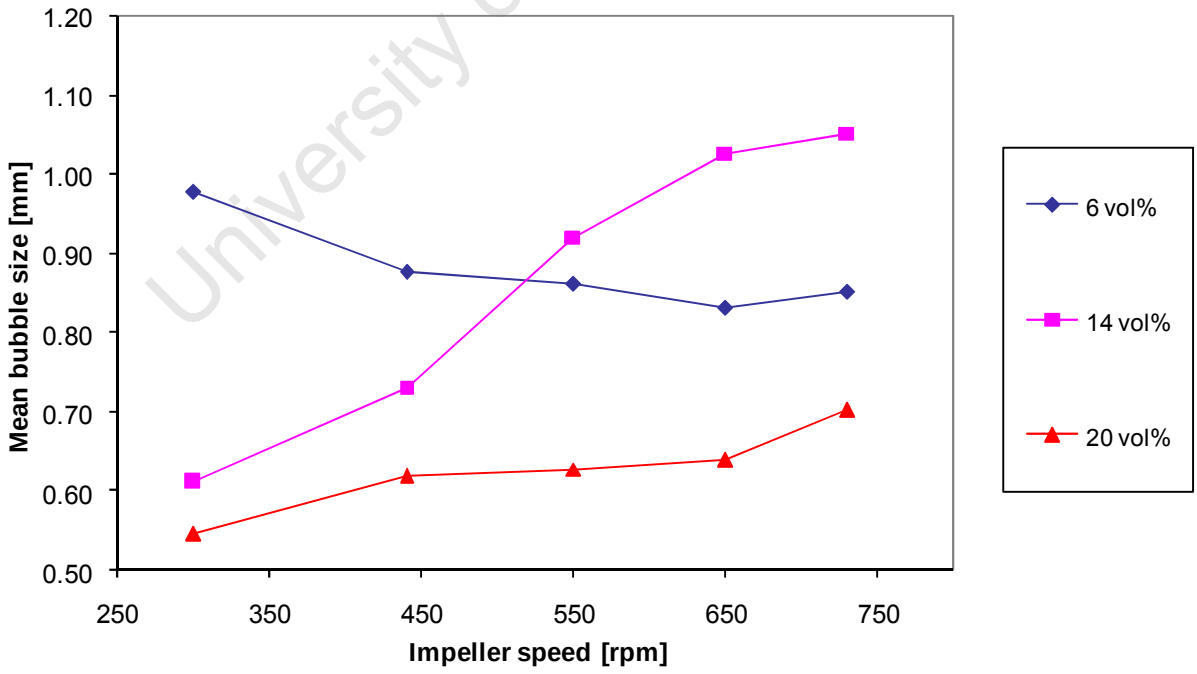

Figure 4.6 Effect of impeller speed on bubble size for kaolin ore.

Bubble size decreases with increasing impeller speed for dilute solids concentrations (as expected) but increases for higher solids concentrations. This increase was unexpected as literature suggests that bubble size should decrease with increasing impeller speed for all slurry types (Gorain *et al.*, 1995a; Grau and Heiskanen, 2005). It should be noted that the bubble size is greater at intermediate solids concentrations (for kaolin and Platreef ores) and lower at high solids concentrations. These findings will be discussed in terms of the effect of slurry rheology on gas dispersion in Section 4.2.1.3. Here, a mechanism will be proposed for the unexpected increase in bubble size.

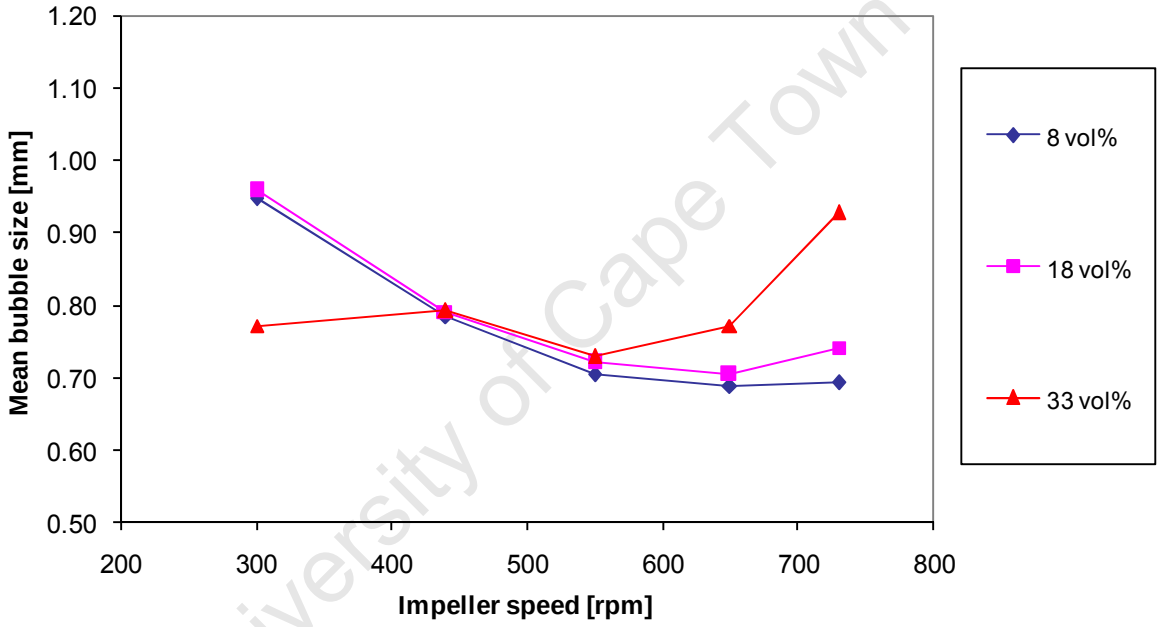

Figure 4.7 Effect of impeller speed on bubble size for Bindura nickel ore.

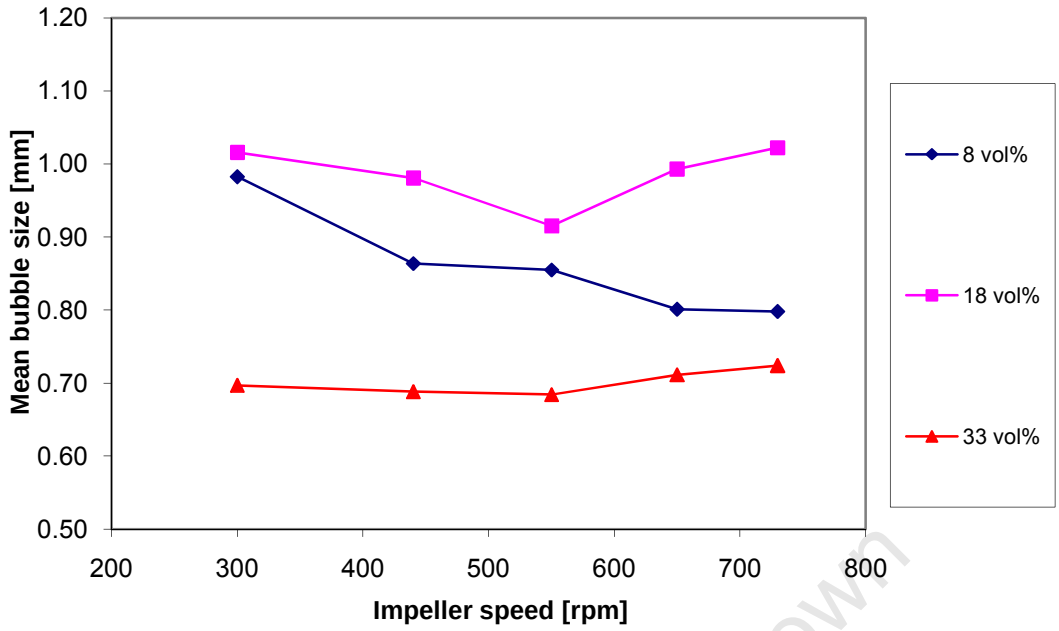

Figure 4.8 Effect of impeller speed on bubble size for Platreef ore.

4.2.1.2 Effect of Solids Concentration

Figures 4.9, 4.10 and 4.11 show the effect of solids concentration on bubble size for kaolin, Bindura nickel and Platreef ores respectively. The bubble size range from 0.55 to 1.10 mm typical of small flotation cells is observed as in Section 4.2.1.1.

Bubble size is observed to decrease for dilute solid concentrations as impeller speed increases as expected. At intermediate solids concentrations an increase in bubble size is observed (for kaolin ore) or the bubble size remains relatively constant (for Bindura nickel and Platreef ores). This result was expected as an increase in bubble size with solids concentration was observed by O'Connor *et al*. (1990) for a viscous slurry, as well as by Tucker *et al*. (1994) and Grau and Heiskanen (2005). At the highest solids concentrations a significant decrease in bubble size is observed, which was not expected.

A description of the mechanism with which bubble size increases and decreases with solids concentrations (particularly at high solid concentrations) is proposed and the discussion of these findings is presented in Section 4.2.1.3.

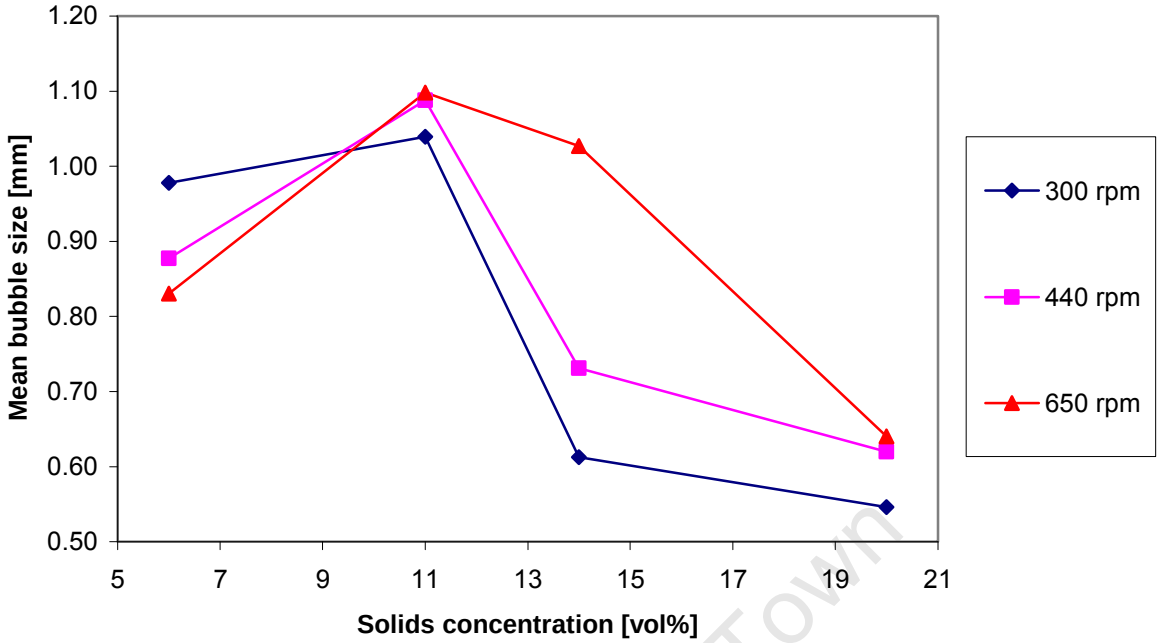

Figure 4.9 Effect of solids concentration on bubble size for kaolin ore.

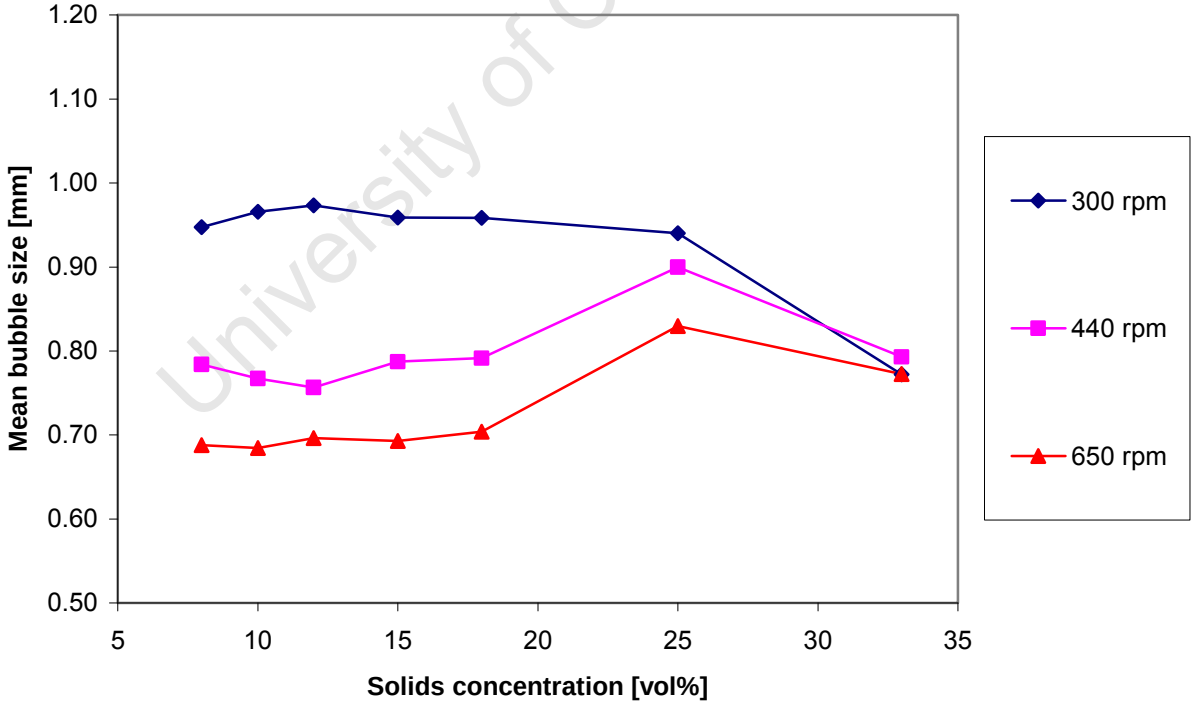

Figure 4.10 Effect of solids concentration on bubble size for Bindura nickel ore.

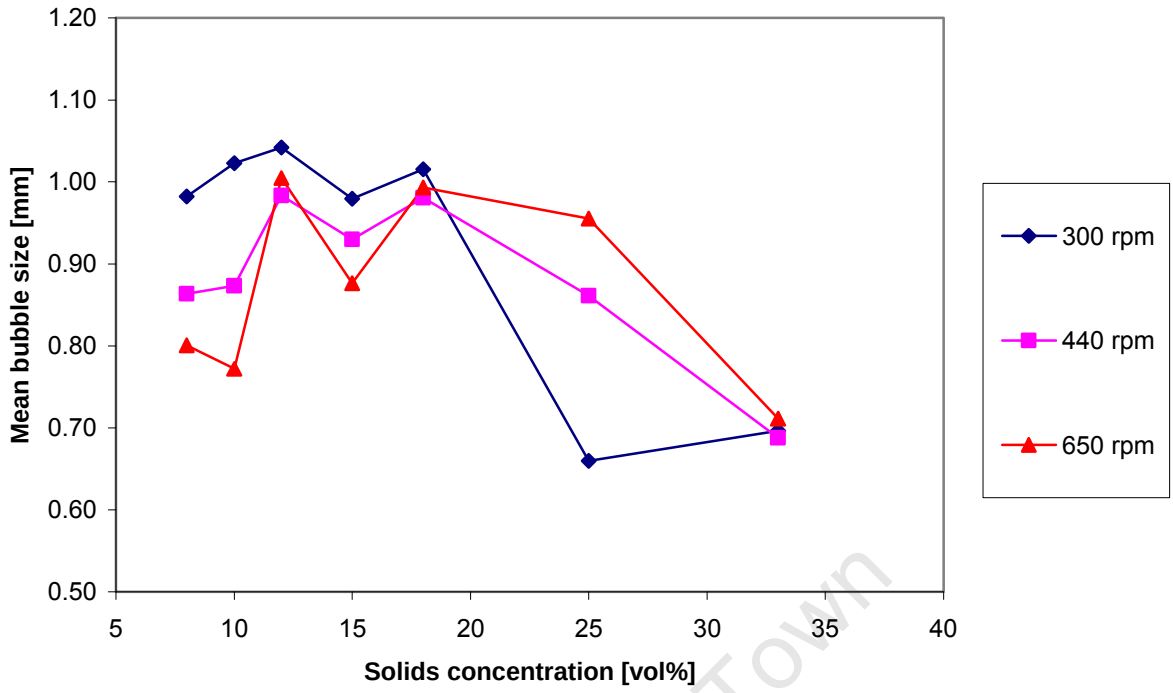

Figure 4.11 Effect of solids concentration on bubble size for Platreef ore.

4.2.1.3 Effect of Rheology on Bubble Size

In Section 4.2.1.1 it was observed that bubble size decreased with increasing impeller speed for dilute systems. This decrease was expected due to the generation of smaller bubbles by turbulent shear as the impeller speed increased as noted by Grau and Heiskanen (2005).

In Section 4.2.1.2 it was observed that bubble size either increased or remained relatively constant at intermediate solids concentration; this was expected and has been observed by O'Connor *et al.* (1990), Tucker *et al.* (1994) and Grau and Heiskanen (2005). An unexpected decrease in bubble size at the highest solids concentration was observed. The deviations from the expected results at high solids concentrations may be explained as follows.

An increase in solids concentration results in an increase in the slurry density. Slurry rheology is characterised by the yield stress and viscosity properties, both of which increase exponentially with solids concentration (c.f. Figures 4.4 and 4.5). In a

flotation cell, high viscosities result in increased turbulence damping with consequent generation of larger bubbles as noted by O'Connor *et al*. (1990). High yield stresses result in the formation of a 'cavern' of mixed slurry around the impeller, while the slurry in the bulk of the cell remains stagnant as noted by Bakker *et al*. (2009, 2010).

Local power intensities in this cavern may be very high resulting in the generation of very small bubbles by turbulent shear (around the impeller), even at moderate overall power input to the flotation cell. The formation of the cavern itself is dependent on the yield stress of the slurry as well as the impeller speed. A cavern tends to form at high yield stresses and low impeller speeds. However as the impeller speed increases the cavern increases in size and eventually disappears. It thus follows that the bubble size depends on a complex combination of mechanisms and whether a cavern is formed due to the conditions existing in the cell.

4.2.2 Gas Hold-Up

4.2.2.1 Effect of Impeller Speed

Figures 4.12 to 4.14 show the effect of impeller speed on gas hold-up. Here, the gas hold-up values range from 2% to 16% for kaolin ore, 1% to 10% for Bindura nickel ore and 2.5% to 16% for Platreef ore. The ranges are towards the lower end of the range observed in mechanical flotation cells as reported in Section 2.5.3.

Gas hold-up increases with impeller speed most significantly for dilute and intermediate solids concentrations. These trends were expected and have been observed as shown in Section 2.5.3. At high solids concentrations an increase in gas hold-up was also observed, however at a smaller degree compared to dilute and intermediate slurries; this result was not expected. The mechanism with which gas hold-up increases with impeller speed is discussed in Section 4.2.2.3.

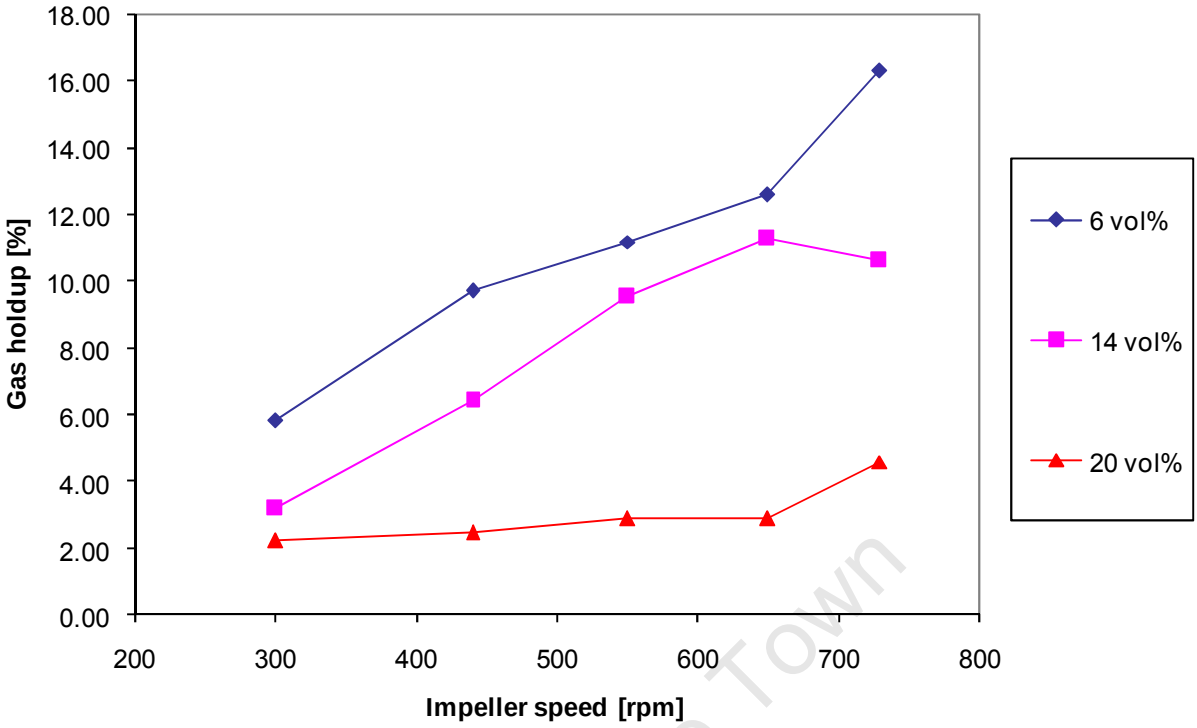

Figure 4.12 Effect of impeller speed on gas hold-up for kaolin ore.

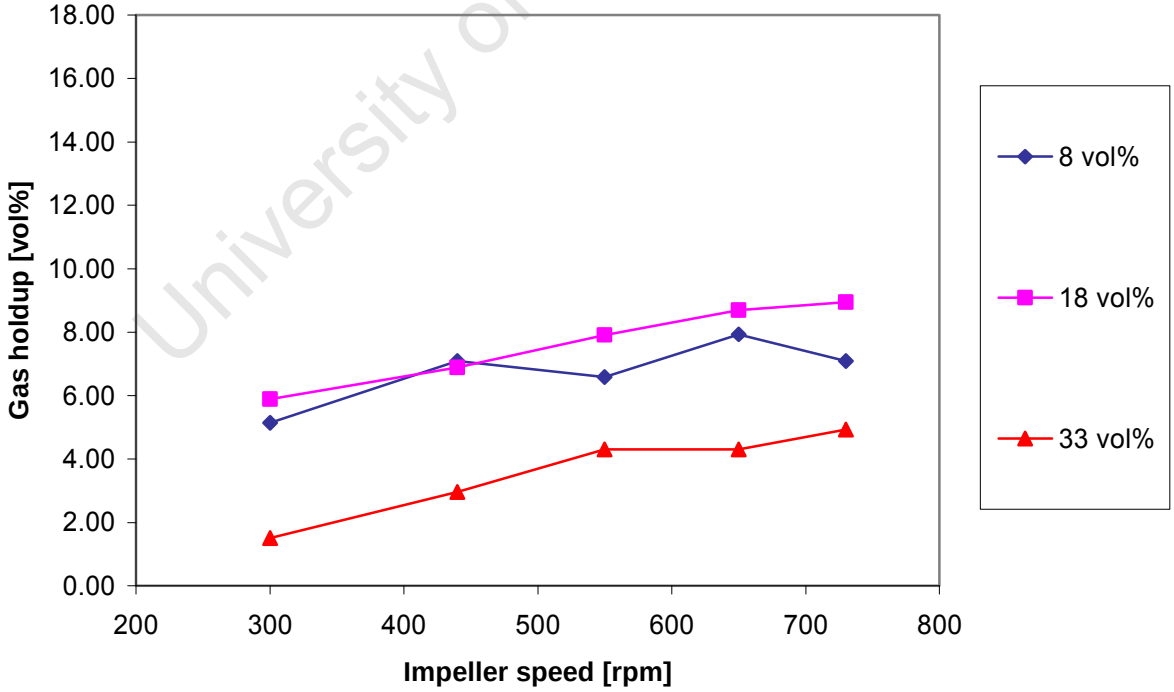

Figure 4.13 Effect of impeller speed on gas hold-up for Bindura nickel ore.

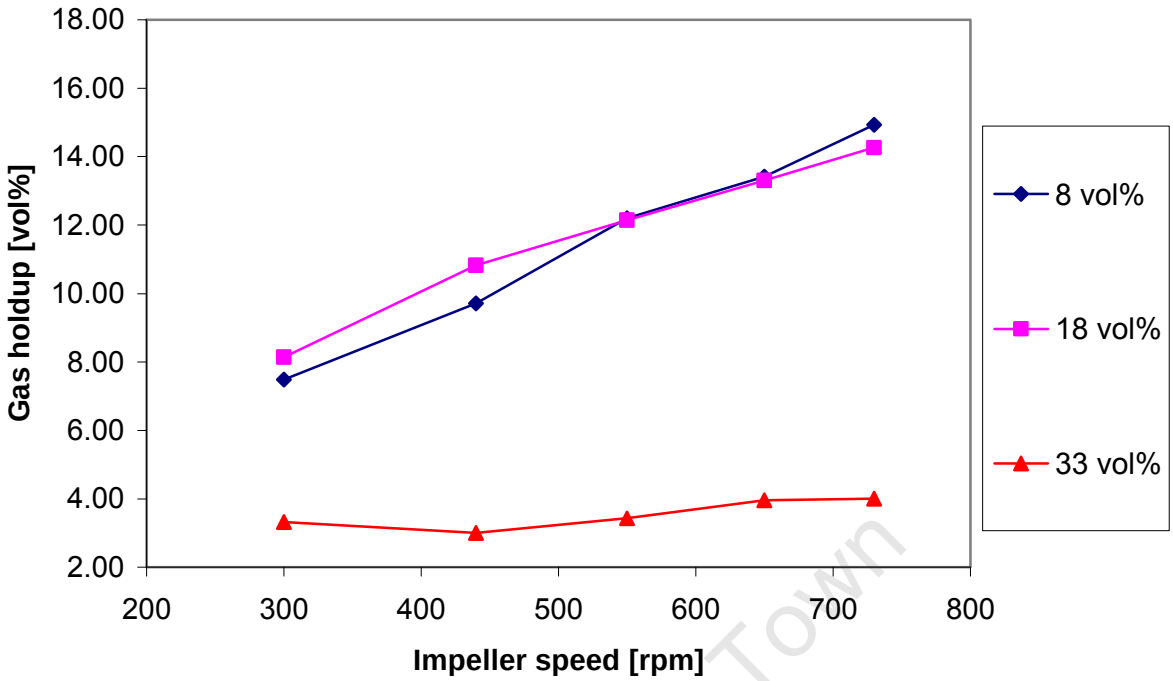

Figure 4.14 Effect of impeller speed on gas hold-up for Platreef ore.

4.2.2.2 Effect of Solids Concentration

Figures 4.15 to 4.17 show the effect of solids concentration on gas hold-up. Here, the gas hold-up ranges from 2.5% to 15%. As observed in Section 4.2.2.1 this range is towards the lower end of the range observed in mechanical flotation cells (see Section 2.6.3).

Gas hold-up decreases with increasing solids concentration for the impeller speeds tested. A dramatic decrease in gas hold-up can be observed at the highest solids concentrations; this result was not expected. Given that bubble size decreases at the highest solids concentration (c.f. Figures 4.9 to 4.11), one would expect that the gas hold-up would increase with decreasing bubble size. This unexpected decrease in gas hold-up however has been observed by several authors as shown in Section 2.7.3.3. Machon *et al.* (1980) however attributed this decrease in gas hold-up to the formation of larger bubbles. The mechanism behind the decrease in gas hold-up is proposed in Section 4.2.2.3.

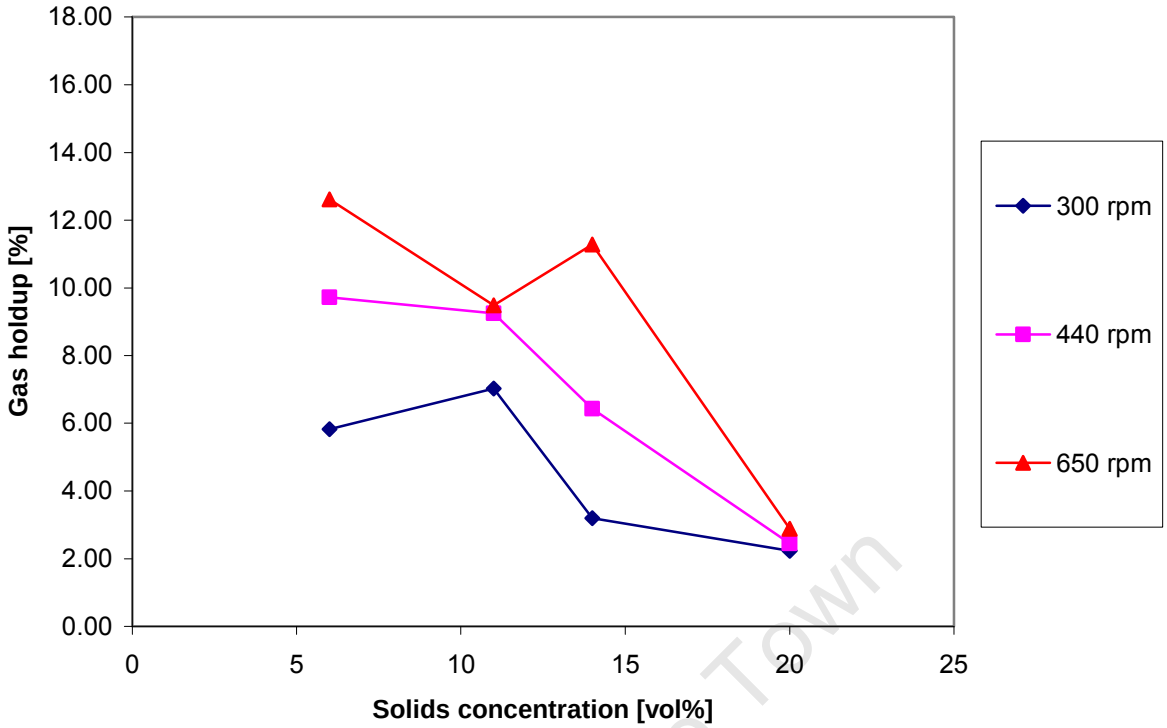

Figure 4.15 Effect of solids concentration on gas hold-up for kaolin ore.

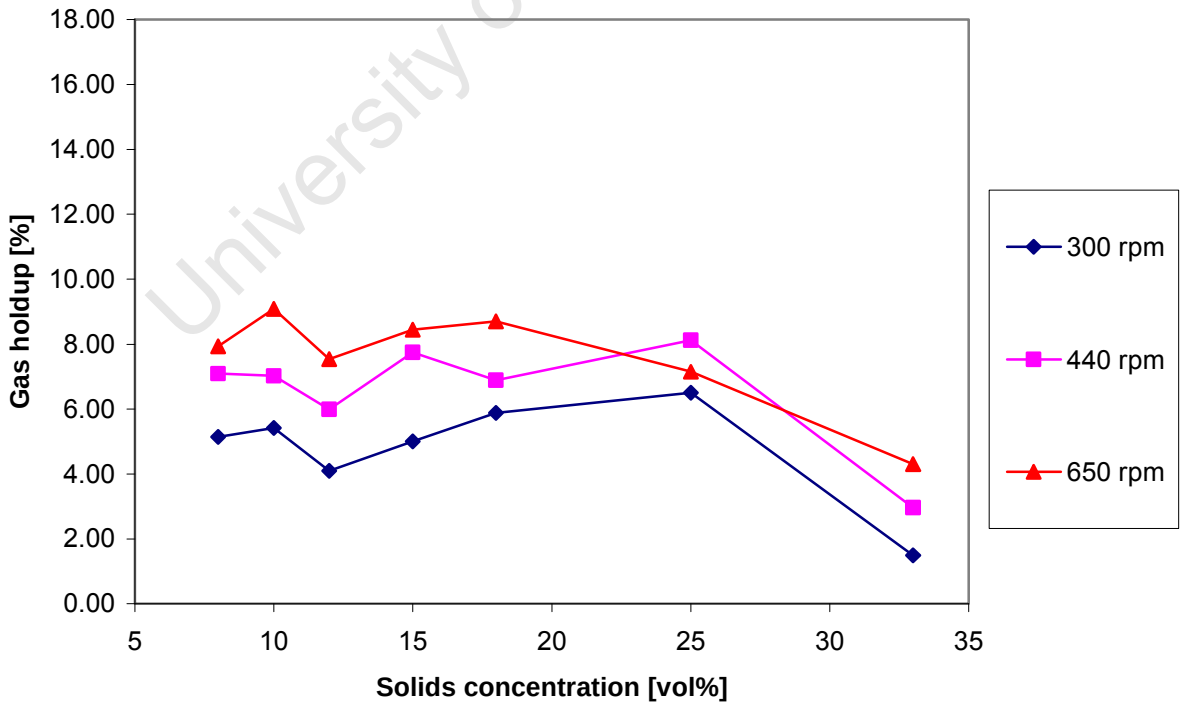

Figure 4.16 Effect of solids concentration on gas hold-up for Bindura nickel ore.

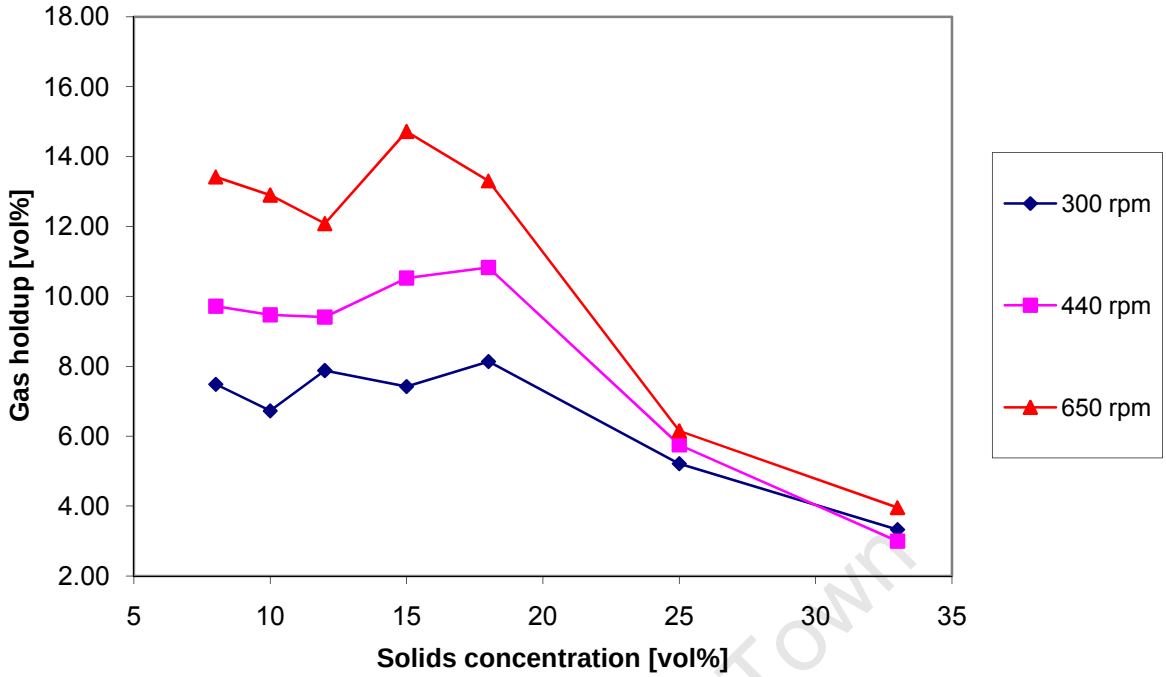

Figure 4.17 Effect of solids concentration on gas hold-up for Platreef ore.

4.2.2.3 Effect of Rheology on Gas Hold-Up

Gas hold-up was observed to increase with impeller speed, more significantly for dilute slurries. This increase in gas hold-up was expected due to a combination of the generation and dispersion of smaller bubbles as observed by Gorain *et al.* (1995b), Finch *et al.* (2000), and Grau and Heiskanen (2005). At intermediate solids concentrations gas hold-up either increased with impeller speed of remained relatively constant; this result has also been observed in literature. The results suggest that increasing solids concentration (the rheology of the slurry) leads to turbulence damping, resulting in the formation of slightly larger bubbles. This increase in slurry rheology was found to have minimal impact on the gas hold-up due to the corresponding increase in the drag forces on the bubbles. This result also supports the results observed for the bubble size at intermediate solids concentrations as described in Section 4.2.1.3. At the highest solids concentration there is a dramatic reduction in gas hold-up. This decrease was not expected as it also contradicts the observation of small bubbles formed at the highest solids concentrations. This contradiction may be explained as follows.

An increase in solids concentration results in an increase in yield stress and viscosity of slurries. This increase affects the generation of bubbles due to a combination of turbulence damping and the formation of a cavern as discussed in Section 4.2.1.3. However, this also affects the dispersion of bubbles throughout the flotation cell which has major impact on the gas hold-up in the flotation cell.

At very high solids concentrations a cavern forms which results in the generation of small bubbles. These bubbles however are poorly dispersed, mostly found in the near vicinity of the impeller (where there are high local power intensities) which results in low gas hold-ups through-out the rest of the flotation cell. The small bubbles rise directly to the surface of the cell from the cavern and are not distributed throughout the cell. Bakker *et al*. (2009, 2010) clearly noted the formation of a cavern at the highest solids concentrations for kaolin and Bindura nickel ores. Consequently, a high solids concentration may result in the generation of small bubbles but overall results in poor gas dispersion and a consequent low gas hold-up. Vlaev *et al*. (2008) observed similar results.

4.3 Effect of Rheology on Gas Dispersion

Figures 4.18 and 4.19 show the effect of yield stress on bubble size and gas hold-up for kaolin, Bindura nickel and Platreef ores for all impeller speeds and solids concentrations. These graphs provide a generic view of the effect of rheology on gas dispersion and further confirm the observations made in Section 4.2. Plots of bubble size and gas hold-up against viscosity were not generated as the rheology results in Section 4.1 indicated that the slurries were dominated by the yield stress. The yield stress therefore will be used as the primary rheological property that governs the quality of gas dispersion in the flotation cell.

Figure 4.18 shows that bubble size initially increases and then decreases with increasing yield stress. Figure 4.19 shows that the gas hold-up decreases with increasing yield stress. The results observed in Figures 4.18 and 4.19 are a result of slurry rheology. The reasons for this behaviour have been discussed in Section 4.2.

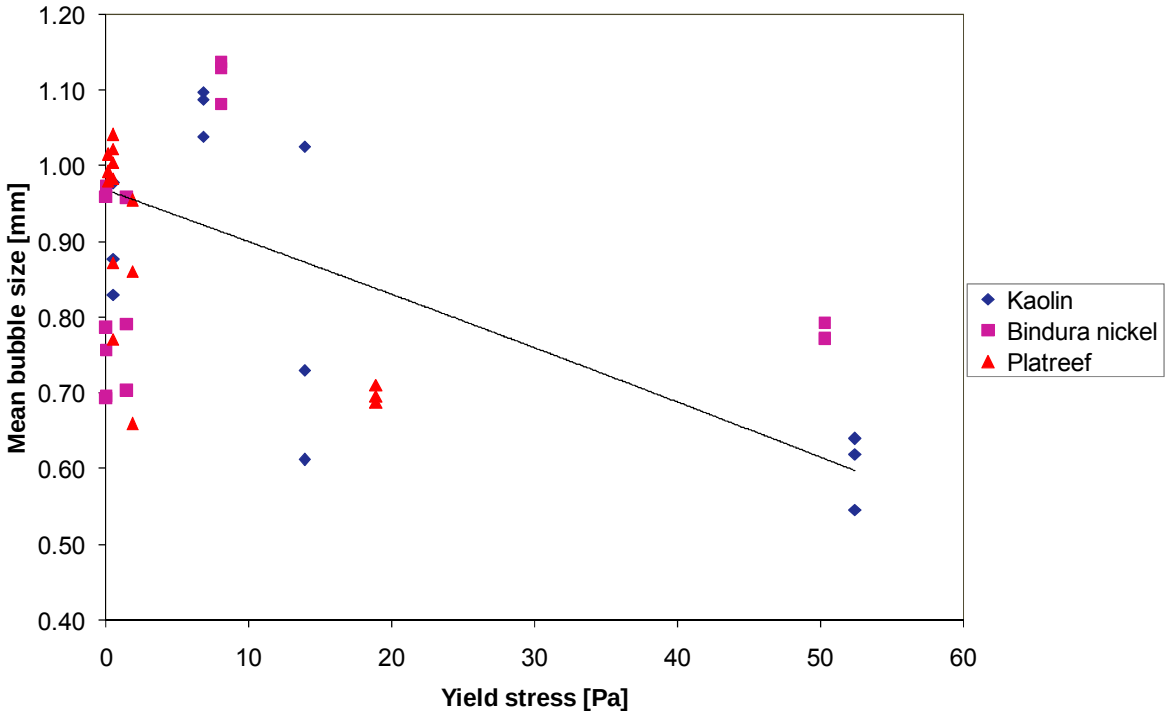

Figure 4.18 Effect of yield stress on bubble size for kaolin, Bindura nickel and Platreef ores at all impeller speeds and solids concentrations.

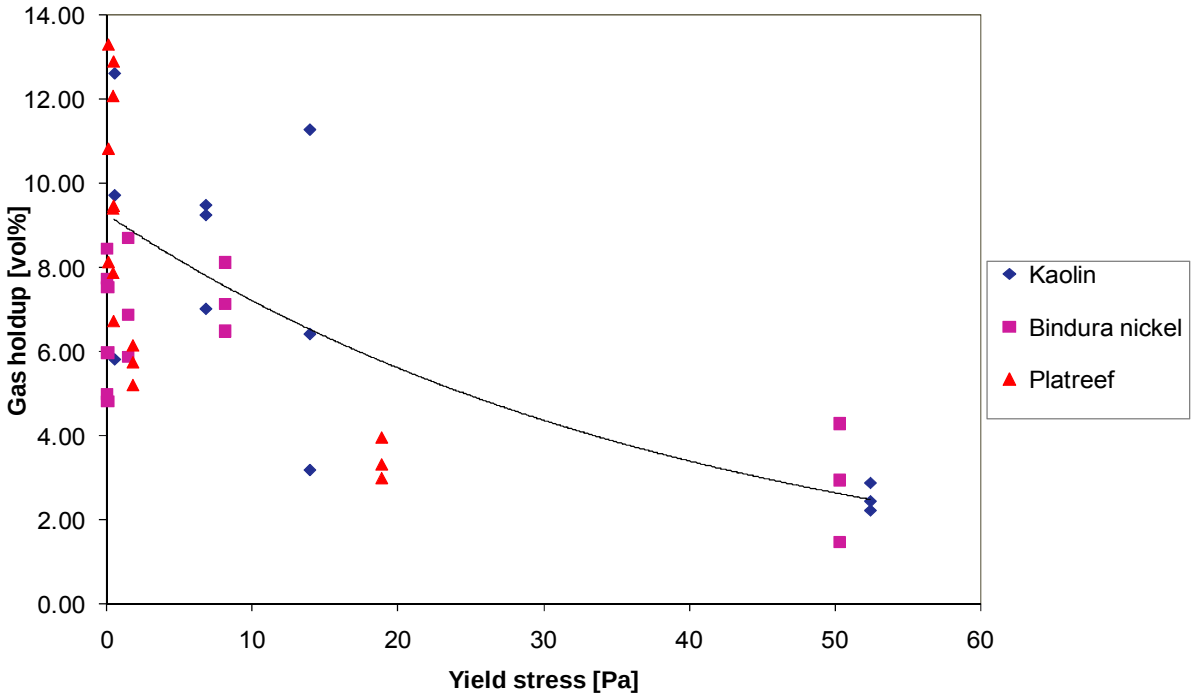

Figure 4.19 Effect of yield stress on gas hold-up for kaolin, Bindura nickel and Platreef ores at all impeller speeds and solids concentrations.

CHAPTER 5 Conclusions

This thesis investigates the effect of slurry rheology on gas dispersion in a pilot scale mechanical flotation cell. The study was conducted using kaolin, Bindura nickel and Platreef slurries. The following conclusions can be made from this study.

5.1 Rheology

The effect of slurry rheology was investigated at different solids concentrations for kaolin, Bindura nickel and Platreef ores. It was found that all three ores displayed typical non-Newtonian rheological behaviour. The three ores were found to exhibit Bingham plastic behaviour within the shear rate range tested. The slurry yield stresses and viscosities increased exponentially with increasing solids concentration. A much greater increase in slurry yield stress was observed compared to the viscosity. It was thus concluded that the yield stress was the dominant rheological characteristic for each ore type.

5.2 Gas Dispersion

Bubble size varied from 0.55 to 1.10 mm; this is towards the lower end of the range of bubble sizes observed in mechanical flotation cells. The observed trends in bubble size with increasing solids concentration displayed characteristics that were both expected and unexpected. At low solids concentrations the bubble size decreased with increasing impeller speed as expected. At intermediate solids concentrations the bubble size increased or remained relatively constant for the higher impeller speeds; this result was also expected. These characteristic trends have been observed in other literature studies. At the highest solids concentrations however, bubble size was found to decrease significantly, which was unexpected.

Overall gas hold-up varied from 2 to 15%. This is within the range observed in mechanical flotation cells. At low solids concentrations, gas hold-up increased with increasing impeller speed, as expected. At intermediate solids concentrations the gas hold-up was found to either increase or remain constant, as observed in literature. An unexpected and dramatic decrease in gas hold-up was observed particularly at the

highest solids concentrations for all ore types. This result highly contradicted the dramatic decrease in bubble size observed at these solids concentrations.

The unexpected decrease in bubble size and gas hold-up is attributed to slurry rheology. At the highest solids concentrations, the slurry rheology is distinctly non-Newtonian. This non-Newtonian effect is reflected in the high yield stresses observed for all three ores, resulting in the formation of a 'cavern' of slurry around the impeller. This leads to the generation of small bubbles in the impeller zone, but poor dispersion of these bubbles throughout the cell, resulting in low gas hold-ups.

5.3 Recommendations for Future Work

The following recommendations can be made based on the findings of this thesis:

- Given that only the global gas hold-up was measured, it is recommended that further work be conducted such that local gas hold-up be measured since local bubble size was measured.
- Local and global superficial gas velocity is recommended for measurement. These measurements would complete the gas dispersion study by adding the determination of the bubble surface area flux.
- Given that it was established in this study that slurry rheology has a significant effect on gas dispersion, it is recommended that studies indicating the addition of dispersants (to reduce yield stress and viscosity) be carried out. The effect of reduction of the slurry rheology parameters (yield stress and viscosity) on gas dispersion can thus also be investigated.
- Qualitative information was obtained on the ores that were tested. It is recommended that a more detailed mineralogical study be done, to further interpret the results.

References

1. Ahmed, N., Johnson, G. J., 1989, Flotation kinetics, Minerals Processing and Extractive Metallurgy Review, 5, 77-99.
2. Aldrich, C., Feng, D., 2000, The effect of frothers on bubble size distributions in flotation pulp phases and surface froths, Minerals Engineering, 13, 1049-1057.
3. Alejo, B., Barrientos, A., 2009, Model for yield stress of quartz pulps and copper tailings, International Journal of Mineral Processing, 93, 213–219.
4. Arratia, P.E., Kukura, J., Lacombe J., Muzzio, F.J., 2006, Mixing of shear-thinning fluids with yield stress in stirred tanks, AIChE Journal, 52, 2310 – 2322.
5. Aston, J.R., Drummond, C.J., Healy, T.W., 1983, The chemistry of action of simple and complex flotation frothers, AMIRA Project Report 79/P119.
6. Avotins, P.V., Ahschlager, S.S., Wicker, G.R., 1979, The rheology and handling of laterite slurries. In: Proceedings of the International Laterite Symposium, New Orleans, SME, 610–635.
7. Bakker, C. W., Meyer, C. J., Deglon, D. A., 2009, Numerical modelling of non-Newtonian slurry in a mechanical flotation cell, Minerals Engineering, 22, 944 – 950.
8. Bakker, C. W., Meyer C. J., Deglon, D. A., 2010, The development of a cavern model for mechanical flotation cells, Minerals Engineering, 23, 968 – 972.
9. Balerin, C., Aymard, P., Ducept, F. Vaslin S., Cuvelier, G., 2006, Effect of formulation and processing factors on the properties of liquid food foams, Journal of Food Engineering, 78, 802 – 809.
10. Barnes, H. A., 1999, The yield stress- a review or ‘παντα ρει’- everything flows?, Journal of Non-Newtonian Fluid Mechanics, 81, 137 – 178.
11. Blakey, B.C., James, D.F., 2003, Characterizing the rheology of laterite slurries, International Journal of Mineral Processing, 70, 23–39.
12. Brown, D. A. R., Jones, P. N., Middleton, J. C., Papadopoulos, G., Arik, E. B., 2004, Experimental Methods. In: E.L. Paul, V. Atiemo-Obeng and S.M. Kresta, Editors, The Handbook of Industrial Mixing, Wiley, New York.
13. Bruijn, W., Van’t Riet, K., Smith, J.M. , 1974, Power consumption with aerated Rushton turbines, Trans. Inst. Chem. Eng., 52, 88 – 104.

14. Burdukova, E., Becker, M., Bradshaw, D. J., and Laskowski, J. S., 2007, Presence of negative charge on the basal planes of New York talc, Journal of Colloid Interface Science, 315, 337–342.
15. Burgess, F.L., 1997, OK100 tank cell operation at Pasmisko-Broken Hill, Minerals Engineering, 10, 723-741.
16. Calderbank, P.H., 1958, Interfacial area in gas-liquid contacting with mechanical agitation, Trans. Inst. Chem. Eng., 36, 443-463.
17. Cawthorn, R. G., 1999, Platinum group elements mineralization in the Bushveld Complex - A critical reassessment of geochemical models, South Africa Journal of Geology, 102, 268-281.
18. Chalkley, M. E., Toirac, I. L., 1997, The acid pressure leach process for nickel and cobalt laterite. Part I: Review of operations at Moa. In: W.C. Cooper and I. Mihaylov, Editors, Proceedings of the Nickel–Cobalt 97 International Symposium-Volume I, August 17–20, The Metallurgical Society of CIM, Sudbury, Canada, 341–353.
19. Chhabra, R. P., Richardson, J. F., 1999, Non-Newtonian flow in the process industries, Butterworth-Heinemann, Oxford.
20. Cheng, D. C-H., Richmond, 1978, Some observations on the rheological behaviour of dense suspensions, Rheol. Acta., 17, 446- 453.
21. Chen, F., Gomez C.O., Finch, J.A., 2001, Bubble size measurement in flotation machines, Minerals Engineering, 14, 427-432.
22. Chimimba, L. R., Ncube, S. M. N., 1986, Nickel sulphide mineralization at Trojan Mine, Zimbabwe. In Anhaeusser C R, Maske S, Editors, Mineral Deposits of South Africa Geology Society, South Africa, Johannesburg, 1, 249-253.
23. Cho, Y.S., Laskowski, J.S., 2002, Effect of flotation frothers on bubble size and foam stability, International Journal of Mineral Processing, 64, 69-80.
24. Çınar, M., Şahbaz, O., Çınar , F., Kelebek, Ş, Öteyaka, B., 2007, Effect of the Jameson cell operating variables and design characteristics on quartz-dodecylamine flotation system, Minerals Engineering, 20, 1391 – 1396.
25. Cooke, M., Heggs, P.J., Rodgers T.L., 2008, The effect of solids on the dense phase gas fraction and gas–liquid mass transfer at conditions close to the heterogeneous regime in a mechanically agitated vessel, Chemical Engineering Research and Design, 86, 869–882.

26. Das, G.K., Kelly, N., Muir, D.M., 2011, Rheological behaviour of lateritic smectite ore slurries, Minerals Engineering, 24, 594 - 602.
27. Deglon, D. A., Harris, M.C., Franzidis, J-P., Tucker, J. P., O'Connor, C. T., 1993, An evaluation of bubble size and distribution in different flotation systems, Internal Report, University of Cape Town, South Africa.
28. Deglon, D., Sawyerr, F., O'Connor, C., 1999, A model to relate the flotation rate constant and the bubble surface area flux in mechanical flotation cells, Minerals Engineering, 12, 599-608.
29. Deglon, D.A., Egya-Mensah, D., Franzidis, J.P., 2000, Review of hydrodynamics and gas dispersion in flotation cells on South African platinum concentrators. Minerals Engineering, 13, 235-244.
30. Deglon, D. A., 2004, Surface Processes (CHE 338S) notes, University of Cape Town, South Africa.
31. Deglon, D.A., 2005, The effect of agitation on the flotation of platinum ores. Minerals Engineering, 18, 839–844.
32. De Lorgeril, C., Cuvelier, G., Vaslin, S., Launay, B., 2000, Etude rheologique d'un produit alimentaire foisonne: influence du procede et suivi veiillissement. Les cahiers de Rheologie, 17, 131 – 146.
33. Djelveh, G., Gros, J. B., 1995, Estimation of physical properties of foamed foods using energy dissipation in scraped-surface heat exchangers, Journal of Food Engineering, 26, 45 – 56.
34. Djelveh, G., Cornet, J. F., Gros, J. B., 1999, Combined effects of substrates and process parameters in food foaming processes. In G. M. Campbell, C. Webb, S. S. Pandellia, & K. Niaranjan, Editors, Bubbles in foods. St Paul, Minnesota: Eagan Press.
35. Du, H., 2008, Flotation chemistry of selected alkali halide salts and naturally hydrophobic minerals: a molecular dynamics simulation study, PhD Dissertation, University of Utah.
36. Duarte, A.C.P., Grano, S.R., 2007, Mechanism for the recovery of silicate gangue minerals in the flotation of ultrafine sphalerite, Minerals Engineering, 20, 766-775.
37. Egyah-Mensah, D., Hydrodynamics and gas dispersion in industrial flotation cells, 1998, MSc. Thesis, University of Cape Town, South Africa.

38. Elson, T. P., Cheesman, D. J., Nienow, A. W., 1986, X-ray studies of cavern sizes and mixing performance with fluids possessing a yield stress, Chemical Engineering Science, 41, 2555-2562.
39. Falutsu, M., 1994, Direct measurement of gas rate in a flotation machine, Minerals Engineering, 7, 1487 – 1494.
40. Fangary, Y.S., Barigou, M., Seville, J.P.K., Parker, D.J., 2000, Fluid trajectories in a stirred vessel of non-Newtonian liquid using positron emission particle tracking, Chemical Engineering Science, 55, 5969–5979.
41. Finch, J.A., Dobby, G., Column flotation, 1990, Pergamon Press, Oxford.
42. Finch, J. A., Xiao, C., Hardie, C., Gomez, C. O., 2000, Gas dispersion properties: bubble surface area flux and gas hold-up, Minerals Engineering, 13, 365 – 372.
43. Finch, J.A., Gelinas, S., Moyo, P., 2006, Frother-related research at McGill University, Minerals Engineering, 19, 726-733.
44. Fuerstenau, M. C., Han, K. N., 2003, Principles of mineral processing, Society for Mining, Metallurgy, and Exploration, Inc. (SME), Littleton, Colorado.
45. Fuerstenau, M. C., Jameson, J. G., Yoon, R., 2007, Froth flotation: A century of innovation, Society for Mining, Metallurgy, and Exploration, Littleton, Colorado.
46. Gain, S. B., Mostert, A. B., 1982, The geological setting of the platinoid and base metal sulfide mineralisation in the Platreef of the Bushveld Complex in Drenthe, north of Potgietersrus, Economic Geology, 77, 1395–1404.
47. Gao, M., Forssberg, E., 1993, The influence of slurry rheology on ultra-fine grinding in a stirred ball mill, 18th International Mineral Processing Congress, Sydney, CA (Conference Article), Australia, 237 – 244.
48. George, P., Nguyen, A. V., Jameson, G. J., 2004, Assessment of true flotation and entrainment in the flotation of submicron particles by fine bubbles, Minerals Engineering, 17, 847 – 853.
49. Gomez, C. O., Finch, J. A., 2002, Gas dispersion measurements in flotation cells, International Journal of Minerals Engineering, 84, 51 – 58.
50. Gomez, C.O., Cortés-López, F., Finch, J.A., 2003, Industrial testing of a gas holdup sensor for flotation systems, Minerals Engineering, 16, 493-501.
51. Goodwin, J. W., Ottewill, R. H., 1969, Rheological studies on kaolinite suspensions, Proceedings of the British Ceramic Society, London, 13, 31-45.

52. Gorain, B. K., Franzidis, J. P., Manlapig, E. V., 1995a, Studies on impeller type, impeller speed and air flow rate in an industrial scale flotation cell - Part 1: Effect on bubble size distribution, Minerals Engineering, 8(6), 615 – 635.
53. Gorain, B. K., Franzidis, J. P., Manlapig, E. V., 1995b, Studies on impeller type, impeller speed and air flow rate in an industrial scale flotation cell Part 2: Effect on gas hold-up, Minerals Engineering, 8(12), 1557 – 1570.
54. Gorain, B., Franzidis, J., Manlapig, E., 1996, Studies on impeller type, impeller speed and air flow rate in an industrial scale flotation cell -Part 3: Effect on superficial gas velocity, Minerals Engineering, 9 (6), 639–654.
55. Gorain, B. K., Franzidis, J. P., Manlapig, E. V., 1997, Studies on impeller type, impeller speed, and air flow rate in an industrial scale flotation cell - Part 4: Effect of bubble surface area flux on flotation performance, Minerals engineering, 10, 367 – 379.
56. Gorain, B. K., Oravainen, H., Allenius, H., Peaker, R., Weber, A., Tracyzk, F., 2007, Mechanical froth flotation cells. In Fuerstenau, M. C., Jameson, G., and Yoon, R. H., (Eds), Froth flotation: A century of innovation, SME, 637 – 680.
57. Grau, R. A., Heiskanen, K., 2003, Gas dispersion measurements in a flotation cell, Minerals Enginerering, 16, 1081 – 1089.
58. Grau, R. A., Heiskanen, K., 2005, Bubble size distribution in laboratory scale flotation cells, Minerals Engineering, 18, 1164 – 1172.
59. Grau, R. A., 2006, An investigation of the effect of physical and chemical variables on bubble generation and coalescence in a laboratory scale flotation cells, Doctoral Thesis, Helsinki University of Technology, Espoo, Finland.
60. Grenville, R. K., Nienow, A. W., 2004, Blending of miscible liquids. In: E.L. Paul, V. Atiemo-Obeng and S.M. Kresta, Editors, The Handbook of Industrial Mixing, Wiley, New York.
61. He, M., Wang, Y., Forssberg, E., 2004, Slurry rheology in wet ultrafine grinding of industrial minerals: A review, Powder Technology, 147, 94-112.
62. He, M., Wang, Y., Forssberg, E., 2006, Parameter studies on the rheology of limestone slurries, International Journal of Mineral Processing, 78, 63–77.
63. He, M., Forssberg, E., 2007, Influence of slurry rheology on stirred media milling of quartzite, International Journal of Mineral Processing, 84, 240 – 251.
64. Hernandez, H., Gomez, C. O., Finch, J. A., 2003, Gas dispersion and de-inking in a flotation column, Minerals Engineering, 16, 739 – 744.

65. Hintikka, V.V., Kalapuda, S., Viitanen, P.I., 1999, Effect of rheology on grinding efficiency in the laboratory scale continuous classifying mill, 20, 133 – 154.
66. Hinze, J. O., 1955, AIChEJ, 289.
67. Huynh, L., Jenkins, J., Ralston, J., 2000, Modification of the rheological properties of concentrated slurries by control of mineral-solution interfacial chemistry, International Journal of Minerals Processing, 59, 305 – 325.
68. Jahani, Y, Ehsani, M., 2009, The rheological modification of talc-filled polypropylene by epoxy–polyester hybrid resin and its effect on morphology, crystallinity, and mechanical properties, Polymer Engineering Science, 49, 619–629.
69. Jenkins, P., Ralston, J., 1997, The adsorption of a polysaccharide at the talc aqueous solution interface, Colloids and Surfaces, 27, 40.
70. Johnson, S. B., Russell, A. S., Scales, P. J., 1998, Volume fraction effects in shear rheology and electro acoustic studies of concentrated alumina and kaolin suspensions, Colloids and Surfaces A: Physicochemical and Engineering Aspects, 141, 119-130.
71. Kelly, E.G, Spottiswood, D.J., 1982, Introduction to minerals processing, John Wiley & Sons, 301 – 305.
72. King, R. P., Hatton, T. A., Hulbert, D. G., 1974, Bubble loading during flotation, Transactions of The Institution of Mining and Metallurgy, 83, C112 – C115.
73. King, R. P., 1982, Flotation of fine particles: In Principles of flotation, SAIMM Monograph series, 3, 215 – 225.
74. Kirjavainen, V.M, Heiskanen, K., 2007, Some factors that affect beneficiation of sulphide nickel-copper ores, Minerals Engineering, 20, 629 – 633.
75. Klimpel, R. R., 1988, Grinding aids based on slurry rheology control. In: Somasundaran, P., Moudgil, B. M., Reagents in Mineral Technology, Marcel Dekker, New York, 179-194.
76. Kroezen, A. B. J., Groot Wassink, J., 1987, Bubble size distribution and energy dissipation in foam mixer, Journal of the Society of Dyers and Coulorists, 103, 386 – 394.
77. Kuan, H., Finch, J. A., 2010, Impact of talc on pulp and froth properties in F150 and 1-pentanol frother systems, Minerals Engineering, 23, 1003–1009.
78. Kumar, B., 2010, Energy dissipation and shear rate with geometry of baffled surface aerator, Chemical Engineering Research Bulletin, 14, 92 – 96.

79. Kushalkar, K. B., Pangarkar, V. G., 1995, Particle mass transfer in three phase mechanically agitated contactors: Power law fluids, , 34, 2485.
80. Kyle, J.H., Furfaro, D., 1997, The Cawse nickel/cobalt laterite project metallurgical process development. Part I: Review of operations at Moa. In: W.C. Cooper and I. Mihaylov, Editors, Proceedings of the Nickel–Cobalt 97 International Symposium-Volume I, August 17–20, The Metallurgical Society of CIM, Sudbury, Canada, 379–389.
81. Loginov, M., Larue, O., Lebovka, N., Vorobiev, E., 2008, Fluidity of highly concentrated kaolin suspensions: Influence of particle concentration and presence of dispersant, Colloids and Surfaces A: Physicochemical and Engineering Aspects, 325, 64 - 71.
82. Machon, V., Vlcek, J., Nienow, A.W., Solomon, J., 1980, Some effects of pseudoplasticity on hold-up in aerated, agitated vessels, Chemical Engineering Journal, 19(1), 67-74.
83. Machon, V., Pacek, A. W., Nienow, A. W., 1997, Bubble sizes in electrolyte and alcohol solutions in a turbulent stirred vessel, Trans IChemE Part A, 75, 339-348.
84. Massola, C. P., Chaves, A. P., Lima, J. R. B., Andrade, C. F.,2009, Separation of silica from bauxite via froth flotation, Minerals Engineering, 22, 315–318.
85. Metz, B., Kossen, N. W. F., van Suijdam, J. C., 1979, The rheology of mould suspensions, Advances in Biochemical Engineering, 11, 103 – 156.
86. Metzner, A. B., Otto, R. E., 1957, Agitation of non-Newtonian fluids, AIChE J., 3, 3-10.
87. Moore, I. P. T., Cossor, G., Baker, M., 1995, Velocity distributions in a stirred tank containing a yield stress fluid, Chemical Engineering Science, 50(15), 2467 – 2481.
88. Motteram, G., Ryan, M., Weizenbach, R., 1997, Application of the pressure acid leach process to Western Australian nickel/cobalt laterites. In: W.C. Cooper and I. Mihaylov, Editors, Proceedings of the Nickel–Cobalt 97 International Symposium-Volume I, August 17–20, The Metallurgical Society of CIM, Sudbury, Canada, 391–407.
89. Muster, T. H., Prestidge, C. A., 1995, Rheological investigations of sulphide mineral slurries, Minerals Engineering, 8, 1541-1555.

90. Nagata, S., Nishikawa, M., Tada,H., Hirabayashi, H., Gotoh, S., 1970, Power consumption of mixing impellers in Bingham plastic liquids, Journal of Chemical Engineering of Japan, 3, 237–243.
91. Naik, S., van Drunick, W., 2007, Anglo Research (AR) experience with integrated comminution and flotation plant modelling, Journal of The South African Institute of Mining and Metallurgy, 107, 641-650.
92. Ndlovu, B.N., Burdukova, E., Becker, M., Deglon, D.A., Franzidis, J.P., Laskowski, J.S., 2010, An investigation on the effects of chrysotile particle shape and anisotropic properties on the rheology of chrysotile suspensions. In Proceedings of XXV International Mineral Processing Congress, Brisbane, 6-10 September.
93. Ndlovu, B., Becker, M., Forbes, E., Deglon, D., Franzidis, J. P., 2011, The influence of phyllosilicate mineralogy on the rheology of mineral slurries, Minerals Engineering, 24 (12), 1314 – 1322.
94. Nesse, T., Schubert, H., Mockel, H.O., 1979, Tubulenzmessung in Mehrphasenstromungen gasformig/flussig and fest/flussig mittels einer Piezsonde, 2nd European Symposium on Particle Measurement Techniques, Nurnberg, 431-445.
95. Nesset, J.E., Hernandez-Aguilar, J.R., Acuna, C., Gomez, C.O., Finch, J.A., 2006, Some gas dispersion characteristics of mechanical flotation machines, Minerals Engineering, 19, 807-815.
96. Newell, R., Grano, S., 2006, Hydrodynamics and scale up in Rushton turbine flotation cells: Part 1- Cell hydrodynamics, International Journal of Minerals Processing, 81, 1-13.
97. Nguyen, Q. D., Boger, D. V., 1985, Direct yield stress measurement with the vane method, Journal of rheology, 29, 335 – 347.
98. Nienow, A. W., Elson T. P., 1988, Aspects of mixing in rheologically complex fluids, Chemical Engineering Research and Design, 66, 5 – 15.
99. Nienow, A. W., Ulbrecht, J. J., 1985, Gas liquid mixing and mass transfer in high viscosity liquids, Mixing of liquids by mechanical agitation, edited by J. J. Ulbrecht and G. K. Patterson, Gordon & Breach, New York, Chapter 6.
100. Nonaka, M., Inoue, T., Imaizumi, T., 1982, A micro-hydrodynamic flotation model and its application to the flotation process, Proceedings XIV, International Minerals Processing Congress, Toronto, III-9. I-III-9.19.

101. O'Connor, C.T., Randall, E.W., Goodall, C.M., 1990, Measurement of the effect of physical and chemical variables on bubble size, International Journal of Mineral Processing, 28, 139 – 149.

102. Oldshue, J.Y., 1983, Fluid mixing technology and practice, Chemical Engineering, 83 – 108.

103. Parolis, L. A. S., van der Merwe, R., van Leerdam, G. C., Prins, F. E., Smeink, R. G., 2007, The use of ToF-SIMS and microflotation to assess the reversibility of binding CMC onto talc, Minerals Engineering, 20, 970 – 978.

104. Parthasarathy, R., Jameson, G.J., Ahmed, N., 1991, Bubble breakup in stirred vessels-predicting the Sauter mean diameter, Trans. Inst. Chem. Eng., Part A 69, 295-301.

105. Parthasarathy, R., Ahmed, N. , 2004, Bubble size distribution in a gas sparged vessel agitated by a Rushton turbine, Chemical Engineering Science, 33, 703.

106. Pease, J. D., Curry, D. C., Young, M. F., 2006, Designing flotation circuits for high fines recovery, Minerals Engineering, 19, 831-840.

107. Poncin, S., Nguyen, S., Midoux, N., Breysse, J., 2002, Hydrodynamics and volumetric gas-liquid mass transfer coeffiecient of a stirred vessel equipped with a gas-inducing impeller, Chemical Engineering Science, 57, 3299 – 3306.

108. Power, A., Franzidis, J.P., 2000, The characterization of hydrodynamic conditions in industrial flotation cells, Proceedings AusIMM 7th Mill Operators Conference, Kalgoorlie, WA, 243-255.

109. Pradip, M. S. M., Malghan, S. G., 1998, Shear yield stress of flocculated alumina-zirconia mixed suspensions: effect of solid loading, composition and particle size distribution, Chemical Engineering Science, 53, 3073 – 3079.

110. Preen, B. V., 1961, Gas-liquid mass transfer in a mechanically agitated vessel, PhD dissertation, University of Natal, Durban, South Africa.

111. Prestidge, C.A., 1997, Rheological investigations of ultrafine galena particle slurries under flotation-related conditions, International Journal of Mineral Processing, 51, 241–254.

112. Pryor, E. J., 1965, Mineral processing, 3rd Ed., Applied Science Publishers Ltd, London.

113. Quinn, J.J., Kracht, W., Gomez, C.O., Gagnon, C., Finch, J.A., 2007, Comparing the effect of salts and frother (MIBC) on gas dispersion and froth properties, Minerals Engineering, 20, 1296–1302.

114. Rennie, J., Valentin, F. H. H., 1968, Gas dispersion in agitated tanks, Chemical Engineering Science, 23, 663-664.

115. Sánchez Pérez, J.A., Rodríguez Porcel, E.M., Casas López, J.L., Fernández Sevilla, J.M., Chisti, Y., 2006, Shear Rate in Stirred Tank and Bubble Column Bioreactors, 124, 1 – 5.

116. Savreux, F., Jay, P., Magnin, A., 2007, Viscoplastic fluid mixing in a rotating tank, Chemical Engineering Science, 62, 2290 – 2301.

117. Sawyerr, F., Deglon, D. A., O'Connor, C. T., 1998, Prediction of bubble size distribution in mechanical flotation cells, The Journal of the South African Institute of Mining and Metallurgy, 179-186.

118. Schubert, H., Bischofberger, C., 1978, On the hydrodynamics of flotation machines, International Journal of Minerals Processing, 5, 131-142.

119. Schubert, H., Bischofberger, G., Koch, P., 1982, Influence of hydrodynamics on flotation processes, Autbereitungs-Tech., 23, 306 – 315.

120. Schubert, H., 1999, On the turbulence controlled micro processes in flotation machines, International Journal of Mineral Processing, 56, 257–276.

121. Schwarz, S., Alexander, D., 2006, Gas dispersion measurements in industrial flotation cells, Minerals Engineering, 19, 554-560.

122. Shi, F. N., Napier-Munn, T. J., 1996, A model for slurry rheology, International Journal of Mineral Processing, 47, 103–123.

123. Sjöberg, M., Bergström, L., Larsson, A., Sjöström, E., 1999, The effect of polymer and surfactant adsorption on the colloidal stability and rheology of kaolin dispersions, Colloids and Surfaces A: Physical and Engineering Aspects, 159, 197-208.

124. Solomon, J., Nienow, A. W., Pace, G. W., 1981, Flow patterns in agitated plastic and pseudo-plastic fluids, In: Fluid Mixing, Inst. Chem. Eng. Symp. Ser., 64, 1773-1781.

125. Street, N., Buchanan, A. S., 1956, The ζ-potential of kaolinite particles, Australian Journal of Chemistry, 9, 450-466.

126. Sweet, C., van Hoogstraten, J., Harris, M., Laskowski, J.S., 1997, The effect of frothers on bubble size and frothability of aqueous solutions, In: Finch, J.A., Rao, S.R., Holubec, I., Processing of complex ores, Proc. 2nd UBC-McGill Int. Symp. Met Soc of CIM, Montreal, 235-245.

127. Tangsathitkulchai, C., Austin, L. G., (1989), Slurry density effects on ball milling in a laboratory ball mill, Powder Technology, 59, 285 – 293.

128. Tangsathitkulchai, C., 2003, The effect of slurry rheology of fine grinding in a laboratory mill, 69, 29–47.

129. Tatterson, G. B., 1991, Fluid mixing and gas dispersion in agitated tanks, McGraw-Hill, Inc.

130. Taute, J. J., 2006, Anglo Platinum bubble sizer user manual, Divisional Metallurgical Laboratory, Rustenburg, South Africa.

131. Thakur, R. K., Vial, C., Djelveh G., 2003, Foaming of commercial grade food products in continuous stirred column, Transactions of IChemE, 81(A), 1083 – 1089.

132. Trahar, W. J., Warren, L. J., 1976, The floatability of very fine particles- a review, International Journal of Mineral Processing, 3, 103 -131.

133. Tucker, J.P., Deglon, D.A., Franzidis, J.P., Harris, M.C., O'Connor, C.T., 1994, An evaluation of a direct method of bubble size distribution measurement in a laboratory batch flotation cell, Minerals Engineering, 7(5–6), 667 –680.

134. Tyndale-Biscoe, R., 1972, The geology of the country around Gwanda, Southern Rhodesia Bulletin No. 36 (reprinted 1972), Geological Survey, Salisbury.

135. Van der Westhuizen, A. P., 2004, The evaluation of solids suspension in a pilot scale mechanical flotation cell, MSc. Thesis, University of Cape Town, South Africa.

136. Van der Westhuizen, A.P., Deglon, D.A., 2007, Evaluation of solids suspension in a pilot-scale mechanical flotation cell, Minerals Engineering, 20(3), 233-240.

137. Van der Westhuizen, A.P., Deglon, D.A., 2008, Solids suspension in a pilot-scale mechanical flotation cell: A critical impeller speed correlation, Minerals Engineering, 21, 621-629.

138. Vera, M.A., Franzidis, J. P., Manlapig, E.V., 1999, The JKMRC high bubble surface area flux flotation cell, Minerals Engineering, 12(5), 477-484.

139. Viti, C., Mellini, M., Rumori, C., 2005, Exsolution and hydration of pyroxenes from partially serpentinized hartzburgites, Mineralogical Magazine, 69(4), 491–507.

140. Vieira, M. G., Peres, A. E. C., 2012, Effect of reagents on the rheological behaviour of an iron ore concentrate slurry, International Journal of Mining Engineering and Mineral Processing, 1(2), 38 – 42.

141. Vlaev, S.D., Valeva, M.D., Mann R., 2002, Some effects of rheology on the spatial distribution of gas holdup in a mechanically agitated vessel, Chemical Engineering Journal, 87, 21-30.

142. Wang, Y., Forssberg, E., 1995, Dispersants in stirred ball mill grinding, Kona 13, 67 – 77.

143. Waters, K. E., Hadler, K., Cilliers, J. J., 2008, The flotation of fine particles using charged microbubbles, Minerals Engineering, 21, 918 – 923.

144. Whittington, B. I., Muir, D. M., 2000, Pressure acid leaching of nickel laterites: a review, Mineral Processing and Extractive Metallurgy Reviews, 21, 527–600.

145. Wichterle, K., Wein, O., 1975, Agitation of concentrated suspensions, Presented in CHISA 75, Paper B4.6, Prague, Czechoslovakia.

146. Wichterle, K., Wein, O., 1981, Threshold of mixing of non-Newtonian fluids, International Chemical Engineering Journal, 21, 116 – 120.

147. Wiese, J.G., Harris, P.J. and Bradshaw, D.J., 2010, The effect of increased frother dosage on froth stability at high depressant dosages, Minerals Engineering, 23(11-13), 1010-1017.

148. Wilkens, D.C., Miller, J.D., Plummer, J.R., Dietz, D.C., Myers, K.J., 2005, New techniques for measuring and modelling cavern dimensions in a Bingham plastic fluid, Chemical Engineering Science, 60, 5269–5275.

149. Williams, D. J. A., Williams, K. P., 1977, Electrophoresis and zeta potential of kaolinite, Journal of Colloid and Interfacial Science, 65(1), 79-87.

150. Wills, B.A., 1997, Mineral processing technology – An introduction to the practical aspects of ore treatment and mineral recovery, 6th Ed., 294 – 297.

151. Wills, B. A., Napier-Munn, T., 2006, Will's mineral processing technology – an introduction to the practical aspects of ore treatment and mineral recovery, 7th Ed., 306 - 307.

152. Woodburn, E. T., King, R. P., Colborn, R. P., 1971, The effects of particle size distribution on the performance of a phosphate flotation process, Met Trans., 2, 3163 – 3174.

153. Yang, H. G., Li, C. Z., Gu, H. C., Fang, T. N., 2001, Rheological behavior of titanium dioxide suspensions, J. Colloid Interface Sci., 236, 96 – 103.

154. Yianatos, J.B., Bergh, L.G., Cortés, G.A., 2001, Hydrodynamic and metallurgical characterization of industrial flotation banks for control purposes, Minerals Engineering, 14(9), 1033-1046.

155. Yianatos, J., Bergh, L., López, R., Molinet, P., Jiménez, P., 1999, Characterization of an industrial flotation column at División Andina, Codelco, Minerals Engineering, 12 (5), 565-569.

156. Yoon, R. H., 2000, The role of surface forces in flotation kinetics: In Proceedings of the XXI International Mineral Processing Congress, B8a, 1 – 7.

157. Yue, J., Klein, B., 2004, Influence of rheology on the performance of horizontal stirred mills, Minerals Engineering, 17, 1169-1177.

Appendices

Appendix A: Rheology data

Table 7.1 Kaolin shear rate and shear stress data

Measuring Points	6 vol%		11 vol%		14 vol%		20 vol%	
	Shear Rate [1/s]	Shear Stress [Pa]	Shear Rate [1/s]	Shear Stress [Pa]	Shear Rate [1/s]	Shear Stress [Pa]	Shear Rate [1/s]	Shear Stress [Pa]
1	1000.00	6.73	1000.00	13.60	1000.00	23.40	1000.00	75.30
2	728.00	4.64	728.00	11.80	728.00	21.00	728.00	70.90
3	530.00	3.06	530.00	10.50	530.00	19.30	530.00	67.30
4	386.00	2.40	386.00	9.58	386.00	18.10	386.00	64.10
5	281.00	2.01	281.00	8.88	281.00	17.00	281.00	61.20
6	204.00	1.73	204.00	8.31	204.00	16.20	204.00	58.50
7	149.00	1.52	149.00	7.84	149.00	15.40	149.00	56.10
8	108.00	1.36	108.00	7.44	108.00	14.70	108.00	53.70
9	78.80	1.24	78.80	7.09	78.80	14.10	78.80	51.40
10	57.40	1.13	57.40	6.78	57.40	13.60	57.40	49.10
11	41.80	1.05	41.80	6.51	41.80	13.00	41.80	46.90
12	30.40	0.97	30.40	6.25	30.40	12.50	30.40	44.50
13	22.10	0.91	22.10	6.01	22.10	12.00	22.10	42.00
14	16.10	0.86	16.10	5.78	16.10	11.50	16.10	39.20
15	11.70	0.82	11.70	5.55	11.70	10.90	11.70	36.10
16	8.53	0.78	8.53	5.33	8.53	10.40	8.53	31.80
17	6.21	0.74	6.21	5.07	6.21	9.66	6.21	27.70
18	4.52	0.70	4.52	4.80	4.52	8.96	4.52	23.00
19	3.29	0.68	3.29	4.54	3.29	7.99	3.29	20.40
20	2.40	0.66	2.40	4.23	2.40	6.83	2.39	19.20
21	1.74	0.63	1.74	3.86	1.74	5.78	1.74	17.60
22	1.27	0.61	1.27	3.42	1.27	4.96	1.27	16.10
23	0.92	0.57	0.92	2.98	0.92	4.39	0.92	14.90
24	0.67	0.55	0.67	2.64	0.67	3.99	0.67	13.60
25	0.49	0.52	0.49	2.41	0.49	3.71	0.49	12.40
26	0.36	0.48	0.36	2.26	0.36	3.47	0.36	11.40
27	0.26	0.44	0.26	2.16	0.26	3.27	0.26	10.70
28	0.19	0.41	0.19	2.07	0.19	3.12	0.19	10.10
29	0.14	0.39	0.14	2.01	0.14	3.00	0.14	9.75
30	0.10	0.37	0.10	1.96	0.10	2.93	0.10	9.46

Table 7.2 Bindura nickel ore shear rate and shear stress data.

Measuring Points	8 vol%		10 vol%		13 vol%		18 vol%		25 vol%		33 vol%	
	Shear Rate [1/s]	Shear Stress [Pa]	Shear Rate [1/s]	Shear Stress [Pa]	Shear Rate [1/s]	Shear Stress [Pa]	Shear Rate [1/s]	Shear Stress [Pa]	Shear Rate [1/s]	Shear Stress [Pa]	Shear Rate [1/s]	Shear Stress [Pa]
1	1000.00	5.84	1000.00	6.58	1000.00	7.41	1000.00	11.30	1000.00	22.90	1000.00	127.00
2	728.00	3.71	728.00	4.25	728.00	4.87	728.00	7.05	728.00	18.80	728.00	105.00
3	530.00	2.34	530.00	2.73	530.00	3.18	530.00	5.55	530.00	15.90	530.00	91.30
4	386.00	1.75	386.00	1.91	386.00	2.09	386.00	4.55	386.00	13.90	386.00	81.30
5	281.00	1.35	281.00	1.51	281.00	1.69	281.00	3.84	281.00	12.40	281.00	73.60
6	204.00	1.08	204.00	1.23	204.00	1.40	204.00	3.34	204.00	11.30	204.00	67.60
7	149.00	0.88	149.00	1.03	149.00	1.20	149.00	2.98	149.00	10.40	149.00	62.60
8	108.00	0.73	108.00	0.88	108.00	1.05	108.00	2.70	108.00	9.60	108.00	58.00
9	78.80	0.61	78.80	0.76	78.80	0.94	78.80	2.48	78.80	8.97	78.80	52.90
10	57.40	0.52	57.40	0.66	57.40	0.85	57.40	2.30	57.40	8.45	57.40	47.40
11	41.80	0.44	41.80	0.58	41.80	0.77	41.80	2.15	41.80	8.01	41.80	41.90
12	30.40	0.37	30.40	0.51	30.40	0.70	30.40	2.03	30.40	7.63	30.40	35.60
13	22.10	0.32	22.10	0.45	22.10	0.64	22.10	1.92	22.10	7.27	22.10	28.00
14	16.10	0.27	16.10	0.39	16.10	0.58	16.10	1.83	16.10	6.90	16.10	22.90
15	11.70	0.23	11.70	0.35	11.70	0.54	11.70	1.75	11.70	6.47	11.70	18.20
16	8.53	0.19	8.53	0.31	8.53	0.49	8.53	1.67	8.53	5.70	8.53	14.00
17	6.21	0.16	6.21	0.27	6.21	0.46	6.21	1.60	6.21	4.40	6.21	12.20
18	4.52	0.13	4.52	0.23	4.52	0.41	4.52	1.49	4.52	3.38	4.52	9.89
19	3.29	0.10	3.29	0.20	3.29	0.38	3.29	1.25	3.29	2.88	3.29	8.19
20	2.40	0.09	2.40	0.17	2.40	0.34	2.40	0.96	2.40	2.60	2.39	7.77
21	1.74	0.07	1.74	0.14	1.74	0.29	1.74	0.83	1.74	2.37	1.74	7.89
22	1.27	0.06	1.27	0.12	1.27	0.25	1.27	0.73	1.27	2.18	1.27	7.86
23	0.92	0.05	0.92	0.11	0.92	0.22	0.92	0.64	0.92	2.03	0.92	7.64
24	0.67	0.04	0.67	0.09	0.67	0.20	0.67	0.59	0.67	1.93	0.67	7.43
25	0.49	0.04	0.49	0.09	0.49	0.19	0.49	0.56	0.49	1.87	0.49	7.26
26	0.36	0.04	0.36	0.08	0.36	0.18	0.36	0.54	0.36	1.84	0.36	7.19
27	0.26	0.03	0.26	0.08	0.26	0.18	0.26	0.53	0.26	1.83	0.26	7.21
28	0.19	0.03	0.19	0.07	0.19	0.17	0.19	0.51	0.19	1.82	0.19	7.31
29	0.14	0.03	0.14	0.07	0.14	0.17	0.14	0.50	0.14	1.78	0.14	7.43
30	0.10	0.03	0.10	0.06	0.10	0.15	0.10	0.49	0.10	1.77	0.10	9.30

Table 7.3 Platreef ore shear rate and shear stress data.

Measuring Points	6 vol%		8 vol%		12 vol%		18 vol%		25 vol%		33 vol%	
	Shear Rate [1/s]	Shear Stress [Pa]	Shear Rate [1/s]	Shear Stress [Pa]	Shear Rate [1/s]	Shear Stress [Pa]	Shear Rate [1/s]	Shear Stress [Pa]	Shear Rate [1/s]	Shear Stress [Pa]	Shear Rate [1/s]	Shear Stress [Pa]
1	1000.00	4.50	1000.00	4.89	1000.00	5.94	1000.00	8.25	1000.00	13.00	1000.00	47.90
2	728.00	2.81	728.00	3.13	728.00	3.82	728.00	5.34	728.00	8.25	728.00	39.90
3	530.00	1.79	530.00	1.97	530.00	2.46	530.00	3.43	530.00	6.59	530.00	34.40
4	386.00	1.11	386.00	1.25	386.00	1.57	386.00	2.22	386.00	5.41	386.00	30.40
5	281.00	0.70	281.00	0.77	281.00	0.94	281.00	1.76	281.00	4.56	281.00	27.40
6	204.00	0.41	204.00	0.45	204.00	0.69	204.00	1.44	204.00	3.96	204.00	25.10
7	149.00	0.26	149.00	0.32	149.00	0.54	149.00	1.21	149.00	3.53	149.00	23.30
8	108.00	0.19	108.00	0.24	108.00	0.44	108.00	1.04	108.00	3.21	108.00	21.80
9	78.80	0.14	78.80	0.18	78.80	0.36	78.80	0.92	78.80	2.96	78.80	20.70
10	57.40	0.11	57.40	0.14	57.40	0.31	57.40	0.83	57.40	2.77	57.40	19.80
11	41.80	0.09	41.80	0.12	41.80	0.26	41.80	0.76	41.80	2.62	41.80	19.00
12	30.40	0.07	30.40	0.09	30.40	0.23	30.40	0.71	30.40	2.51	30.40	18.20
13	22.10	0.05	22.10	0.08	22.10	0.20	22.10	0.66	22.10	2.42	22.10	17.50
14	16.10	0.04	16.10	0.06	16.10	0.18	16.10	0.62	16.10	2.36	16.10	16.80
15	11.70	0.03	11.70	0.05	11.70	0.17	11.70	0.60	11.70	2.31	11.70	15.60
16	8.53	0.03	8.53	0.04	8.53	0.14	8.53	0.57	8.53	2.27	8.53	13.20
17	6.21	0.02	6.21	0.03	6.21	0.13	6.21	0.55	6.21	2.24	6.21	11.40
18	4.52	0.01	4.52	0.02	4.52	0.11	4.52	0.53	4.52	2.20	4.52	9.56
19	3.29	0.01	3.29	0.02	3.29	0.10	3.29	0.52	3.29	2.17	3.29	7.75
20	2.40	0.01	2.40	0.02	2.40	0.10	2.40	0.51	2.40	2.13	2.40	6.78
21	1.74	0.01	1.74	0.01	1.74	0.09	1.74	0.49	1.74	1.97	1.74	6.58
22	1.27	0.00	1.27	0.01	1.27	0.08	1.27	0.48	1.27	1.64	1.27	6.30
23	0.92	0.00	0.92	0.00	0.92	0.06	0.92	0.46	0.92	1.34	0.92	6.12
24	0.67	0.00	0.67	0.00	0.67	0.06	0.67	0.43	0.67	1.18	0.67	5.98
25	0.49	0.00	0.49	0.00	0.49	0.05	0.49	0.37	0.49	1.07	0.49	5.83
26	0.36	0.00	0.36	0.00	0.36	0.04	0.36	0.30	0.36	0.96	0.36	5.74
27	0.26	0.00	0.26	0.00	0.26	0.03	0.26	0.24	0.26	0.86	0.26	5.69
28	0.19	0.00	0.19	0.00	0.19	0.02	0.19	0.21	0.19	0.78	0.19	5.68
29	0.14	0.00	0.14	0.00	0.14	0.02	0.14	0.18	0.14	0.72	0.14	5.70
30	0.10	0.00	0.10	0.00	0.10	0.01	0.10	0.16	0.10	0.68	0.10	5.75

Appendix B: Gas Dispersion Data

Bubble Size

Table 7.4 Kaolin ore mean bubble size data.

Solids Concentration [vol%]	Mean Bubble Size [mm]				
	300 rpm	440 rpm	550 rpm	650 rpm	730 rpm
6	0.98	0.87	0.86	0.83	0.85
11	1.04	1.09	1.09	1.10	1.11
14	0.61	0.73	0.92	1.03	1.05
20	0.53	0.61	0.62	0.63	0.69

Table 7.5 Bindura nickel ore mean bubble size data.

Solids Concentration [vol%]	Bubble size [mm]				
	300 rpm	440 rpm	550 rpm	650 rpm	730 rpm
8	0.95	0.78	0.70	0.69	0.69
10	0.97	0.77	0.72	0.68	0.69
13	0.97	0.76	0.71	0.70	0.70
15	0.96	0.79	0.69	0.69	0.69
18	0.96	0.79	0.72	0.70	0.74
25	0.94	0.90	0.87	0.83	0.80
33	0.77	0.79	0.73	0.77	0.93

Table 7.6 Platreef ore mean bubble size data.

Solids Concentration [vol%]	Mean Bubble Size [mm]				
	300 rpm	440 rpm	550 rpm	650 rpm	730 rpm
8	0.98	0.85	0.85	0.81	0.80
10	1.02	0.87	0.86	0.77	0.78
12	1.03	0.98	0.98	1.02	0.96
15	0.98	0.93	0.85	0.88	0.89
18	0.99	0.98	0.89	0.95	0.93
25	0.66	0.86	0.73	0.96	1.27
33	0.70	0.69	0.68	0.71	0.72

Table 7.7 Kaolin ore gas hold-up data.

Solids Concentration [vol%]	Gas Hold-up [vol%]				
	300 rpm	440 rpm	550 rpm	650 rpm	730 rpm
6	5.81	9.56	11.14	12.58	16.14
11	7.02	9.25	8.96	9.48	8.85
14	3.20	6.43	9.53	11.28	10.60
20	2.23	2.43	2.80	2.90	4.41

Table 7.8 Bindura nickel ore gas hold-up data.

Solids Concentration [vol%]	Gas Hold-up [vol%]				
	300 rpm	440 rpm	550 rpm	650 rpm	730 rpm
8	5.14	7.09	6.58	7.93	7.08
10	5.42	7.02	8.07	9.09	7.29
13	4.84	5.99	6.80	7.54	6.61
15	5.00	7.75	7.49	8.45	7.35
18	5.88	6.88	7.91	8.70	8.95
25	6.50	8.12	8.32	7.14	6.88
33	1.50	2.96	4.30	4.30	4.93

Table 7.9 Platreef ore gas hold-up data.

Solids Concentration [vol%]	Gas Hold-up [vol%]				
	300 rpm	440 rpm	550 rpm	650 rpm	730 rpm
8	7.49	9.72	12.20	13.42	14.93
10	6.73	9.47	11.84	12.90	14.38
12	7.88	9.41	11.07	12.08	13.59
15	7.42	10.52	12.20	14.71	15.81
18	8.13	10.82	12.14	13.30	14.27
25	5.21	5.75	5.88	6.15	6.16
33	3.32	3.00	3.43	3.96	4.01

Appendix C: Standard Deviation and Standard Errors

Table 7.10 Standard deviation and errors of mean bubble size for kaolin ore.

Solids Content [vol%]	Mean Bubble Size [mm]									
	300 rpm		440 rpm		550 rpm		650 rpm		730 rpm	
	STDEV	Error	STDEV	Error	STDEV	Error	STDEV	Error	STDEV	Error
6	0.0014	0.0010	0.0051	0.0036	0.0016	0.0011	0.0005	0.0004	0.0016	0.0011
11	0.0693	0.0490	0.0950	0.0672	0.0106	0.0075	0.0211	0.0149	0.0327	0.0232
14	0.0252	0.0178	0.0098	0.0069	0.0150	0.0106	0.0617	0.0436	0.0342	0.0242
20	0.0185	0.0131	0.0141	0.0099	0.0058	0.0041	0.0143	0.0101	0.0165	0.0117

Table 7.11 Standard deviation and errors of mean bubble size for Bindura nickel ore.

Solids Content [vol%]	Bubble size [mm]									
	300 rpm		440 rpm		550 rpm		650 rpm		730 rpm	
	STDEV	Error	STDEV	Error	STDEV	Error	STDEV	Error	STDEV	Error
8	0.0135	0.0078	0.0409	0.0236	0.0292	0.0169	0.0097	0.0097	0.0141	0.0081
10	0.0698	0.0403	0.0186	0.0107	0.0141	0.0081	0.0027	0.0027	0.0079	0.0045
13	0.0246	0.0142	0.0273	0.0158	0.0251	0.0145	0.0013	0.0013	0.0101	0.0058
15	0.0370	0.0214	0.0359	0.0207	0.0015	0.0009	0.0101	0.0101	0.0104	0.0060
18	0.0521	0.0301	0.0118	0.0068	0.0135	0.0078	0.0054	0.0054	0.0257	0.0148
25	0.0188	0.0108	0.0113	0.0065	0.0202	0.0117	0.0155	0.0155	0.0041	0.0024
33	0.0174	0.0100	0.0068	0.0039	0.0400	0.0231	0.0216	0.0216	0.0461	0.0266

Table 7.12 Standard deviation and errors of mean bubble size for Platreef ore.

Solids Content [vol%]	Bubble size [mm]									
	300 rpm		440 rpm		550 rpm		650 rpm		730 rpm	
	STDEV	Error	STDEV	Error	STDEV	Error	STDEV	Error	STDEV	Error
8	0.0065	0.0038	0.0118	0.0068	0.0104	0.0060	0.0113	0.0065	0.0065	0.0038
10	0.0157	0.0091	0.0250	0.0144	0.0253	0.0146	0.0053	0.0031	0.0200	0.0115
13	0.0269	0.0155	0.0650	0.0375	0.0050	0.0029	0.0230	0.0133	0.0154	0.0089
15	0.0100	0.0058	0.0800	0.0462	0.0352	0.0203	0.0255	0.0147	0.0150	0.0087
18	0.0271	0.0157	0.0058	0.0033	0.0259	0.0150	0.0452	0.0261	0.1106	0.0639
25	0.0209	0.0120	0.1917	0.1107	0.0088	0.0051	0.0085	0.0049	0.0136	0.0079
33	0.2170	0.1253	0.2202	0.1271	0.1982	0.1144	0.1590	0.0918	0.1789	0.1033

Table 7.13 Standard deviation and errors of gas hold-up for kaolin ore.

Solids Content [vol%]	Gas Hold-up [vol%]									
	300 rpm		440 rpm		550 rpm		650 rpm		730 rpm	
	STDEV	Error	STDEV	Error	STDEV	Error	STDEV	Error	STDEV	Error
6	0.0237	0.0167	0.2249	0.1590	0.0616	0.0435	0.0418	0.0296	0.2155	0.1524
11	0.8399	0.5939	0.1334	0.0943	0.8053	0.5694	2.9175	2.0630	2.0178	1.4268
14	1.6690	1.1801	0.8508	0.6016	0.7953	0.5624	0.6374	0.4507	2.5873	1.8295
20	0.0063	0.0045	0.0405	0.0287	0.1352	0.0956	0.0062	0.0044	0.2537	0.1794

Table 7.14 Standard deviation and errors of gas hold-up for Bindura nickel ore.

Solids Content [vol%]	Gas Hold-up [vol%]									
	300 rpm		440 rpm		550 rpm		650 rpm		730 rpm	
	STDEV	Error	STDEV	Error	STDEV	Error	STDEV	Error	STDEV	Error
8	0.8614	0.4973	0.6333	0.3656	2.5119	1.4502	0.9750	0.5629	1.1297	0.6523
10	0.2049	0.1183	0.8586	0.4957	0.2954	0.1705	0.6106	0.3525	0.4949	0.2857
13	2.0988	1.2118	2.3123	1.3350	1.9761	1.1409	0.9712	0.5607	1.6250	0.9382
15	0.5484	0.3166	0.4910	0.2835	0.2991	0.1727	0.6734	0.3888	0.8874	0.5123
18	1.1811	0.6819	0.4910	0.7423	2.0058	1.1580	1.1254	0.6497	1.4290	0.8250
25	0.3056	0.1764	1.1859	0.6847	0.9916	0.5725	1.3840	0.7990	1.5963	0.9216
33	0.7169	0.4139	0.5421	0.3130	1.0407	0.6009	0.8519	0.4919	0.7277	0.4201

Table 7.15 Standard deviation and errors of gas hold-up for Platreef ore.

Solids Content [vol%]	Gas Hold-up [vol%]									
	300 rpm		440 rpm		550 rpm		650 rpm		730 rpm	
	STDEV	Error	STDEV	Error	STDEV	Error	STDEV	Error	STDEV	Error
8	0.1131	0.0653	0.3240	0.1871	0.2036	0.1175	0.4325	0.2497	0.4768	0.2753
10	0.2155	0.1244	0.1767	0.1020	0.1676	0.0968	0.0820	0.0473	0.3970	0.2292
13	0.1835	0.1059	0.0885	0.0511	0.1710	0.0987	0.1445	0.0835	0.1610	0.0930
15	0.1603	0.0925	0.1731	0.1000	0.0833	0.0481	0.0785	0.0453	0.3498	0.2020
18	0.2955	0.1706	0.3148	0.1818	0.1020	0.0589	0.1721	0.0994	0.2574	0.1486
25	0.3360	0.1940	0.5839	0.3371	1.0006	0.5777	0.9319	0.5380	0.6641	0.3834
33	0.0000	0.0000	0.4571	0.2639	0.4531	0.2616	0.0000	0.0000	0.3730	0.2154

Appendix D: Formulas and Equations used

Rheology

The Bingham plastic model was used to determine the yield stress and the viscosity.

$$t = t_B + \left(h_B \cdot g\right)$$

Gas dispersion

In order to calculate the bubble size, the mean area of the bubbles from the Anglo Platinum Bubble sizer were used. It was assumed that the bubbles are spherical such that:

$A_{bubble} = \frac{p d_b^{\,2}}{4}$, then the mean bubble size is

$$d_b = \sqrt{\frac{4A_{bubble}}{p}}$$

To calculate the gas hold-up (ε_G) the change in volume in the presence of air (V_2) and absence of air (V_1) was taken into account; the equation used was thus:

$$e_G = \frac{V_2 - V_1}{V_1}$$

Error Analysis

The standard deviation is a measure of the wide distribution between values and the mean value. It can be estimated by equation 3.5:

$$s = \sqrt{\sum \frac{\left(x_i - \bar{x}\right)^2}{\left(N-1\right)}}$$

where:

s -estimated standard deviation

N -number of observed values

x_i -ith observed value

$\bar{x}$ -average of all observed values

The standard error provides a confidence value of the mean of the set of data, equation 3.6 shows the relationship:

$$s_{\bar{x}} = \frac{s}{\sqrt{N}}$$

where:

$s_{\bar{x}}$ -standard error

s -estimated standard deviation

N -number of observed values